Author:
Beritza, Konstantina

Title:
Developing plant chassis for heterologous expression of the pleuromutilin biosynthetic gene cluster

Developing plant chassis for heterologous expression of the pleuromutilin biosynthetic gene cluster

Konstantina Beritza

School of Biological Sciences
University of Bristol

Research supervisors: Prof Gary Foster & Dr Andy Bailey

A dissertation submitted to the University of Bristol in accordance with the requirements of the degree of ***Master of Science by Research*** in the Faculty of Science

September 2020

Word count: 24,287

Abstract

In an era of widespread antibiotic resistance, basidiomycete fungi are a useful source of possible antimicrobials, with pleuromutilin being one of them. Due to its mechanism of action which comprises the binding of the conserved peptidyl transferase centre, resistance to pleuromutilin is slow to be developed and has minimal cross-resistance with other antibiotics. The pleuromutilin biosynthetic gene cluster and pathway of chemical intermediates is known, and its heterologous expression has been achieved in fungi. This thesis reports attempts to express parts of the pleuromutilin pathway in different plant hosts, including *Marchantia polymorpha* and *Nicotiana tabacum*. Prior to genetic engineering of the hosts, this work shows that pleuromutilin, mutilin and a diverse selection of antibiotics impact on growth and morphology of *Physcomitrella patens* and *M. polymorpha*, when supplemented into growing media, indeed the pleuromutilin derivative, tiamulin led to inhibition of growth of *P. patens* and *M. polymorpha*.

The construction of multigene expression plasmids using Golden Gate technology is described. Transient expression was performed in *N. tabacum* and stable transformants obtained in *M. polymorpha*. Expression analysis using qPCR was carried out to validate the heterologous expression of the genes. The results from HPLC analysis were unclear and did not prove the presence of pleuromutilin metabolic intermediates, indicating that more work is needed to fine-tune the biosynthetic pathway *in planta*.

Acknowledgements

First of all, I am grateful to Prof Gary Foster and Dr Andy Bailey for giving me the opportunity to work in their research group, as well as their mentoring during my studies. Their guidance and constant encouragement played a major role in my aspiration of continuing doing research.

I have been really fortunate to work in a wonderful environment, and I cannot thank enough all the members of Lab321, especially Dr Ian Prosser, Dr Katherine Williams, Dr Amy James and the PhD student Helen Rees for every valuable advice inside and outside the lab. Also, my sincere thanks to Dr Jill Harrison and PhD student Zoe Nemec Venza for their help in plant propagation and transformation.

Last but not least, I would like to thank my family, my partner and close friends, being always there to support me in their way, while trying to understand with what kind of ‘’jelly stuff’’ I am working in the lab.

COVID-19 statement

The unprecedented situation of the Covid-19 lockdown had a significant impact on my research project. The lockdown prevented the production and testing of additional transformants of *Marchantia polymorpha* or any repeats of the HPLC and qPCR analyses. Furthermore, transformation of *Physcomitrella patens* and further analysis of any stable transformants could not proceed. Last but not least, thesis writing was being disrupted due to IT issues and unforeseen relocation to Greece.

Author's declaration

I declare that the work in this dissertation was carried out in accordance with the requirements of the University's *Regulations and Code of Practice for Research Degree Programmes* and that it has not been submitted for any other academic award. Except where indicated by specific reference in the text, the work is the candidate's own work. Work done in collaboration with, or with the assistance of, others, is indicated as such. Any views expressed in the dissertation are those of the author.

Signed: Konstantina Beritza **Date**: 22/09/2020

Contents

List of Figures

List of Tables

List of Abbreviations

(w/v)	Weight/Volume
°C	Degree Celcius
35S/CaMV 35S	Cauliflower mosaic virus 35S promoter
Act2	Actin 2
$AlK(SO_4)_2$	Aluminum potassium sulfate
AT	di-ammonium tartrate
atf	Acetyltransferase gene
ATP	Adenosine triphosphate
BGC	Biosynthetic gene cluster
BLAST	Basic local alignment search tool
bp	Base pairs
$Ca(NO_3)_2$	Calcium nitrate
$CaCl_2$	Calcium chloride
CARB	Community-acquired bacterial pneumonia
cDNA	Complementary DNA
CDS	Coding sequence
CHO	Chinese hamster ovary
$CoCl_2$	Cobalt(II) chloride
Cq	Cycle of quantification value
CRISPR/Cas9	Clustered regularly interspaced short palindromic repeats/ Caspase 9
Ct	Threshold cycle
CTAB	Cetyl trimethylammonium bromide
$CuSO_4$	Copper(II) sulfate
cyc	Terpene cyclase gene
dH_2O	Deionised water
dig-lig	Digestion-ligation
DMSO	Dimethyl sulfoxide
DNA	Deoxyribonucleic acid
dNTP	Deoxyribonucleotide triphosphate
dpi	Days post infection
EDTA	Ethylenediaminetetraacetic acid
ELSD	Evaporate light scattering detector
ER	Endoplasmic reticulum
ES+/ES-	Positive/negative electrospray ionization

EtOH	Ethanol
FDA	Food and Drug Administration
$FeSO_4$	Iron(II) sulfate
FF	Forward primer
g	Gravitational force
G418	Geneticin®
GCMS	Gas chromatography-Mass spectrometry
GFP	Green fluorescent protein
ggpps	Geranylgeranyl pyrophosphate synthase gene
GGS	Geranylgeranyl pyrophosphate synthase
GOI	Gene of interest
GT	Gene targeting
H_2O	Water
H_3BO_3	Boric acid
HCl	Hydrochloric acid
HPLC-MS	High-pressure liquid chromatography-Mass spectrometry
HSP	Heat-shock protein
IPTG	Isopropyl β-D-1-thiogalactopyranoside
IV	Intravenous
K_2HPO_4	Dipotassium phosphate
kb	Kilo bases
KBr	Potassium bromide
KH_2PO_4	Monopotassium phosphate
KI	Potassium iodide
KNO_3	Potassium nitrate
KOH	Potassium hydroxide
LacZ	β-galactosidase
LB	Lysogeny Broth
LB	Left Border
LiCl	Lithium chloride
mas	Mannopine synthase
MeOH	Methanol
MES	2-(N-morpholino)ethanesulfonic acid
$MgCl_2$	Magnesium chloride
$MgSO_4$	Magnesium sulfate
$MnCl_2$	Manganese(II) chloride
MoClo	Modular Cloning

mRNA	Messenger RNA
MRSA	Methicillin-resistant *Staphylococcus aureus*
N_2	Nitrogen
NaCl	Sodium chloride
NaFe(III)	Sodium iron
$NaMoO_4$	Sodium molybdate
NaOH	Sodium hydroxide
NCBI	National center for Biotechnology Information
NH_4NO_3	Ammonium nitrate
NHK	Nozaki–Hiyama–Kishi cyclization
nos	Nopaline synthase
nptII	Neomycin phosphotransferase II gene
NTC	Non-template control
OD_{600}	Optical density at a wavelength of 600nm
osc	Oxidosqualene cyclase
P/Pro	Promoter
P450	Cytochrome P450
PCR	Polymerase chain reaction
PEG	Polyethylene glycol
pH	Potential of hydrogen
PIPES	Piperazine-N,N'-bis(2-ethanesulfonic acid)
PKS	Polyketide synthase
pri-miRNA	Primary micro-RNA
PVP-40	Polyvinylpyrrolidone
R/FR	Red/ Far red light
RB	Right Border
REU	Relative expression unit
RNA	Ribonucleic acid
rpm	Revolutions per minute
RR	Reverse primer
rRNA	Ribosomal RNA
Rt	Retention time
RT-qPCR	Quantitative reverse transcription polymerase chain reaction
sdr	Short-chain dehydrogenase/reductase
SDS	Sodium dodecyl sulfate
$SnCl_2$	Tin(II) chloride
SP	Signal peptide

T	Terminator
TALEN	Transcription activator-like effector nuclease
T-DNA	Transfer DNA
TES	Trace elements solution
TU	Transcription unit
UTR	Untranslated region
UV	Ultraviolet
X-gal	5-bromo-4-chloro-3-indolyl-β-D-galactopyranoside
YM	Yeast Malt
$ZnSO_4$	Zinc sulfate

Chapter 1: Introduction

1.1 From traditional medicine to drug discovery

Natural products have likely been used as medicinal agents since the origins of mankind, coming from a variety of sources, including plants, microbes and fungi. Ancient written records date back to 2,600BC in Mesopotamia, whilst Egyptian medicine has even earlier reports, from 2,900BC, with the *Ebers Papyrus* (Borchardt, 2002; Newman & Cragg, 2010). Records from the Chinese *Materia Medica* demonstrate 52 prescriptions, documented from 1,100BC (Chang & But , 1986), while Ayuverda, the Hindu system of alternative medicine, dates back to 1,000BC (Kapoor, 2001).

In ancient Greece, the philosopher and natural scientist, Theophrastus (100BC), reported the use of medicinal herbs in his book *Historia Plantarium,* while Galen (200AC), who practiced pharmacy and medicine in Rome, published prescriptions and formulas made of multiple ingredients (‘’galenicals’’). During the eighth century, Arabs created the first private drug stores and were the ones that preserved and expanded the existing Greco-Roman, Chinese and Indian records (Newman & Cragg, 2010).

1.2 Bioactive natural products from fungi

Filamentous fungi are a source of bioactive natural products, which can have further applications in industry, agriculture or human medicine (Figure 1.1). Approaches where the native host is manipulated in order to increase the yields of these metabolites might be challenging, due to low efficiency genetic engineering or

highly demanding culture conditions (Alberti et al., 2017). For this reason, most approaches for heterologous expression of natural products are focused on *Escherichia coli* and the yeast *Saccharomyces cerevisiae.* Although *E. coli* is the most characterized prokaryotic model for protein expression and purification, and has been used for partial or sequential recreation of biosynthetic pathways, expression of large proteins such as polyketide synthases (PKSs) has been mostly unsuccessful. Amongst the limitations of this bacterial host is the inability to promote post-translational modifications that are required for functionality of some enzymes, and the fact that it has a different codon usage than eukaryotic fungi might compel codon optimisation for expression. Similarly, the most commonly researched group of natural products is antibiotics and antibiotic production in bacterial hosts can lead to toxicity or growth complications. *S. cerevisiae* is sometimes used for purification and catalytic characterisation of enzymes, by incubation of the substrate and the enzyme *in vitro.* This unicellular ascomycete fungus is widely used due to its rapid growth, the amenability for transformation and the promotion of most typical eukaryotic post-translational modifications (Alberti et al., 2017; Da Silva & Srikrishnan, 2012; Sørensen & Mortensen, 2005).

The fungal-derived β-lactam antibiotics, such as penicillins (1) and cephalosporins (2), contribute to over 40% of antibiotics in the human and veterinary drug market (Gidijala et al., 2010). Furthermore, fungal-derived fungicides as griseofulvin (3) and echinocandin (4) are used mainly for dermatophyte infections and candidiasis, respectively (Denning, 2002; Finkelstein et al., 1996). Strobilurins (12) are antifungal polyketides that paved the way for the production of synthetic derivatives, such as the β-methoxyacrylate class, used in crop protection. This class of fungicide gained a considerable 25% of the agricultural fungicide market (Nofiani et

al., 2018). Statins compromise another group of fungal natural products used in medicine, in order to lower cholesterol levels, including lovastatin (5) and mevastatin (6) (Manzoni & Rollini, 2002). Cyclosporin (7), originated from the fungus *Tolypocladium inflatum*, is an immunosuppressive agent for use in clinical organ transplantation (Cohen et al., 1984; Kahan, 1985). Another immunosuppressive agent, which also has anti-atherogenic properties and it is used as a treatment for multiple sclerosis, is the natural product myriocin (8) (Hojjati et al., 2005; Strader et al., 2011).

Mycotoxins are a group of fungal secondary metabolites which contaminate food supplies and may cause mycotoxicosis in human and animals (Liew & Mohd-Redzwan, 2018). Among mycotoxins, aflatoxins (9), derive from polyketides and are produced by *Aspergillus flavus, A. parasiticus*, and *A. nomius* (Kumaret al., 2017), ochratoxins (10) are produced by both *Aspergillus* and *Penicillium* species (Reddy & Bhoola, 2010), and trichothecenes (11) are found in genera including *Fusarium, Myrothecium, Spicellum, Stachybotrys, Cephalosporium, Trichoderma* and *Trichothecium* (McCormick et al., 2011).

A group of natural products produced by bacteria, fungi and plants is tropolones (13), which consist of a core structure that is still rare among other natural products, including key steps of ring expansion (Cox & Al-Fahad, 2013). Cladosporin (14) is a nanomolar inhibitor of growth in both blood- and liver-stage of *Plasmodium* (Baragaña et al., 2019; Hoepfner et al., 2012).

1.2.1 Using filamentous fungi as heterologous platforms

When it comes to expression of complete biosynthetic pathways for secondary metabolites, filamentous fungi are preferred, since they can grow quickly using simple and inexpensive growth conditions and for this reason a lot of work is focused on cultivation and genetic engineering advancements (Nevalainen et al., 2005). In addition, fungal genes have relatively long exons and short introns compared to those of higher eukaryotes (Kupfer et al., 2004), and are generally compatible in translation folding and post-translational modifications. Moreover, their already active secondary metabolite machinery increases the availability of common precursors (Kjærbølling et al., 2019).

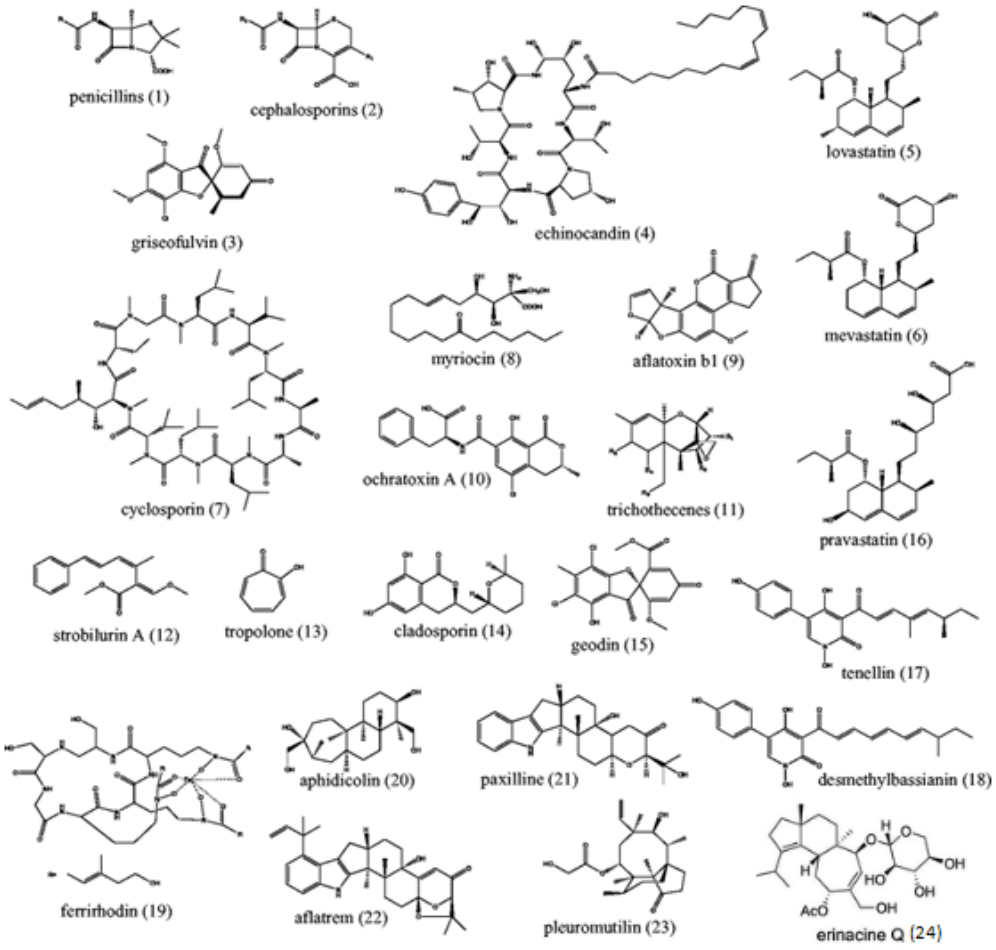

Figure 1.1 Diversity of fungal bioactive natural products (adapted from Alberti et al., 2017).

Aspergillus species are the main platforms used for heterologous studies of gene clusters from different species. Nielsen and co-workers (2013), managed to incorporate the 13-genegeodin (15) cluster from *A. terreus* into *A. nidulans*, based on a successive gene targeting approach, geodin seems to act as a glucose uptake stimulator in rat adipocytes (Sato et al., 2005) and as an antifungal agent (Hargreaves et al., 2002). In the category of cholesterol-lowering agents, pravastatin (16), was successfully produced by McLean and co-workers, using *P. chrysogenum,* with the additional expression of a cytochrome P450 from *Amycolatopsis orientalis* to catalyze the conversion of compactin to pravastatin (McLean et al., 2015). Heneghan et al. managed to re-build the whole biosynthetic pathway of tenellin (17) derived from the insect pathogenic fungus, *Beauveria bassiana,* into *Aspergillus oryzae* and obtain the metabolite at a fivefold concentration (Heneghan et al., 2010). Apart from heterologous expression of the whole biosynthetic pathway, Fisch et al. proposed the reprogramming of polyketide synthases by rational domain swaps for the expression of tenellin (17) and desmethylbassianin (18) (Fisch et al., 2011). Ferrirhodin (19) acts as a siderophore related to iron acquisition and the characterisation of a nonribosomal peptide synthetase gene was accomplished by heterologous expression of the gene from *F. sacchari* to *A. oryzae* (Munawar et al., 2013).

The first attempt at producing terpenoids into fungal hosts by transferring the whole biosynthetic pathway, was achieved by Fujii et al., where they followed a sequential transformation approach to express the four genes of the antibiotic aphidicolin (20) cluster into *A. oryzae* (Fujii et al., 2011). Paxilline (21) is a fungal indole-alkaloid tremorgenic known for its anti-MRSA properties and its biosynthetic pathway was reconstructed step-by-step from *P. paxillin* to *A. oryzae,* allowing the authors to elucidate the substrates of each enzyme (Tagami et al., 2013). Similarly to paxilline, aflatrem (22) was successfully produced after two rounds of *A. oryzae*

transformation, enabling the reconstruction of the 7-gene pathway from *A. flavus* (Tagami et al., 2014). The first effective heterologous reconstruction of a secondary metabolism biosynthetic pathway from a basidiomycete to an ascomycete fungus was accomplished by Bailey et al., where a 7-gene cluster, encoding for the antibiotic pleuromutilin (23), was stepwise introduced from *Clitopilus passeckerianus* to *A. oryzae*, leading to a significant twentyfold increase in production (Bailey et al., 2016). Another example of total biosynthesis comes from the work of Liu et al., where a basidiomycete metabolite erinacine Q (24), a diterpene with neuroprotective properties derived from *Hericium erinaceus*, was produced in *A. oryzae* by applying CRISPR/Cas9-mediated homologous recombination (Liu et al., 2019).

1.2.2 From gene clusters to biosynthetic pathways

Secondary metabolites are usually encoded by genes that are physically grouped in the genome, called biosynthetic gene clusters (BGCs) and can be found in bacteria, fungi and plants (Osbourn, 2010; Tran et al., 2019). A BGC contains all the genes encoding the functional enzymes of the pathway, tailoring enzymes and regulatory elements, such as transcription factors (Figure 1.2). In some cases, it might also contain genes responsible for exportation and transportation of the produced molecules or resistance genes to protect the producer from the potentially harmful metabolites (Medema & Fischbach, 2015; Tran et al., 2019). Physical clustering provides the opportunity for coordinated regulation of gene expression as all the genes would be in a similar chromatin context, allowing the coordinated activation of cryptic clusters using chromatin modifying agents (Hurst et al., 2004; Sproul et al., 2005). Another reason for co-localisation of these genes may be linked to the selective advantage of coinheritance of the entire pathway and of favourable combinations of

alleles (Nei, 1967; Osbourn, 2010). Transcriptional regulation of fungal BCGs is complex and can be affected by various environmental stimuli such as carbon and nitrogen concentrations, temperature, light, pH, reactive oxygen species, amino acids and stimuli from other organisms. Regulation can occur at a global level, where the regulatory proteins are globally acting transcription factors regulating a plethora of genes that do not participate in secondary metabolism (e.g. LaeA, PacC, Cre1; Figure 1.2) and a pathway-specific level, where those specific transcription factors are also encoded by genes involved in the respective cluster (Brakhage, 2013).

Clustering of genes that produce secondary metabolites facilitates their identification. Most secondary metabolites fall into a limited group of chemical classes (terpenes, polyketides or non-ribosomal peptides) and the core synthases for these are readily identifiable by homology searches such as BLAST. The adjacent genomic regions can then be analysed for likely tailoring genes and other elements needed for secondary metabolite production. Analysis of the rapidly expanding number of fungal genomic sequences led to the observation that the BGCs outnumbered the known natural products, therefore indicating a bigger variety of these products within the same organism and that therefore most BGCs are silent or not active enough during laboratory conditions to lead to a detectable product (Kjærbølling et al., 2019). In order to associate a secondary metabolite with a BGC, it is important to take into consideration whether the native strain is amenable to transformation and/or it can grow quickly in laboratory conditions. The next question is whether this BGC is silent or active within the strain, so as to follow external stimuli or genetic engineering to activate it, or gene deletion strategies to eliminate its expression. Heterologous expression is still considered the most preferred option when elucidating and characterising biosynthetic genes and pathway precursors.

Various bioinformatic tools facilitate the assembly and identification of BGCs following one of the strategies: (1) Homology search – having a known similar compound in two organisms, where the biosynthetic cluster has been identified in either of those (2) Retro biosynthesis – having a known compound but no cluster identification, predicting the enzymes activities and therefore any putative clusters that encode these enzymes and (3) Comparative genomics – comparing genomes of a set of organisms that may or may not produce the compound under study and discover gene clusters that are homologous in the producing species and filter them based on no homologs in the non-producing (Kjærbølling et al., 2019; Lazarus et al., 2014; Schmidt-Dannert, 2015).

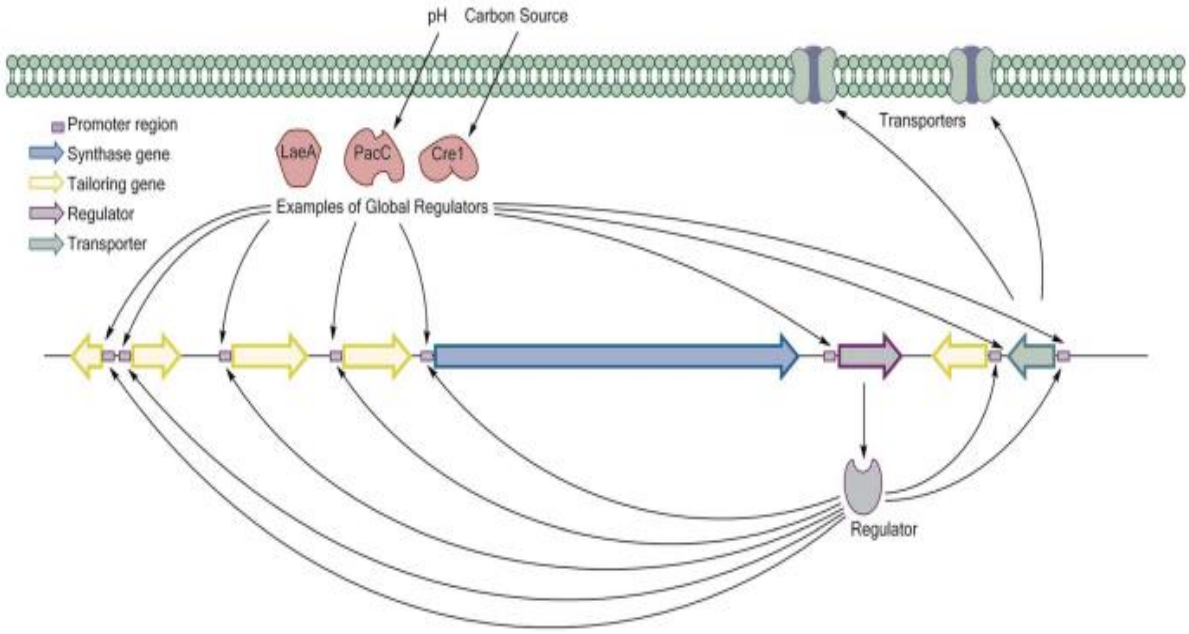

Figure 1.2 A generalised biosynthetic gene cluster, consisting of backbone synthase genes, tailoring genes, regulatory elements and transporters(Lazarus et al., 2014).

1.3 An introduction to pleuromutilins and their clinical potential

1.3.1 Isolation, origin and mechanism of action

Pleuromutilin is a tricyclic diterpene, produced by the basidiomycetes *Pleurotusmutilus* (*Clitopilusscyphoides*) and *Pleurotus passeckerianus* (*Clitopilus passeckerianus*), and its skeleton can be used for semi-synthesis of derivatives (Figure 1.3) (Bailey et al., 2016). The basidiomycetes belong to the subkingdom *Dikarya* and are an often underexploited phylum of fungi that can deliver various medicinal benefits, including not only antibacterial, but also immunomodulatory, anticancer, antiviral, cardio and hepatoprotective properties (de Mattos-Shipley et al., 2016). In most fungal natural products, the yields in the native host are very low, and fermentation or isolation of these compounds can be demanding. This also applies to *C. passeckerianus*, where traditional strain improvement, like random mutagenesis is achievable due to their dikaryotic nature (Bailey et al., 2016).

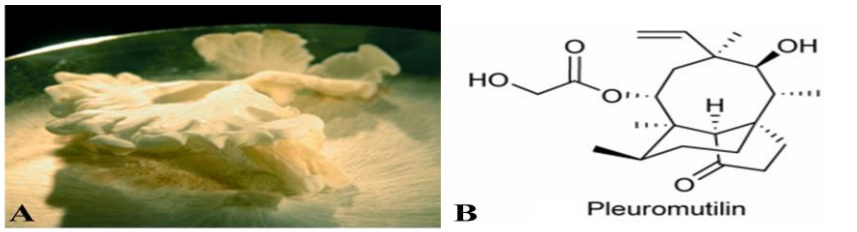

Figure 1.3 (A) A mature *Clitopilus passeckerianus* fruiting body. **(B)** Chemical structure of pleuromutilin (de Mattos-Shipley et al., 2017; Newman & Cragg, 2010).

Pleuromutilin and its producing strains were first isolated and reported by Kavanagh et al. in the early 1950s (Kavanagh et al., 1951; Kavanagh et al., 1952), where it displayed a potent activity against Gram-positive bacteria, particularly *Staphylococcus aureus.* The unique mechanism of action involves binding to the highly conserved peptidyl transferase centre of the bacterial ribosome. Hence, resistance to pleuromutilin is slow to be established, and it demonstrates minimal

potential for cross-resistance with existing antibiotics. The glycolic acid residue interacts via hydrogen bonding with the P-site of the protein translation centre (Figure 1.4) (Davidovich et al., 2007; Paukner & Riedl, 2017). The primary binding interactions of pleuromutilin with the ribosome originates from its tricyclic centre (Murphy et al., 2017). The majority of semi-synthetic efforts have focused on modification of the C14 side chain (Fazakerley & Procter, 2014; Paukner & Riedl, 2017), indeed more than 3,000 C14 derivatives have been produced. Until now, the three mechanisms of resistance to pleuromutilin consist of mutations in 23S rRNA and *rplC* genes encoding the ribosomal protein L3, methylation of the nucleotide A2503 which blocks pleuromutilin binding, and drug efflux by ATP-binding cassette (ABC) transporters (Goethe et al., 2018).

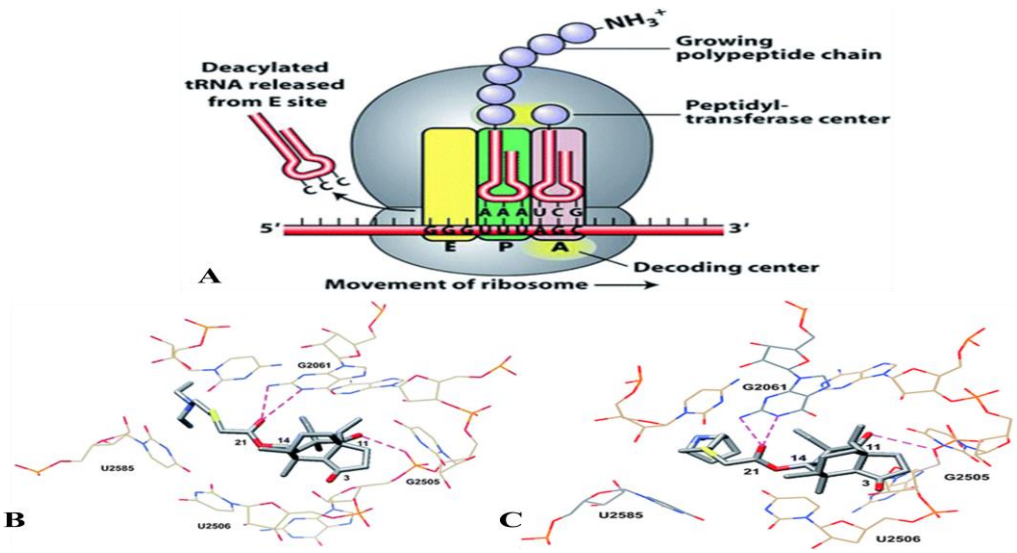

Figure 1.4 (A) Schematic of protein translation. **(B)** Partial structure of tiamulin and **(C)** retapamulin bound to the 50S ribosomal subunit of *D. radiodurans* (Davidovich et al., 2007; Goethe et al., 2018; Schlünzen et al., 2004).

1.3.2 Early studies of structure and biosynthesis of pleuromutilin

Structural studies were first published in 1952, describing the molecular structure of pleuromutilin ($C_{22}H_{34}O_5$) and correctly accrediting three of the five oxygen atoms

as two non-phenolic hydroxyl groups and one hindered carbonyl group. The remaining two oxygen atoms were experimentally assigned to a lactone ring (Anchel, 1952); this was later corrected, and shown to be the ester functionality at C14. Birch and Arigoni eventually generated the full and correct structure of pleuromutilin, giving also a proposed biosynthetic pathway, thus identifying pleuromutilin as the glycolic ester of the diterpene mutilin (Birch et al., 1966; Arigoni, 1968).

1.3.3 Chemical Synthesis of pleuromutilins

The first attempt of pleuromutilin chemical synthesis reported in 1980 by Kahn, where he focused on access to the synthetic core, examining the coupling of a vinyl anion fragment to a spirocyclobutanone derivative which would lead to the skeleton of pleuromutilin via the oxy-Cope rearrangement (Kahn, 1980). Two years later, Gibbons reported the total synthesis of pleuromutilin through a 12-step procedure, initiating with a sequential Michael reaction. After acquiring the tricyclic core, he started modifying it and completed the synthesis of pleuromutilin in a further 17 steps (Gibbons, 1982). In 2013, Fazakerley et al. reported the first enantiospecific total synthesis of pleuromutilin (Fazakerley et al., 2013). An 18-step synthesis of pleuromutilin was revealed by Farney et al. that enabled the preparation of mutilin derived antibiotics (Farney et al., 2018). In contrary to semisynthesis, *de novo* synthesis of pleuromutilins was reported by Liu et al., where ring-closing metathesis led to a modified pleuromutilin core via Nozaki–Hiyama–Kishi (NHK) cyclization to create C5, C6, C10-des-methyl pleuromutilin derivatives (Liu et al., 2011). These chemical syntheses were all constrained by being multi-step and typically low-yielding, so limited the exploitation of pleuromutilin from a purely synthetic route.

1.3.4 Recent identification of pleuromutilin gene cluster

In 2016, Bailey et al. attempted to identify the genes involved in the biosynthesis of pleuromutilin (Bailey et al., 2016). Fungal diterpene pathways typically include a pathway-specific geranylgeranyl pyrophosphate synthetase (GGS), so their study looked to isolate such genes by PCR and identify which was the best candidate for pleuromutilin synthesis. Northern blots performed on RNA extracted from the fungus grown under production and repression conditions identified a GGS whose expression was consistent with pleuromutilin production and sequencing the surrounding genomic region identified more candidate genes as being part of the cluster. After testing gene expression levels, a cluster of seven genes appeared to be tightly co-regulated and were attributed to the gene cluster responsible for pleuromutilin biosynthesis. The cluster is composed of 3 cytochrome P450 genes (*p450-1*,*-2*,*-3*), an acetyltransferase (*atf*) and terpene cyclase (*cyc*) gene, a geranylgeranyl pyrophosphate synthase (*ggpps*) and a short-chain dehydrogenase/reductase (*sdr*) gene (Figure 1.5 A). The link between those genes and pleuromutilin production was proved by a gene silencing approach, where silence of *ggpps* or *cyc* led to an 87% reduction of pleuromutilin titre and a direct decline in bacterial clearing zones. It is also noteworthy that gene silencing of an individual gene from the cluster generated downregulation of all other cluster genes.

One year later, Yamane et al., (2017) characterised all of the biosynthetic intermediates of pleuromutilin pathway and through draft-genome sequencing of the closely related strain *C. pseudo-pinsitus,* they reported an identical gene organisation to that of Bailey et al., 2016. In summary, in order to propose the detailed pathway of pleuromutilin and characterize the function of all enzymes of the

pathway they conducted in vitro enzymatic reactions using a diterpene synthase, and in vivo synthesis by heterologous expression in *A. oryzae* (Figure 1.5 B).

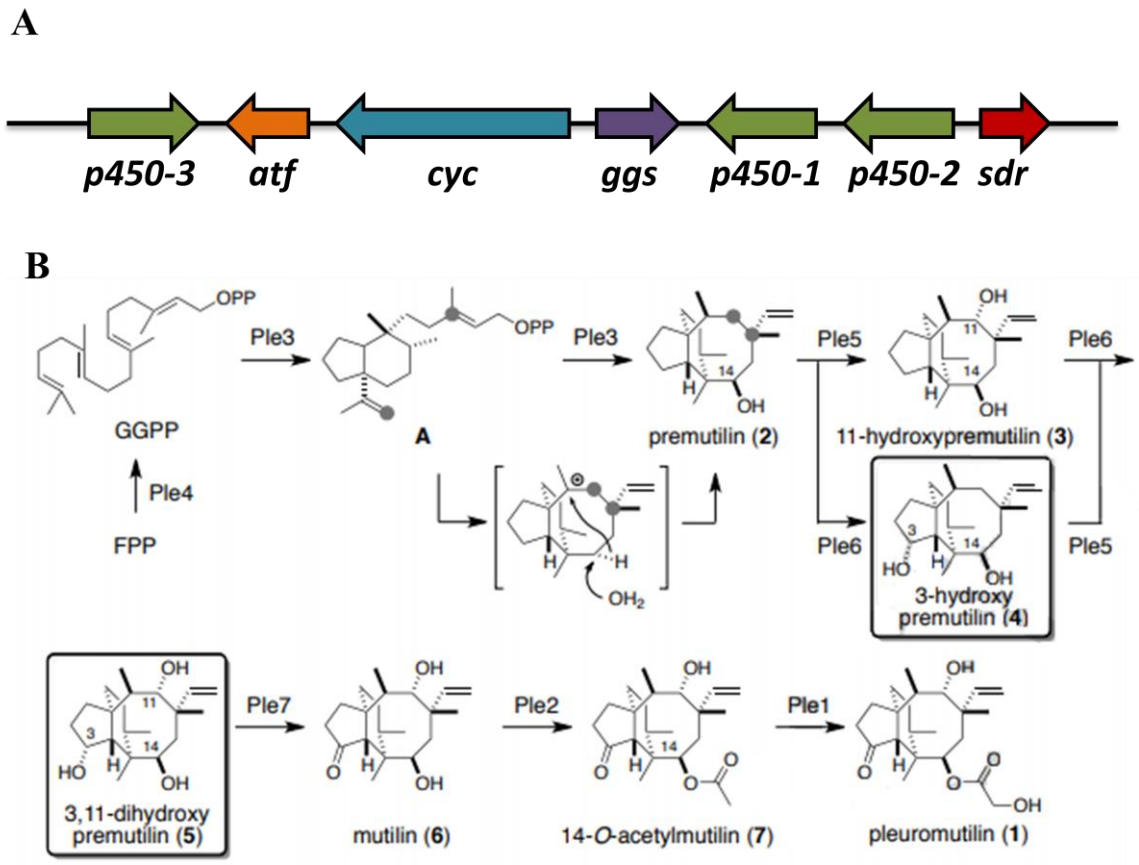

Figure 1.5 (A) Pleuromutilin BGC: *ggs*, GGPP synthase gene; *cyc*, terpene synthase gene; *p450-1*,-*2*,-*3*, cytochrome P450s genes; *sdr*, short-chain dehydrogenase gene; *atf*, acetyltransferase gene (Bailey et al., 2016). **(B) Proposed biosynthetic pathway of pleuromutilin** (1) (Yamane et al., 2017); GGPP, geranylgeranyl diphosphate; ggs/ ple4, GGPP synthase; cyc/ ple3, terpene synthase; p450-1,2,3/ ple1, ple5, and ple6, cytochrome P450s; sdr/ ple7, short-chain dehydrogenase/ reductase; atf/ ple2, acetyltransferase.

However, the proof-of-principle for gene function was accomplished by conducting stepwise heterologous expression in *A. oryzae*, which resulted to detailed structural elucidation of the pleuromutilin pathway intermediates (Figure 1.6) (Alberti, et al., 2017).

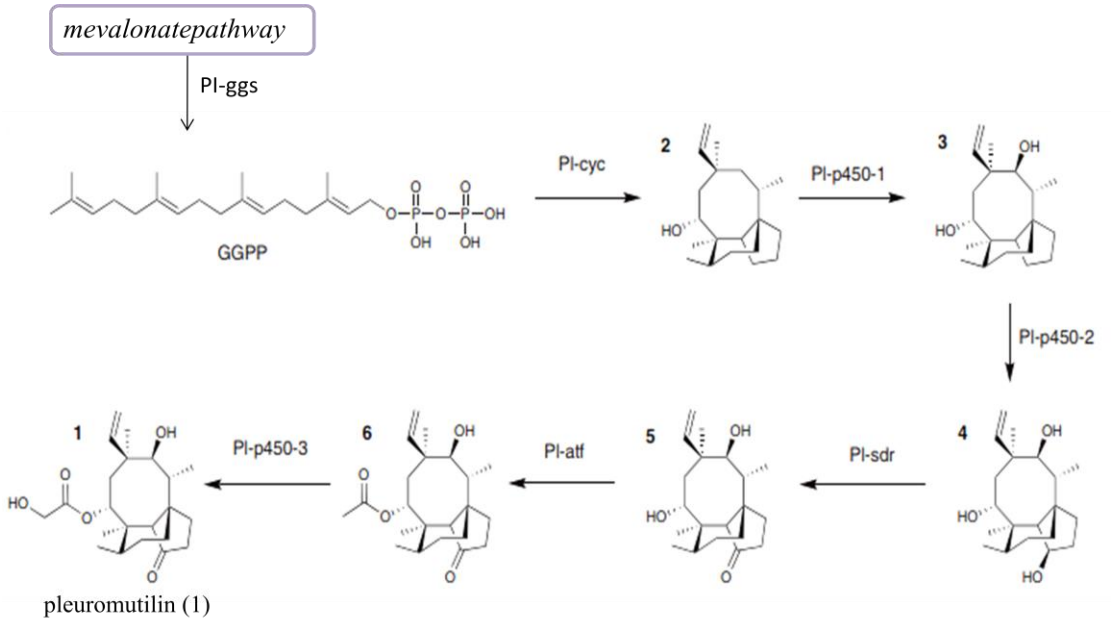

Figure 1.6 Proposed biosynthetic pathway of pleuromutilin (Alberti, et al., 2017); GGPP, geranylgeranyl diphosphate; ggs, GGPP synthase; cyc, terpene synthase; p450-1, 2, 3, cytochrome P450s; sdr, short-chain dehydrogenase/reductase; atf, acetyltransferase.

1.3.5 Enhancement of pleuromutilin production

1.3.5.1 Attempted overexpression in the native host *C. passeckerianus*

Experimental overexpression of the putative gene cluster was carried out in the native host *C. passeckerianus* using either native promoters or the constitutive promoter gpdII from *Agaricus bisporus.* However, in both cases not only there was no significant increase in pleuromutilin production but also often reduced or no bacterial clearing zones were observed, thus proving a complete loss of antibacterial activity, likely indicating a type of endogenous sense-suppression in *C. passeckerianus* (Bailey et al., 2016). As a final attempt, the whole putative gene cluster along with the neighboring genes was expressed in the native host, thus

revealing that only 16 out of 119 transformants showed a 20-40% increase in clearing zone diameter.

1.3.5.2 Successful heterologous expression in *Aspergillus oryzae*

Heterologous expression of the putative pleuromutilin gene cluster from a basidiomycete (*C. passeckerianus*) to an ascomycete (*A. oryzae*) and successful *de novo* production of pleuromutilin were first accomplished by Bailey and co-workers (Bailey et al., 2016). In this study, every transformant that successfully expressed all seven genes of the cluster resulted in expansion of the clearing zone, thus confirming the production and secretion of an antibacterial compound. HPLC-MS analyses demonstrated a considerable increase of 2,016% in pleuromutilin production, but the yield was still very limited for pharmaceutical purposes (Alberti et al., 2017). According to the study, this poor yield might due to the use of the enolase promoter used for the genes cyclase, p450-1 and short-chain dehydrogenase.

1.3.6 Pleuromutilin derivatives and clinical potential

All of the pleuromutilin derivatives used in veterinary and human medicine have modifications in the C14 side chain, where some of the analogues consist of carbamate or acyl carbamate linkers (Figure 1.7). It is worth mentioning that only the sulfanylacetyl derivatives were successful in proceeding to clinical trials (Goethe et al., 2018). Tiamulin and valnemulin were the first pleuromutilin derivatives used for veterinary purposes, being active against a broad spectrum of Gram-positive bacteria (Poulsen et al., 2001). Moreover, the approval of retapamulin in 2007 for the treatment of methicillin-resistant *Staphylococcus aureus* (MRSA) infections (Jones et al., 2006) and the development of lefamulin for the treatment of community-acquired bacterial pneumonia (CARB), which has been recently approved by the Food and Drug Administration (FDA) for human oral and intravenous use, pave the way for

more studies in the field (File et al., 2019). The lefamulin C14 side chain contains a thioether bond that increases its solubility and metabolic stability, which promotes the oral and intravenous use. This side chain also eliminates resistance development by increasing the number of hydrogen bonds to the target (Veve, 2018).

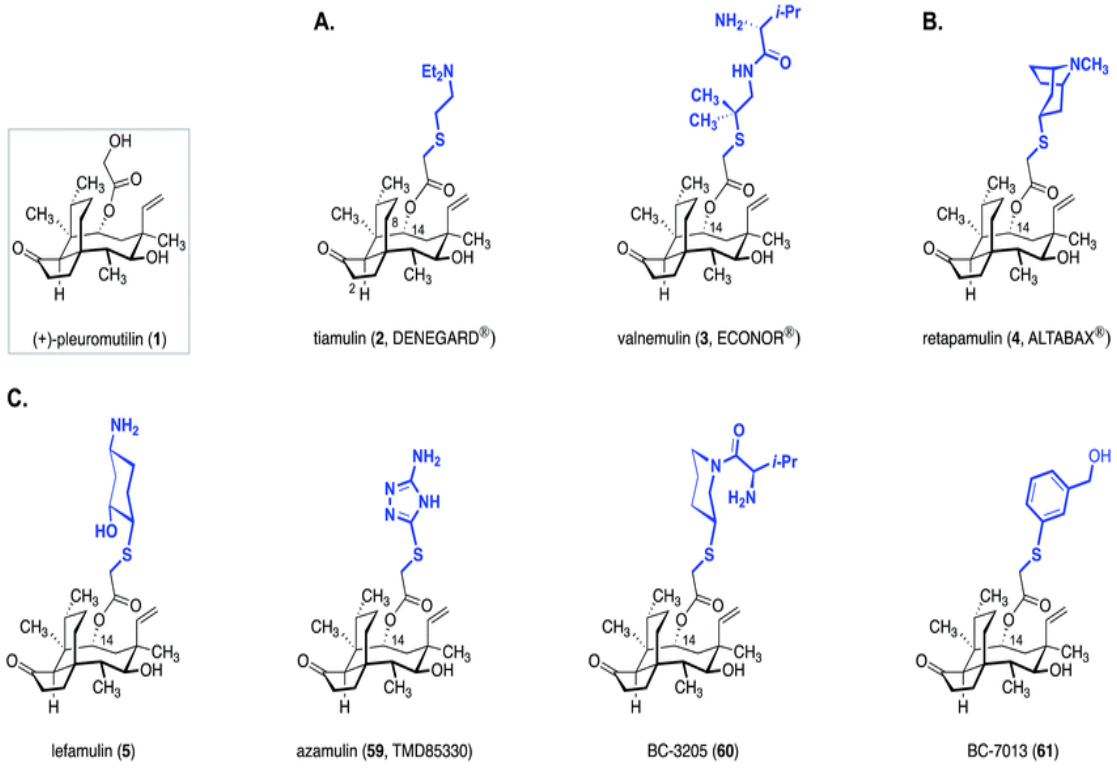

Figure 1.7 Clinical and pre-clinical pleuromutilins (1): **(A)** Veterinary antibiotics tiamulin (2) and valnemulin (3), **(B)** Retapamulin (4): human topical, short-term treatment for skin and soft tissue infections, **(C)** Lefamulin (5): human systemic use for various clinical conditions including community acquired bacterial pneumonia (CARB), pre-clinical agents azamulin (59), BC-3205 (60) and BC-7013 (61) (Goethe et al., 2018).

1.4 Plants as biosynthetic machinery for secondary metabolites

When it comes to heterologous hosts, plants have several benefits that make them a preferable expression platform. In order to grow, they simply require water, carbon dioxide, inorganic nutrients and light rather than expensive culture media. They will grow on a field-scale with conventional farming equipment rather than needing specialist facilities such as fermentors so are ideal for use in developing countries as well as those with more developed biotech industries. The challenges in finding the ideal host for heterologous production are numerous, including fine-tuning of expression levels, delivering cofactors, precursors and obtaining the desired post-translational modifications (Smanski et al., 2017).

1.4.1 A moss-based expression platform

Mosses belong to the bryophyte sister lineage of vascular plants, sharing many gene families with *Arabidopsis* but with less redundancy (Ishizaki, 2017). The dominant phase of moss lifecycle is haploid (gametophytic), like in algae, while the dominant phase in all seed plants is at least diploid (sporophytic) (Figure 1.8; Reski et al., 2015). The moss *Physcomitrella patens* is a well-established model organism, with a fully sequenced genome and efficient homologous recombination, making it an attractive biotechnological candidate. Due to the dominant haploid lifecycle, backcrossing for establishment of homozygous transgenic lines is not necessary. As a photosynthetic organism, its subcellular compartments can create tailored microenvironments. It is able to grow in large-scale liquid culture, while ensuring homogeneity and reproducibility of production. The simple terpenoid profile means it has fairly a clean metabolic background, although *P. patens* produces large quantities

of endogenous diterpenes (Khairul Ikram et al., 2017; King et al., 2016). For this reason, *Physcomitrella* has been used as a production host for commercial diterpenoids, such as taxadiene and sesquiterpenoids like the anti-malarial drug artemisinin. In addition to simple metabolites, mosses display a diverse engineering platform with applications in pharmaceutical protein production, biomimetics for regenerative medicine and indeed in modifying extreme environments for halting greenhouse gas emissions (Decker & Reski, 2020).

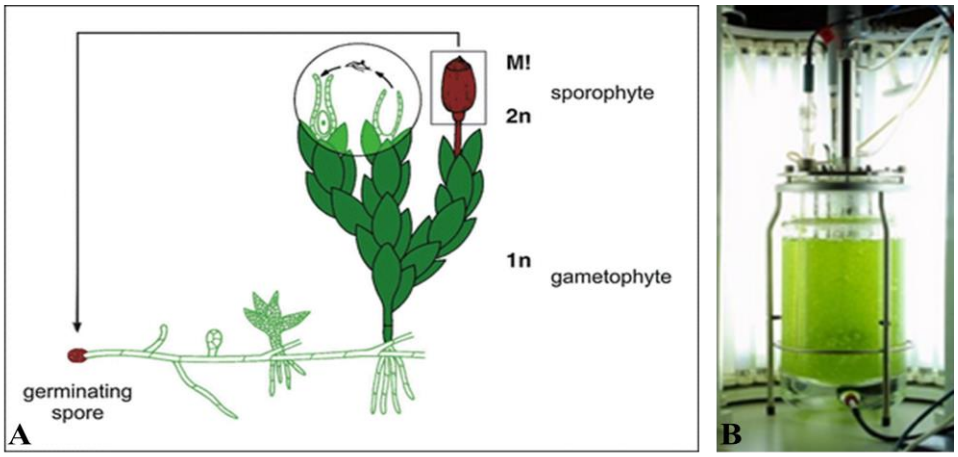

Figure 1.8 ***Physcomitrella patens*** **(A)** life cycle, where development starts from the haploid spore, which forms protonema, a tip growing filamentous tissue. During the juvenile-to-adult transition of the moss gametophyte, the protonema forms buds which contain a three-faced apical meristematic cell (Harrison et al. 2009) able to generate the leafy gametophore. Within several weeks of inducing conditions (15 °C short day), male and female sexual organs are produced and an example of **(B)** a stirred tank photobioreactor for small-scale production (Decker & Reski, 2020; Harrison et al., 2009; Müller et al., 2016).

1.4.1.1 Methods and approaches in moss genetic engineering

The high rate of accurate gene targeting (GT) via homologous recombination is a clear benefit for engineering of moss compared to similar approaches in seed plants (Reski et al., 2015). Furthermore, base-specific genome modifications are

relatively easy to obtain and production of fusion proteins is possible (Mosquna et al., 2009; Mueller et al., 2014), along with down-regulation of native gene expression via synthetic microRNAs (Khraiwesh et al., 2008; Reski et al., 2018). In addition, *in planta* assembly of gene constructs was accomplished in the same moss (King et al., 2016), an approach initially established in *Saccharomyces cerevisiae* (Gibson, 2009). An additional benefit is that the rescue of episomally replicating DNA is also possible in *P. patens* (Murén et al., 2009), making it easy to manipulate and exploit as a synthetic biology platform. These results showed the possibility of integrating megabase extended gene constructs into the moss genome, an important tool of synthetic biology so far only known from yeast. Advancement of protocols for culture media, protoplast isolation and regeneration, and for PEG-mediated transformation, enables the incorporation of multiple different genes in a single experiment (Hohe et al., 2004; Hohe & Reski, 2002; Reski et al., 2018).

Development of auxotrophic moss mutants led the way for new selection markers (Ulfstedt et al., 2017) and these facilitate multiple rounds of transformation. Transgene expression methods in moss use various promoter elements, such as endogenous, bacterial and seed plant promoters (Holtorf et al., 2002; Jost et al., 2005; Reutter et al., 1998). The combination of suitable promoters enables regulated gene expression control, (Horstmann et al., 2004), induced either by temperature, chemicals or red light (Kubo et al., 2013; K. Müller et al., 2014; Saidi et al., 2005).

Elements important for transcription, translation or secretion used in *P. patens* were first established and optimised for recombinant protein production in CHO cells (Gitzinger et al., 2009). Recent studies reveal that artificial promoters can be an excellent option for the expression of multiple genes (Peramuna et al., 2018). Synthetic promoters have relatively short sizes but possess sufficient activity.

Moreover, recombinant proteins can directly be secreted through the ER to the medium where *P. patens* grows by utilizing endogenous signal sequences (Schaaf et al., 2005). As an alternative, there is a case where the product is integrated into the cell membrane, thus giving to this moss extracellular catalytic or binding properties (Morath et al., 2014).

Although plants reveal a high consistency of N-glycosylation throughout tissues and across species, the basic structure of N-glycosylation is conserved between humans and plants (Bosch et al., 2013). Where glycosylation was inappropriate, genes that encoded plant-derived glycosyltransferases have been identified and eliminated from the moss (Koprivova et al., 2004; Parsons et al., 2012). A different approach involved a moss mutant with the ultimate aim to ‘‘humanise’’ glycosylation in moss by expressing human beta-1,4-galactosyltransferase (Huether et al., 2005).

1.4.2 Liverworts in biotechnology

Liverworts, along with mosses and hornworts, belong to the non-vascular group of bryophytes. The dominant form of their development is a gametophyte thallus that is haploid and dioecious, while they can propagate both sexually and asexually through vegetative propagules, called gemmae (Figure 1.9) (Kubota et al., 2013). The majority of secondary metabolites found in liverworts are lipophilic mono-, sesqui-, diterpenoids, aromatic compounds and acetogenins, however nitrogen- and sulfur-containing compounds are very rare. The most characteristic feature of their chemical diversity is that most of sesqui- and diterpenoids are enantiomers of those found in higher plants (Adam & Becker, 1993; Asakawa & Ludwiczuk, 2013; Asakawa et al., 2013). Interestingly, Marchantin A, the first characterized cyclic

bis(bibenzyls) from *Marchantia polymorpha* has pharmacological potential, showing anticancer, antifungal, antimicrobial, antioxidant and muscle relaxing activity (Gaweł-Bęben et al., 2019; Jantwal et al., 2019; Takahashi & Asakawa, 2017). The liverwort *M. polymorpha* has been extensively studied, mainly to address the evolution of land plants and gene function. However, it was also used as the first plant platform for prostaglandin production, since it accumulates the substrate arachidonic acid, by introducing a cyclooxygenase gene into the *M. polymorpha* genome from the red alga, *Gracilaria vermiculophylla* (Takemura et al., 2013).

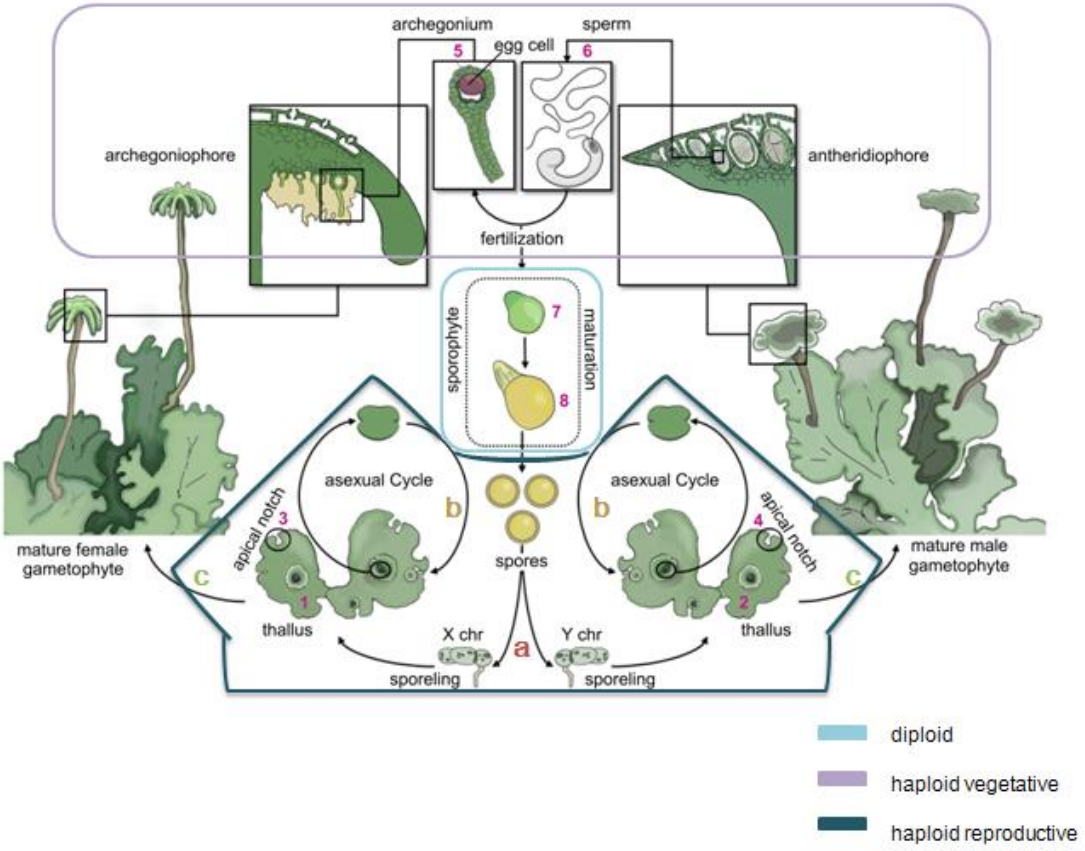

Figure 1.9 Life cycle of *Marchantia polymorpha*. A haploid spore germinates and develops into a thallus. A group of cells developing from a spore is called a sporeling. Under white light a sporeling grows into a sphere-like cell mass (**a.** germination/ high R light). A thallus is a multilayered gametophyte body with dorsoventrality that has a growing point at the apical notch of each lobe, which undergoes periodical bifurcations. In the vegetative growth phase, dozens of clonal progeny, gemmae,

are produced in gemma-cups, which are formed repeatedly on the dorsal side of a thallus. After dispersion and water uptake, each gemma develops into an individual thallus (**b.** vegetative propagation/ gemma to gemmaling). *M. polymorpha* transits from vegetative to reproductive growth under a long-day condition supplemented with far-red light (FR), and develops gametangiophores on the thallus (**c.** transition to reproductive growth phase/ FR light). The male gametangiophore is called an antheridiophore and contains antheridia, and the female gametangiophore is called an archegoniophore and has archegonia. Sperm released into water swim up the neck of the archegonium and fertilize the eggs. The zygote undergoes mitotic divisions, and develops into a multicellular diploid sporophyte. Nutrients are supplied to the developing sporophyte from the surrounding gametophyte tissues. Meiosis occurs inside the sporangium, and hundreds of thousands of haploid spores are produced per sporangium (Ishizaki et al., 2016; adapted from Schmid et al., 2018).

1.4.2.1 Tools and techniques for *Marchantia* research

Given the haploid nature of *M. polymorpha*, genetically homogeneous lines can be established easily. Most characterized gene regulatory elements are common between *Marchantia* and higher plants like angiosperms, while gene families are sparsely populated (Bowman et al., 2017). Whole-genome analysis proves that genes responsible for growth and development are conserved but with low redundancy in *M. polymorpha* (Ishizaki et al., 2016).

M. polymorpha can reproduce both sexually and asexually and for this reason various transformation techniques have been established. Physical DNA delivery via particle bombardment to the nuclear genome was achieved using 2-week old thalli grown from gemmae (Takenaka et al., 2000). *Agrobacterium*-mediated genetic transformation, which is now the most common technique, can generate transgenic plants using sporelings, mature thalli, intact male and female gemmae or regenerating thalli derived from either sex, giving isogenic lines in four to six weeks (Kubota et al., 2013; Tsuboyama & Kodama, 2018). Furthermore, plastid transformation is available

for suspension-cultured cells and sporelings. It is worth mentioning that despite multiple plastid genome copies, homoplasmic transformants of thalli can be obtained immediately after primary selection from sporelings and after 12-16 weeks of repeated subculture from suspension-cultured cells (Chiyoda et al., 2007; Chiyoda et al., 2014).

Although homologous recombination is highly efficient in *P. patens*, gene targeting in this manner is difficult in *M. polymorpha*. While using haploid tissue is theoretically impossible to produce knockout plants for essential genes, conditional gene knockout strategies have been established. Nishihama et al., (2015) created a heat- and dexamethasone-controllable gene expression/deletion system by using a promoter of a heat-shock protein (HSP) gene and the Cre/*lox* P site-specific recombination system. Alternatively, artificial microRNA-mediated knockdown was successfully established, using both endogenous and heterologous primary microRNA (pri-miR) hairpin backbones (Flores-Sandoval et al., 2015). Two different Transcription Activator-Like Effector Nuclease (TALEN) techniques were conducted, using custom and self-assembled TALEN constructs, with both approaches being successful in yielding high efficiencies of over 20% (Kopischke et al., 2017). Moreover, Clustered Regularly Interspaced Short Palindromic Repeat/CRISPR-associated protein 9 (CRISPR-Cas9) technology has been used in *M. polymorpha* using *Arabidopsis*-codon-optimized Cas9 (Sugano et al., 2018).

Recently, Sauret-Güeto et al., (2020) developed the type II OpenPlant toolkit which includes vectors for nuclear and chloroplasts transformation, and for CRISPR genome editing, along with a collection of standardized DNA basic parts for expression in *Marchantia***,** including antibiotic resistance genes, signal peptides, fluorescent proteins for multispectral imaging and promoters for gene expression

(Figure 1.10). Also, they include techniques for high-throughput microscopic imaging of multiple *Marchantia* lines, where gemmae are cultured in multiwell plates.

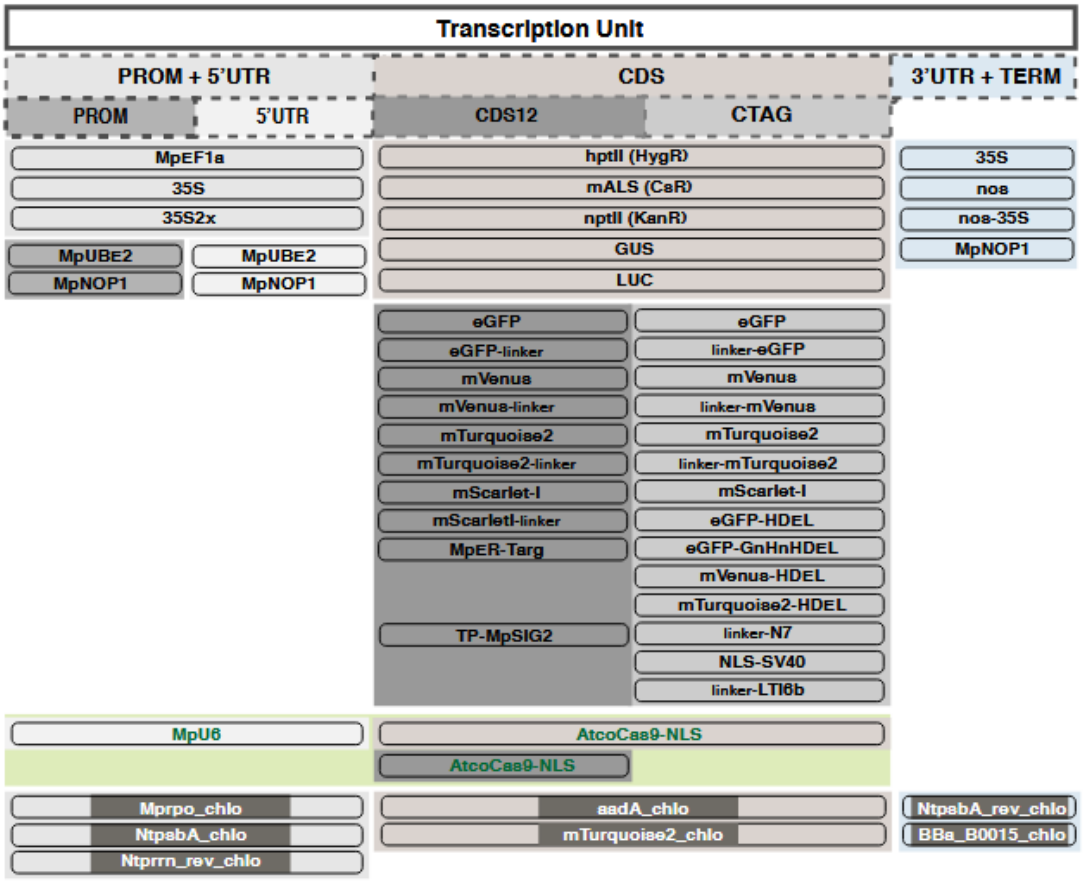

Figure 1.10 Basic (Level 0) DNA parts in the OpenPlant toolkit. The OpenPlant kit contains: promoters with 5' UTR (PROM5), promoters (PROM) and 5' untranslated region (5UTR); coding sequences with start and stop codons (CDS), and for N-terminal (CTAG) and C-terminal (CDS12) protein fusions, and 3' UTR with terminator (3TERM). The OpenPlant toolkit contains 50 basic parts, 43 for nuclear transformation, 3 for CRISPR-Cas9 genome editing (in green), and 7 for chloroplast transformation (name_chlo) (Sauret-Güeto et al., 2020).

1.4.3 *Nicotiana* species for biopharmaceutical production

The cultivated tobacco *Nicotiana tabacum* is the main source for nicotine, given that other plants containing nicotine and nicotine-like alkaloids appear to be toxic for human use (San Andrés Larrea et al., 2014). *N. tabacum* cells are the most frequent plant suspension cells used in biotechnology, grown in stirred tanks and bioreactors, since transformation methods and propagation are simple and reproducible (Wuest et al., 2011). Cell suspensions can be transformed with recombinant plasmids either by co-cultivation with *A. tumefaciens* or particle bombardment (Hellwig et al., 2004). Genetic transformation strategies like CRISPR/Cas9 and TALEN have been also successful (Gao et al., 2015; Y. Zhang et al., 2013). *N. benthamiana* is often used for transient expression, while *N. tabacum* is typically used for production of stable transgenic plants, a procedure that requires a longer period of development (Garabagi et al., 2012). Various valuable therapeutic and diagnostic proteins have been produced in *Nicotiana* plants, including secondary metabolites (Reed & Osbourn, 2018; Bo Wang et al., 2016), enzymes (Kytidou et al., 2017; Vardakou et al., 2012), viral antigens and antibodies (Blokhina et al., 2020; Garabagi et al., 2012; Pang et al., 2019).

1.5 Aims of this project

This project aimed to evaluate the available expression platforms to allow complex multigene expression in various plants. As previously described, the plant hosts that were chosen for this project was *Physcomitrella patens*, *Marchantia polymorpha* and *Nicotiana tabacum*. Prior to transformation it was essential to assess the host plants for sensitivity and/or resistance to mutilins. *P. patens* and *M. polymorpha* were screened due to the stable transformation approach for these plants. Furthermore, in order to express the pleuromutilin pathway in these hosts the appropriate constructs were designed and built to be functional in the different plant chassis. After successful transformation of *M. polymorpha* and transient expression in tobacco, the results of heterologous expression were evaluated by chemical analysis.

Chapter 2: Materials and Methods

2.1 Laboratory supplies

Chemical reagents were purchased from Sigma-Aldrich, Fisher, Honeywell, Acrôs Organics, VWR, Formedium and Merck. Laboratory consumables and glassware were used from Fisher, VWR and Sarstedt, while primers used were supplied from Integrated DNA technologies. DNA ladder, enzymes and buffers derive from New England BioLabs and Thermo. All solutions and media were prepared in deionised water. All solutions, media and glassware were autoclaved at 121°C for 15 minutes unless otherwise stated.

2.2 Species used in this project

2.2.1 Bacterial Species, growth and maintenance

The *Escherichia coli* strain used for plasmid transformation and propagation was *TOP10*. The *Agrobacterium tumefaciens* strain LBA4404 was used for stable or transient transformation methods for *Marchantia polymorpha* and *Nicotiana tabacum*, respectively. Solid and liquid media were autoclaved at 121°C for 15 minutes and allowed to cool to approximately 50°C before adding the appropriate antibiotics or selection reagents (Table 2.1). Agar-based media were poured into sterile 90mm Petri dishes, left to solidify under sterile laminar air flow and stored at 4°C until use. Plates and liquid cultures containing transformed cells were then stored at 4°C until screening and verification via DNA sequencing.

E. coli were grown overnight at 37°C on LB agar (LB Agar Lennox, Tryptone 10g/l, Yeast Extract 5g/l, NaCl 5g/l, agar 15g/l). Liquid cultures were grown with additional agitation at 200rpm (LB Broth Lennox, Tryptone 10g/l, Yeast Extract 5g/l, NaCl 5g/l). All cultures were supplemented with appropriate antibiotics prepared as shown in Table 2.1. Aliquots of liquid cultures of the correct transformed clones were stored in 20% glycerol and kept at -80°C.

A. tumefaciens strain LBA4404 cells were grown for 2-3 days at 28°C, with agitation at 200rpm for liquid cultures, on YM agar or YM broth (Mannitol 10g/l, Yeast Extract 0.4g/l, K_2HPO_4 0.5g/l, NaCl 0.1g/l, $MgSO_4$ $7H_2O$ 0.2g/l, for plates: agar 15g/l), supplemented with appropriate antibiotics as shown in Table 2.1. Aliquots of liquid cultures of the correct transformed clones were stored in 20% glycerol and kept at -80°C.

Table 2.1 Antibiotics used for *E. coli* and *A. tumefaciens* cells.

Organism	Antibiotic/Reagent	Stock Concentration	Dissolve in	Working Concentration
E. coli	Ampicillin	100mg/ml	H_2O	100µg/ml
	Carbenicillin*	50mg/ml	H_2O	100µg/ml
	Kanamycin	50mg/ml	H_2O	50µg/ml
	Spectinomycin	40mg/ml	H_2O	80µg/ml
	X-gal	20mg/ml	DMF	20µg/ml
	IPTG	100mM	H_2O	100µM
A. tumefaciens	Ampicillin	100mg/ml	H_2O	100µg/ml
	Carbenicillin	50mg/ml	H_2O	75µg/ml
	Kanamycin	50mg/ml	H_2O	50µg/ml
	Rifampicin	20mg/ml	MeOH	20µg/ml
	Spectinomycin	40mg/ml	H_2O	250µg/ml

Streptomycin	100 mg/ml	H_2O	100 μg/ml
Acetosyringone	0.1M	DMSO	20-100μM

*carbenicillin can replace ampicillin, as it is more chemically stable

2.2.2 Plant Species, growth and propagation

The moss *Physcomitrella patens WT04* line and the liverwort *Marchantia polymorpha Tak-1* line (or *Takaragaike-1* line, male line) were used for the establishment of stable transformants, while *Nicotiana tabacum SR1* line was used for transient expression experiments. Both *P. patens* and *M. polymorpha* were given by Dr Jill Harrison and *N. tabacum* was provided approximately 4-week old by the Life Sciences Building greenhouse facility. Plant media were autoclaved at 121°C for 15 minutes and allowed to cool to approximately 50°C before adding the appropriate antibiotics or supplements. Agar plates were poured into sterile square 100x100x20mm (Sarstedt, Australia) or 25 compartments (Thermo Fisher Scientific, UK) Petri dishes, left to solidify under laminar flow hood and stored at 4°C until use.

When using plates for propagation, antibiotic treatment assays, PEG-mediated transformation in *P. patens* or during selection, Petri dishes were sealed with 3M Micropore® surgical tape. *P. patens* grew on BCD-AT medium, and *M. polymorpha* on half-strength Gamborg's B5 (Table 2.2), both in a 22°C growth chamber under continuous light and 40% Relative Humidity. *P. patens* can be propagated by subculturing any kind of tissue (e.g. protonemata, leaves) using forceps, while *M. polymorpha* by carefully transferring gemmae into new agar plates using a disposable pipette tip.

Table 2.2 Plant media for *P. patens* and *M. polymorpha.*

Organism	Media	
P.patens	BCD-AT	Stock solutions B, C, D, AT 10ml/l 1x TES 1ml/l, 1M $CaCl_2$ 1ml/l * Plant agar 8g/l <u>Stock solutions*:</u> **B**: $MgSO_4.7H_2O$ 25g/l **C**: KH_2PO_4 12.5g/l pH 6.5 with KOH **D**: KNO_3 101g/l, $FeSO_4.7H_2O$ 1.25g/l 0.5M **AT**: di-ammonium (+) tartrate 92g/l 20x trace elements solution (**TES**): H_3BO_3 12.28g/l, $MnCl_2.4H_2O$ 7.78g/l, $AlK(SO_4)_2.12H_2O$ 1.1g/l, $CuSO_4.5H_2O$ 1.1g/l, $CoCl_2.6H_2O$ 1.1g/l, $ZnSO_4.7H_2O$ 1.1g/l, KBr 0.56g/l, LiCl 0.56g/l, KI 0.56g/l, $SnCl_2.2H_2O$ 0.56g/l
M. polymorpha	Half-strength Gamborg's B5 supplemented with 1% (w/v) sucrose	Gamborg's B5 Basal Salt Mixture (Sigma®)1.5g/l Sucrose 10g/l Plant agar 8g/l pH 5.8 with KOH

*$CaCl_2$ and all stock solutions were filter sterilised and added to the autoclaved plant agar after cooling to 50°C.

2.3 Antibiotic treatment assays

Both *P. patens* and *M. polymorpha* were grown using media described previously, and these were supplemented with dilution series of antibiotics that cover

a wide range of mechanisms of action, including pleuromutilin derivative, tiamulin, and mutilin. Denagard® (tiamulin hydrogen fumarate) was used as a semi-synthetic antibiotic belonging to the pleuromutilin group of antibiotics, while mutilin was organically synthesized by the PhD student Jonathan Davies from the School of Chemistry, University of Bristol. Plant media were supplemented with all of the antibiotics listed in Table 2.3 at concentrations of: 0µg/ml (untreated), 1µg/ml, 5µg/ml, 10µg/ml, 50µg/ml, 100µg/ml, 200µg/ml, 250µg/ml and 500µg/ml.

Table 2.3 Antibiotics used for toxicity tests for *P. patens* and *M. polymorpha*

Mechanism of action	Class	Antibiotic	Stock Concentration
Cell wall synthesis inhibition - transpeptidase inhibition	Aminopenicillins	Ampicillin	100mg/ml in dH_2O
Protein synthesis inhibition – interaction with 30S ribosomal unit	Aminoglycosides	Kanamycin	50mg/ml in dH_2O
Protein synthesis inhibition – interaction with 50S ribosomal unit or peptidyl-transferase inhibition	Chloramphenicol	Chloramphenicol	20mg/ml in EtOH
	Pleuromutilins	Tiamulin, mutilin	125mg/ml in EtOH
DNA synthesis inhibition	1st generation	Nalidixic acid	30mg/ml in 1N NaOH

2.4 Construction of plasmids

The plasmids were assembled using the MoCloPlantToolkit (Addgene Kit #1000000044) and the Golden Gate Plant Parts Kit (Addgene Kit #1000000047), which contain a collection of 95 empty standardized vectors and 95 standardized plant parts, respectively, facilitating the design of multigene constructs for plant transformation (Engler et al., 2014; Marillonnet & Werner, 2015; Weber et al., 2011; Werner et al., 2012).

2.4.1 Modular Cloning (MoClo) using the Golden Gate® assembly

Golden Gate assembly uses type II restriction enzymes, such as *Bsa*I (Eco31I, Thermo Scientific, UK) and *Bpi*I (*Bbs*I, Thermo Scientific, UK) which cleave outside of their recognition sequence, leaving unique four-base flanking overhangs. Since recognition sites are located outside of the cleavage sites, after the digestion-ligation reactions these sites are eliminated, leading to directional, scarless cloning. In order to avoid undesired digestion, the recognition sites must not be present within the fragments that need to be assembled. This can be accomplished through PCR-amplification of the fragments by using overlapping primers that introduce a single nucleotide mismatch at the *Bsa*I/*Bpi*I recognition sites. The domestication of the seven genes of the pleuromutilin gene cluster and of the plant selectable marker *nptII*, encoding an aminoglycoside phosphotransferase, which confers resistance to kanamycin, neomycin and Geneticin® G418, was performed by the PhD student Suphattra Sangmalee and the coding sequences of all seven genes of pleuromutilin pathway and *nptII* gene were provided in the Level zero form. Later in this project, the *nptII* gene was amplified from pISCL70004 plasmid (Golden Gate Plant Parts Kit, C11, $spec^R$) and correctly cloned into the Level zero acceptor for CDS1 modules pICH41308 (MoClo Plant Tool Kit, H2, $spec^R$).

2.4.2 Level generations

The initial step of designing the complete multigene construct was planning the final form and the assembly strategy (Figure 2.1). This includes the final position and orientation of each transcription unit. Up to six transcription units can be cloned in a Level 2 construct at once, because no *Bsa*I/*Bpi*I sites are left after using one of the basic pELE-n end-linkers.

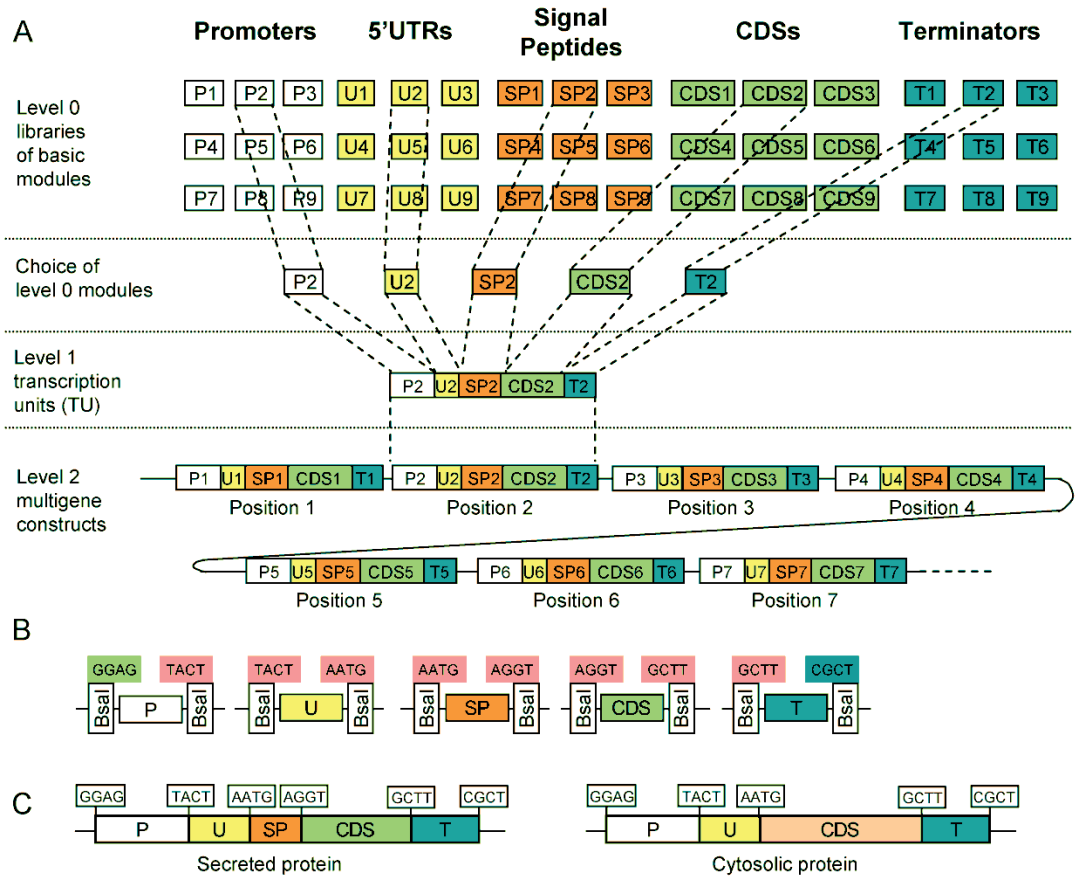

Figure 2.1 Hierarchy of the modular cloning system. (A) Standard parts (Level 0) of promoters (P), 5' untranslated regions (U), signal peptides (SP), coding sequences (CDS) and terminators (T), which are further assembled to form a Level 1 transcription unit and finally multigene constructs. **(B)** Flanking sites of each Level 0 type module. **(C)** Example of two different transcription units encoding a secreted and a cytosolic protein, respectively (Weber et al., 2011).

2.4.2.1 Level -1

The purpose of a universal Level -1 (e.g. pAGM1311, MoClo Plant Tool Kit, A1, kan^R) is to simplify the cloning of large Level 0 modules, while removing any internal *Bsa*I/ *Bpi*I sites. For smaller fragments, sequence domestication can be performed at Level 0.

2.4.2.2 Level 0

Level 0 plasmids consist of the standard parts which compose a transcription unit. These parts include promoters (P), 5' untranslated regions (U), signal peptides (SP), coding sequences (CDS) and terminators (T). Level 0 destination vectors allow blue/ white selection, encoded by a *lacZ* gene and enabling *E. coli* to be resistant to Spectinomycin ($spec^R$). The MoClo Plant Tool Kit provides a series of different destination vectors according to the specific module type (e.g. promoters, coding sequences, terminators). The primers for PCR-amplified sequences were designed with a flanking overhang containing the *Bsa*I or *Bpi*I recognition site, following by the four unique nucleotides according to each module type. At this stage primers could be designed in a way enabling, in parallel, the removal of internal type IIS recognition sites as described above.

2.4.2.3 Level 1

Appropriate combinations of compatible sets of Level 0 modules were assembled into a complete functional transcription unit (TU), giving each Level 1 module (Figure 2.2). All Level 1 destination vectors were designed in order to provide a known position and orientation for TUs (position 1-7, forward or reverse orientation), making the customization of the final construct possible. Also, in contrast to Level 0 backbones, Level 1 cassettes harbor ampicillin/ carbenicillin resistance, while having in common a *lacZ* cassette for blue/ white selection. In order

to prevent the creation of too many Level 1 modules, the 7 destination vectors were designed to be used in a circular mode instead of a linear, by reusing the Level 1 module for position 1 at a later virtual position 8, 15, 22 etc. The special feature of Level 1 vectors is the presence of both *Bpi*I and *Bsa*I sites, in order to compose the Level 1 (TU) module using the *Bsa*I Golden Gate dig-lig reaction and leave intact the *Bpi*I sites, outside the *lac*Z fragment and the *Bsa*I sites, for a later assembly to give Level 2 multigene constructs (Figure 2.2).

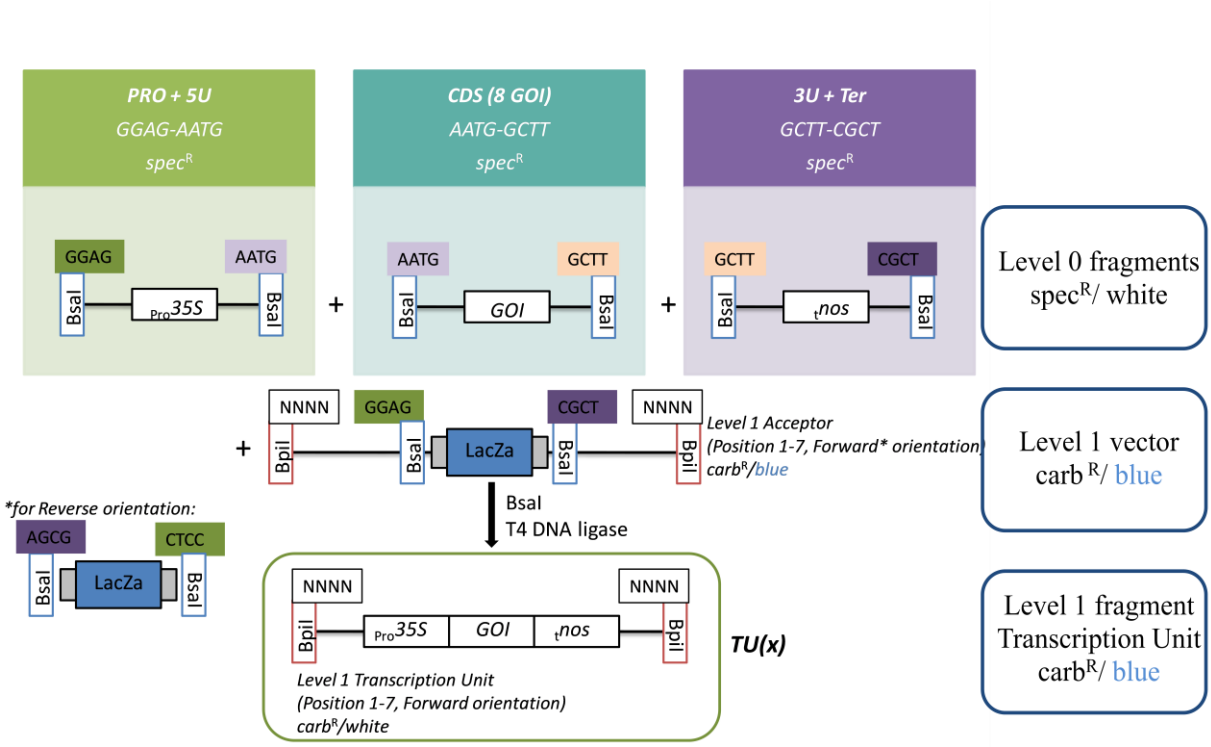

Figure 2.2 Example of a Level 1 Transcription Unit reaction with the unique 4bp overhangs for each Level 0 module. $_{Pro}$35S: 35Spromoter from *Cauliflower Mosaic Virus*, GOI: gene of interest, nos: 3'UTR, polyadenylation signal/ terminator nos (nopaline synthase) from *A. tumefaciens*.

2.4.2.4 Level 2

Separate Level 1 modules (TUs) are then assembled together into multigene constructs by using the *Bpi*I Golden Gate dig-lig reaction. All Level 2 acceptor vectors contain a red colour selectable marker (CRed, containing an artificial bacterial operon necessary for biosynthesis of b-carotene, which is visible, and its conversion

to the more visible on agar plates canthaxanthin, shown in red colour), which is flanked by two *Bpi*I sites, and a resistance gene for kanamycin (kan^R). So, in this case, instead of a blue/ white selection there is a red/ white or a red/ blue selection in relation to pELE-1 to -7 (‘‘closed’’ construct; when there are no restriction sites left to add more modules) or pELB-1 to -7 (‘’open’’ construct; when the *lac*Z cassette is flanked by two *Bsa*I sites and it is possible to add more modules) end-linker. There is also a third type of ‘’open’’ construct end-linker, the pELP-1 to -7, which enables the purple/ red selection by using the type IIS restriction enzyme, *Bsm*BI, which was not used in this project. The different end-linkers allow the colour switching while adding more and more Level 1 TUs, still using the same Level 2 backbone that confers kanamycin resistance.

2.4.2.5 Level M and Level P

Level M destination vectors ($spec^R$) and end-linkers are used for pre-assembling several Level 1 TUs, which can, then, be combined with other M Level constructs into Level P acceptor vectors (kan^R), allowing the simultaneous high-throughput creation of multigene constructs in one step (Figure 2.3).

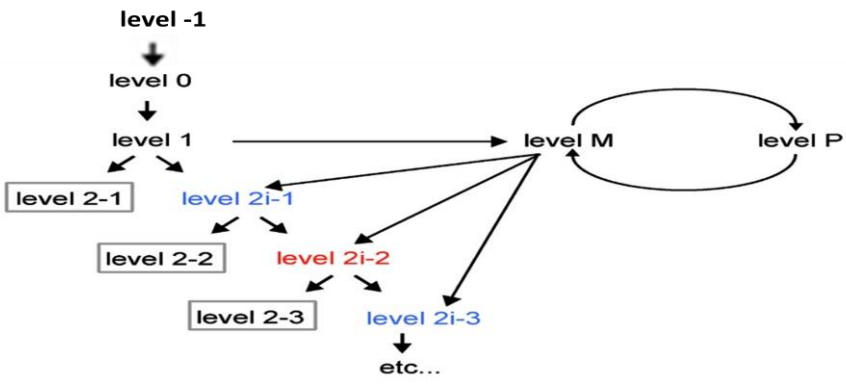

Figure 2.3 Relationship between Levels. Several Level 1 modules can be assembled into Level M, while several Level M modules can be assembled into Level P vectors. Boxes of Level 2-1, 2-2 and 2-3 indicate that they are ‘’closed’’ constructs and further assembly cannot occur (Werner et al., 2012).

2.4.3 One pot digestion-ligation reaction

One of the advantages of Golden Gate assembly is that multiple DNA fragments can be assembled in one-pot, digestion-ligation reaction (dig-lig), reducing the time required for the assembly of multigene constructs. The plasmids used from MoClo Plant Tool Kit and Golden Gate Plant Parts Kit are listed in Tables 2.4 and 2.5, respectively.

Table 2.4 List of destination and end-linker vectors used from MoClo Plant Tool Kit for Golden Gate Assembly.

MoClo Plant Tool Kit

Plate Pos.	Vector Name	Resistance	Description
H2	pICH41308	$spec^R$	Level 0 acceptor for CDS1 modules
A3	pICH41331	$spec^R$	Level 0 acceptor for complete gene modules
B3	pICH47732	$carb^R$	Level 1 acceptor. Position 1. Forward orientation
C3	pICH47742	$carb^R$	Level 1 acceptor. Position 2. Forward orientation
D3	pICH47751	$carb^R$	Level 1 acceptor. Position 3. Forward orientation
E3	pICH47761	$carb^R$	Level 1 acceptor. Position 4. Forward orientation
F3	pICH47772	$carb^R$	Level 1 acceptor. Position 5. Forward orientation
G3	pICH47781	$carb^R$	Level 1 acceptor. Position 6. Forward orientation
H3	pICH47791	$carb^R$	Level 1 acceptor. Position 7. Forward orientation
A4	pICH47802	$carb^R$	Level 1 acceptor. Position 1. Reverse orientation
H4	pAGM4673	kan^R	Level 2 acceptor
B5	pICH41722	$spec^R$	End-link 1 for assembling 1 Level 1 into Level 2 acceptor
C6	pICH49277	$carb^R$	End-link 1 for assembling 3 Level 1 into Level 2 acceptor. With lacZ acceptor site
D6	pICH49283	$carb^R$	End-link 1 for assembling 4 Level 1 into Level 2 acceptor. With lacZ acceptor site
F6	pICH49300	$carb^R$	End-link 1 for assembling 6 Level 1 into Level 2 acceptor. With lacZ acceptor site

D8	pAGM8081	spec^R	Level M acceptor. Position 6
E8	pAGM8093	spec^R	Level M acceptor. Position 7
G8	pICH50881	carb^R	Level M end-link 2
A9	pICH50900	carb^R	Level M end-link 4
B9	pICH50914	carb^R	Level M end-link 5
D9	pICH50932	carb^R	Level M end-link 7
C10	pICH75388	kan^R	Level P acceptor. Position 7
E10	pICH79264	carb^R	Level P end-link 2
B11	pICH79311	carb^R	Level P end-link 7

Table 2.5 List of Level 0 vectors (standard parts) used from Golden Gate Plant Parts Kit for Golden Gate Assembly.

Golden Gate Plant Parts Kit (All plasmid backbones harbor a gene for resistance in spectinomycin/ spec^R)

Plate Pos.	**Vector Name**	**Module name and 4bp overhangs**	**Module Description**
A3	pICH51277	GGAG_ProCaMV35SShort_5UTMV_AATG	promoter (0.4 kb), 35s (*Cauliflower Mosaic Virus*) + 5'UTR, Ω (*Tobacco Mosaic Virus*)
B3	pICH51288	GGAG_ProCaMV35SDouble_5UTMV_AATG	promoter (double), 35s (*Cauliflower Mosaic Virus*) + 5'UTR, Ω (*Tobacco Mosaic Virus*)
D3	pICH87633	GGAG_Pro-AtuNos_5U-TMV_AATG	promoter, nos, (*A.tumefaciens*) + 5'UTR, Ω (*TobaccoMosaicVirus*)
E3	pICH85281	GGAG_Pro-AtuMas_5U- AtuMas _AATG	promoter + 5'UTR, mas, (*A. tumefaciens*) + 5'UTR
F3	pICH88103	GGAG_Pro-AtuOcs_5U- AtuOcs _AATG	promoter + 5'UTR, ocs, (*A. tumefaciens*) + 5'UTR
G3	pICH87644	GGAG_Pro-AtAct2_5U-TMV_AATG	promoter, act2 (AT3G18780, *A.*

			thaliana) and 5'UTR, Ω (*Tobacco Mosaic Virus*)
C11	pICSL70004	GGAG_Pro-AtuNos_5U-TMV_CDNPT_Ter-AtuOcs_CGCT	kanamycin/neomycin/paromomycin resistance cassette (Nos promoter (*A. tumefaciens*) + n*ptII* (*E.coli*) + Ocs terminator (*A. tumefaciens*))
F11	pICH41414	GCTT_3U+Ter-CaMV35S_CGCT	3'UTR, polyadenylation signal/terminator, 35s (*Cauliflower Mosaic Virus*)
H11	pICH41421	GCTT_3U+Ter -AtuNos_CGCT	3'UTR, polyadenylationsignal/terminator, nos (*A. tumefaciens*)
D12	pICH41432	GCTT_3U+Ter -AtuOcs_CGCT	3'UTR, polyadenylation signal/terminator, ocs (*A. tumefaciens*)

The type IIS restriction enzymes *Bsa*I (*Eco*31I) and *Bpi*I (*Bbi*I), and the T4 DNA Ligase (5U/µl) were provided by Thermo Scientific, UK. PCR-amplified products were either cleaned from salts and enzymes or gel extracted before being added to the dig-lig reaction using the Nucleospin® Gel and PCR clean-up from Macherey-Nagel.

To assemble fragments into Level 2 or Level M destination vectors, *Bpi*I digestion was required, following the reaction:

Acceptor plasmid	150ng
Plasmid containing each part to be assembled	2:1 molar ratio of insert:acceptor

10 units of *Bpi*I	1µl
10x Buffer G (with 0.1 mg/ml BSA)	2µl
5 units of T4 DNA ligase (5U/µL)	1µl
10x T4 DNA Ligase Buffer	2µl
Sterile dH_2O	to 15µl
Total volume	**15µl**

To assemble fragments into Level 0, Level 1 or Level P destination vectors, *Bpi*I digestion was required, following the reaction:

Acceptor plasmid	150ng
Plasmid containing each part to be assembled	2:1 molar ratio of insert:acceptor
10 units of *Bpi*I	1µl
10x Buffer G (with 0.1 mg/ml BSA)	2µl
5 units of T4 DNA ligase(5U/µL)	5µl
10X T4 DNA Ligase Buffer	2µl
Sterile dH_2O	to 15µl
Total volume	**15µl**

To assemble fragments into Level 2i (‘’open’’ construct) with a *lac*Z end-linker, digestion with both enzymes, *Bsa*I and *Bpi*I, were required, following the reaction:

Acceptor plasmid	150ng
Plasmid containing each part to be assembled	2:1 molar ratio ofinsert:acceptor
12.5 units of *Bpi*I	1.25µl

7.5 units of *Bsa*I	0.75µl
10x Buffer G (with 0.1 mg/ml BSA)	2µl
5 units of T4 DNA ligase (5U/µL)	1µl
10X T4 DNA Ligase Buffer	2µl
Sterile dH_2O	to 15µl
Total volume	**15µl**

The above reactions for Levels 0, 2i, 2, M and P were run in a PCR machine using the following program (Long protocol):

37°C 20 seconds

37°C 5 minutes
16°C 5 minutes
} x50

50°C 5 minutes

80°C 10 minutes

10°C Final storage

Level 1 constructs were assembled using the short protocol:

37°C 20 seconds

37°C 3 minutes
16°C 4 minutes
} x26

50°C 5 minutes

80°C 10 minutes

10°C Final storage

2.4.4 Expression cassettes design schemes

Four constructs were made for expression in *M. polymorpha* via *Agrobacterium*-mediated transformation, and another four for expression in *P. patens* via PEG-mediated homologous recombination transformation. All of the backbones derive from pBIN19 and pUC19, with ColE1 and RK2 origins of replication to replicate in both *E. coli* and *Agrobacterium*.

The primers used for amplification of a part of *Pp*108 locus for homologous recombination in *P. patens* had additional recognition sites for *Pml*I (*Eco*72I, Thermo Scientific, UK), CAC^GTG, in order to leave blunt ends on both sides of each construct for PEG-mediated transformation and for *Bsa*I, in order to ligate the PCR product into the Level 0 acceptor for making unit modules, pICH41331 (Table 2.6, Figure 2.4**).**

Table 2.6 Primers used for amplification of approximately 1kb of *Pp*108 neutral locus from the *P. patens* genome. GGTCTC(1/5)^ in green colour indicate the recognition site of *Bsa*I (Eco31I), and CAC^GTG in purple the recognition site of *Pml*I (*Eco*72I). L and R indicate the LB (Left Border) and RB (Right Border) of the vector. FF, forward primer; RR, reverse primer.

Primer Name	Sequence (5' → 3')
pp108.1L_FF	ggggtctcaGGAGcacgtggcaaacttgttatctaca
pp108.1L_RR	ggggtctcaAGCGtgtggtacgaggtcataaatata
pp108.1R_FF	ggggtctcaGGAGaatgagccaggtctacacgcagc
pp108.1R_RR	ggggtctcaAGCGcacgtggcatttaaatttgattag
pp108.2L_FF	ggggtctcaGGAGcacgtgttcgcaatgcaatcacca
pp108.2L_RR	ggggtctcaAGCGattaatttttgtattagtagaattc
pp108.2R_FF	ggggtctcaGGAGtcattcaaaaccaagtatgatgt
pp108.2R_RR	ggggtctcaAGCGcacgtgagcccgttctttccctttt

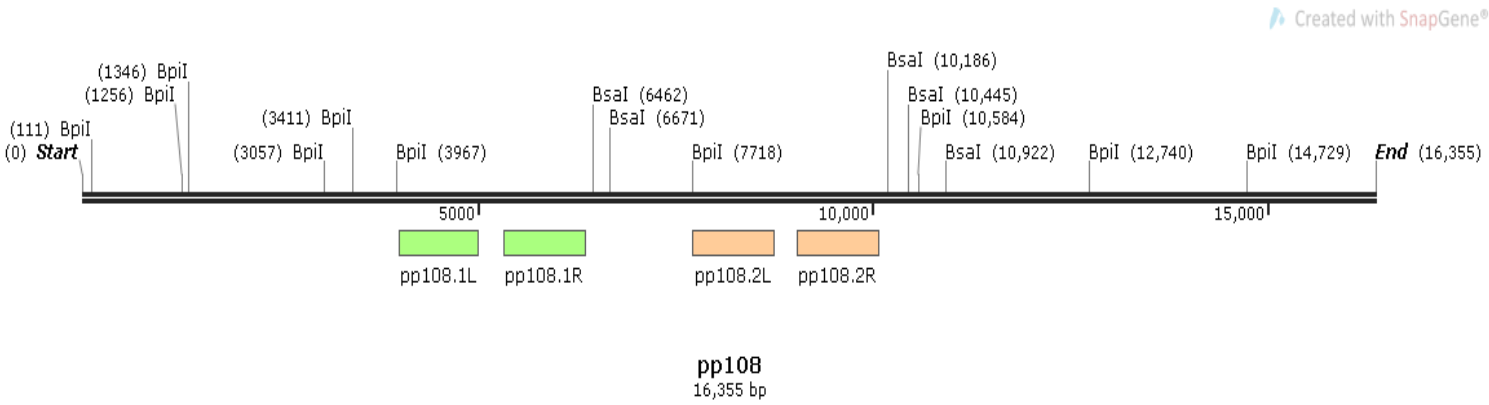

Figure 2.4 Map of the *Pp*108 locus created using SnapGene®. This region was used for targeting homologous recombination of transgenes into *P. patens* genome. The coloured regions specify the regions amplified by PCR (~1-1.2kb) using the primer pairs listed above. *Bsa*I/*Bpi*I recognition sites were not present at the sequences selected for amplification.

The selectable marker *nptII* gene was amplified from pISCL70004 and cloned into the Level zero acceptor for CDS1 modules pICH41308 using primers with flanking *Bsa*I recognition sites:

Table 2.7 Primers used for amplification of the new *nptII* coding sequence, GGTCTC(1/5)^ in green colour indicate the recognition site of *Bsa*I (*Eco*31I). FF, forward primer; RR, reverse primer.

Primer Name	Sequence (5' → 3')
L0_NPTIICDS_FF	ggggtctcaAATGGTTGAACAAGATGGATTG
L0_NPTIICDS_RR	ggggtctcaAAGCTCAGAAGAACTCGTCAAG

pICHnptII or Level 1 empty vector (pL1empty)

The empty vector construct contains only the plant selectable marker NPTII (Figure 2.5).

pAGMggs:cyc:nptII or Level 2.2 (pL2.2)

This construct contains the first 2 genes encoding enzymes of the pleuromutilin pathway, geranylgeranyl pyrophosphate synthetase (GGS) and cyclase (CYC), and the plant selectable marker NPTII (Figure 2.5).

pAGMggs:cyc:nptII:p1:p2:sdr or Level 2.5 (pL2.5)

This construct contains the first 5 genes encoding enzymes of the pleuromutilin pathway, geranylgeranyl pyrophosphate synthetase (GGS), cyclase (CYC), two cytochrome P450s (P450-1, P450-2), a short-chain dehydrogenase/ reductase (SDR), and the plant selectable marker NPTII (Figure 2.5).

pAGMggs:cyc:nptII:p1:p2:sdr:atf:p3 or Level 2.7 (pL2.7)

This is the complete gene cluster construct encoding all seven enzymes of the pleuromutilin pathway, geranylgeranyl pyrophosphate synthetase (GGS) and cyclase (CYC), three cytochrome P450s (P450-1, P450-2, P450-3), a short-chain dehydrogenase/ reductase (SDR), an acetyl transferase (ATF), and the plant selectable marker NPTII (Figure 2.5).

pAGMnptII_pp108.1 or Level M empty vector (p*Pp*LMempty)

The empty vector construct for homologous recombination in *P. patens* contains only the plant selectable marker NPTII and the homologous regions from locus *pp*108.1 from *P. patens* genome (Figure 2.6).

pICHggs:cyc:nptII_pp108.1 or Level P.2 (p*Pp*LP.2)

This construct contains the first 2 genes encoding enzymes of the pleuromutilin pathway, geranylgeranyl pyrophosphate synthetase (GGS) and cyclase

(CYC), the plant selectable marker NPTII, and the homologous regions from *P. patens* (Figure 2.6).

pICHggs:cyc:nptII:p1:p2:sdr_pp108.1 or Level P.5 (p*Pp*LP.5)

This construct contains 5 genes encoding enzymes of the pleuromutilin pathway, geranylgeranyl pyrophosphate synthetase (GGS), cyclase (CYC), two cytochrome P450s (P450-1, P450-2), a short-chain dehydrogenase/ reductase (SDR), the plant selectable marker NPTII, and the homologous regions from *P. patens* (Figure 2.7).

pICHggs:cyc:nptII:p1:p2:sdr:atf:p3_pp108.1 or Level P.7 (p*Pp*LP.7)

This is the complete gene cluster construct encoding all seven enzymes of the pleuromutilin pathway, geranylgeranyl pyrophosphate synthetase (GGS) and cyclase (CYC), three cytochrome P450s (P450-1, P450-2, P450-3), a short-chain dehydrogenase/ reductase (SDR), an acetyl transferase (ATF), the plant selectable marker NPTII, and the homologous regions from *P. patens* (Figure 2.7).

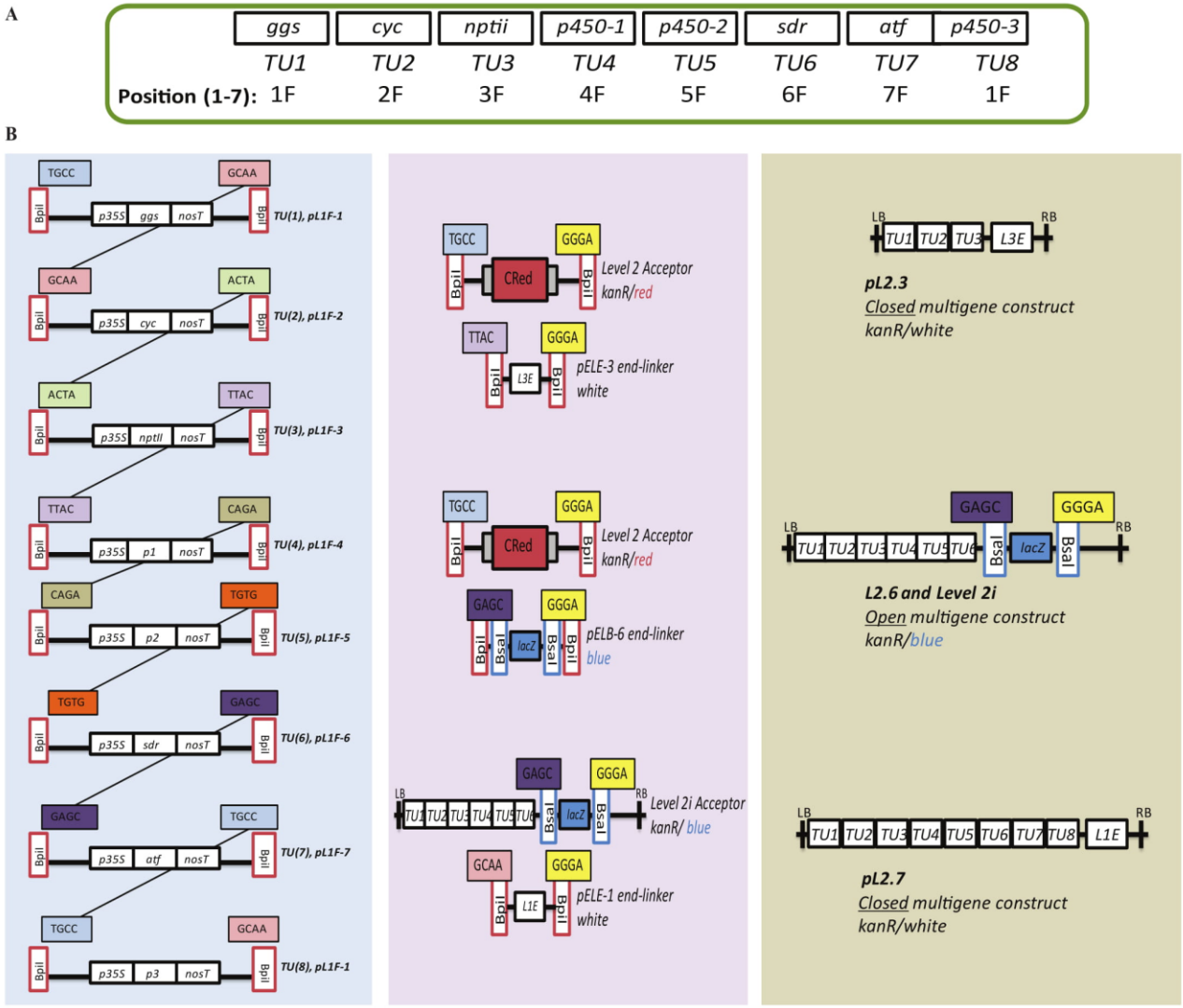

Figure 2.5 Modular Cloning (MoClo) for the construction of the plasmids used for *M. polymorpha* and *N. tabacum* transformation. **(A)** Level 1 of the seven genes of pleuromutilin pathway and the selectable marker *nptII*. **(B)** Schematic of the modular cloning technique; Left column indicates the Level 1 modules, central column the Level 2 destination vectors and end-linkers used, right column the final product of the digestion-ligation reaction.

It is worth mentioning that another approach was followed, where a diversity of promoters and terminators was used to eliminate repetitious use that may lead to transcriptional gene silencing due to promoter methylation and inactivation (Peremarti et al., 2010). More specifically, transcriptional regulatory elements that were proven to be functional in all plant hosts of this project were chosen, shown in Table 2.8 and detailed in Table 2.5.

Table 2.8 Diversity of promoters and terminators used in multigene constructs.

Gene	*ggs*	*cyc*	*nptII*	*P450-1*	*P450-2*	*sdr*	*atf*	*P450-3*
Promoter	35S	Act2	mas	Act2	nos	35S	mas	35S
Terminator	nosT	35ST	oscT	35ST	oscT	nosT	oscT	nosT

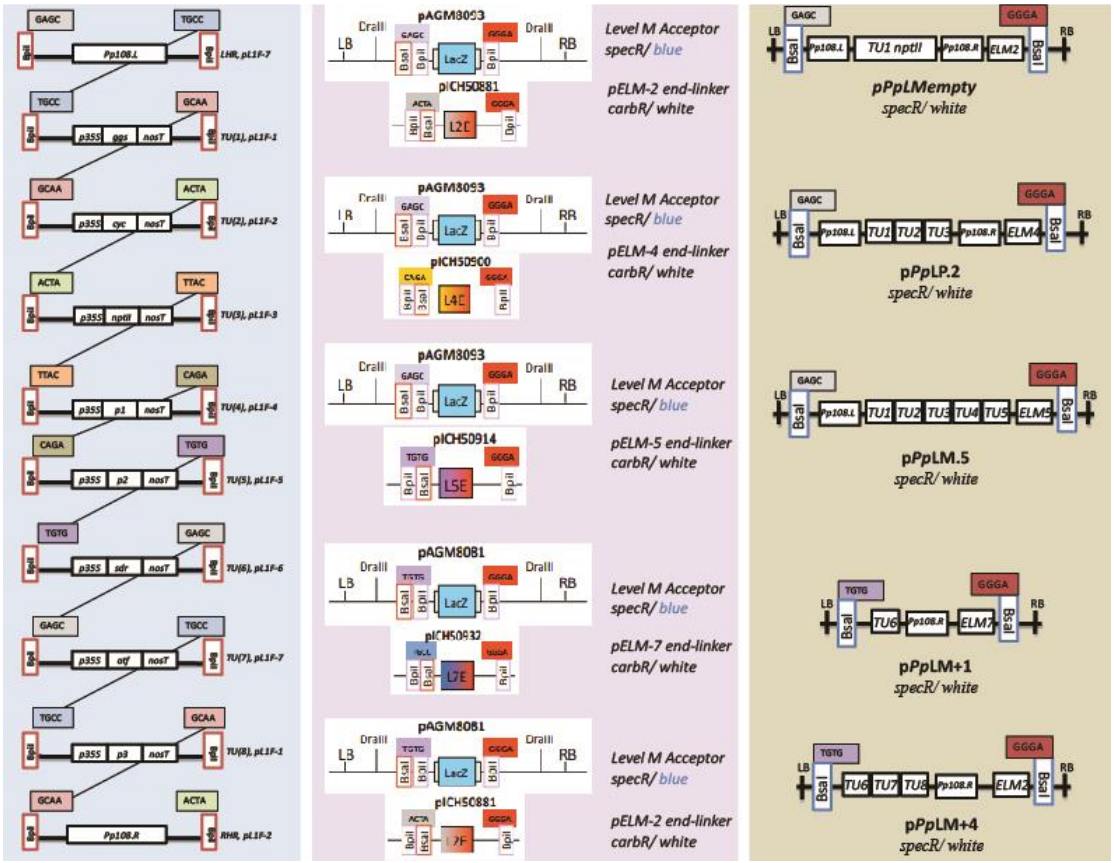

Figure 2.6 Schematic of the modular cloning technique of the plasmids designed for *P. patens* transformation. Left column indicates the Level 1 modules of the seven genes of pleuromutilin pathway, the selectable marker *nptII* and the two homologous regions of *P. patens* genome for homologous recombination, central column the new M destination vectors and end-linkers used, right column the final product of the digestion-ligation reaction. Note that p*Pp*Mempty uses the *nptII* Level 1 in position 1 and *Pp*108.1R Level 1 in position 2. Also, p*Pp*LP.2 uses *Pp*108.1R Level 1 in position 4 and p*Pp*LM+1 in position 7.

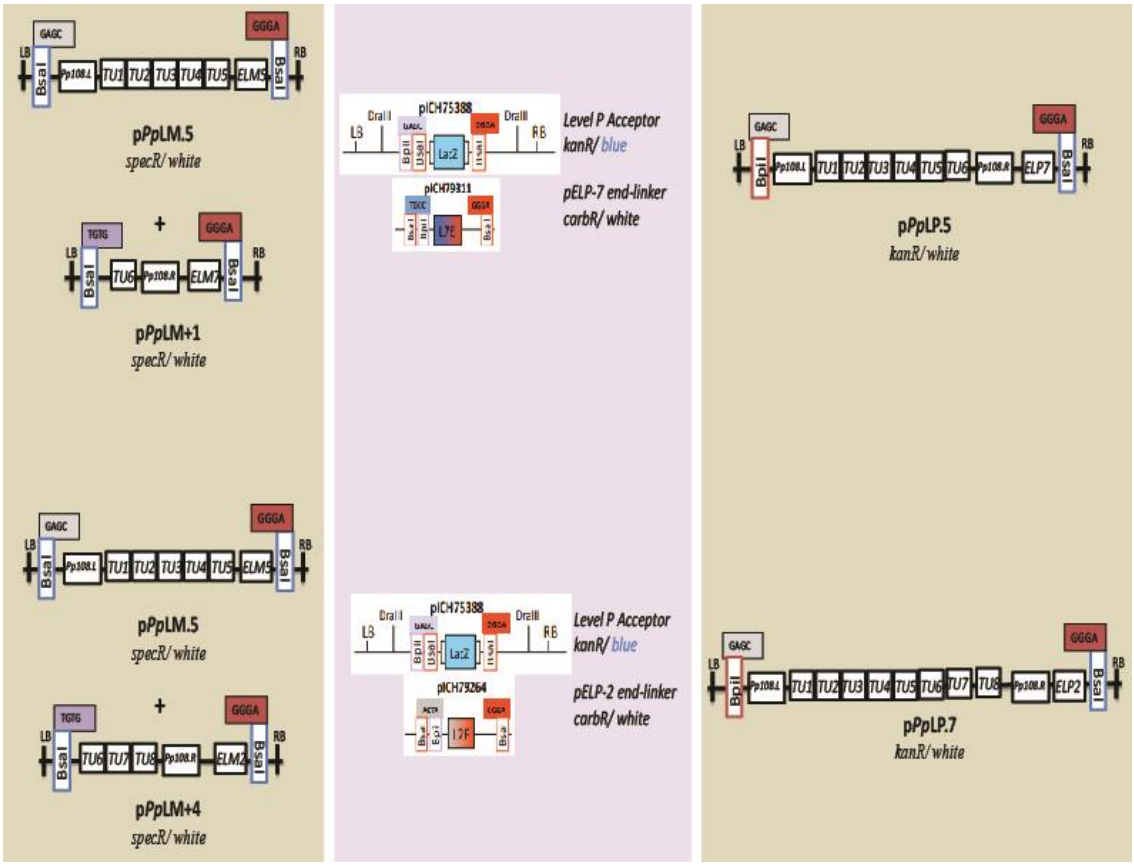

Figure 2.7 Schematic of the modular cloning technique of the plasmids designed for *P. patens* transformation. Left column indicates the Level M modules detailed in Figure 2.6 that are combined, central column the new P destination vectors and end-linkers used, right column the final product of the digestion-ligation reaction.

2.5 Molecular Techniques

2.5.1 DNA extraction

Total DNA from *P. patens* was isolated using a modified CTAB protocol (Doyle, 1991; Langlade Lab, University of Oxford, UK).

Approximately 100mg of tissue was harvested, blotted on sterile Whatman paper, put in a 1.5ml Eppendorf tube and snap-frozen in liquid N_2. Using a sterile cool

plastic pestle, the tissue was ground to a fine powder. 500µl of prewarmed extraction buffer were added and powder was ground further. Another 200µl extraction buffer (Table 2.9) were added to the mixture, along with 7µl 10mg/ml RNase A. The mixture was mixed by vortexing and incubated at 65° C for 10 minutes. Next, 600 µl chloroform-isoamyl alcohol (24:1) were added and the tube was shaken well. After spinning at 13,000g for 10 minutes, the upper aqueous phase was transferred to a new tube, 0.7x volume isopropanol was added to precipitate the DNA, and sample was immediately centrifuged at 13,000g for 10 minutes. The white pellet was washed with 500µl of 70% cold ethanol and left on bench to air-dry. Finally, the pellet was resuspended in 15-30µl TE (10 mM Tris/ 1mM EDTA, pH 8.0) and 1-2µl (~200ng of plant gDNA) was used for each PCR.

Table 2.9 Extraction Buffer used for CTAB DNA extraction method.

Extraction Buffer*	
100 mM Tris-HCl pH8.0	25 ml 2M Tris-HCl pH 8.0
1.42 M NaCl	142 ml 5 M NaCl
2% CTAB	10 g CTAB
20mM EDTA	20 ml 0.5M EDTA
2% PVP-40	10g PVP-40
dH_2O	to 500 ml

*Extraction Buffer was filter sterilised, stored at RT and used within 2-3 days, after prewarming at 65°C. 7µl of beta-mercaptoethanol and 10mg ascorbic acid were added to 10ml buffer immediately before use.

2.5.2 RNA extraction

Isolation of total RNA was performed using the TRIzol® reagent provided by Thermo.

a) Cell lysis and separation of phases

The tissue of plants was ground to a fine powder and 50-100mg was added into microcentrifuge tubes along with 1ml of cold TRIzol reagent for each sample. After rigorous mixing the tubes were incubated at room temperature for 5 minutes. Next, 200µl of chloroform were added, tubes were stored at room temperature for 2-3 minutes and centrifuged for 15 minutes at 12,000g at 4°C. The aqueous phase containing the RNA was transferred to a new tube.

b) Isolation of RNA

Into the aqueous phase, 500µl of isopropanol were added and tubes were stored at room temperature for 10 minutes. Then they were centrifuged for 10 minutes at 12,000g at 4°C. The supernatant was discarded and the white gel-like pellet was resuspended in 1ml of 75% ethanol. After mixing the tubes briefly, they were centrifuged for 5 minutes at 7,500g at 4°C. The supernatant was discarded and the RNA pellet was air dried for 10 minutes. The pellet was resuspended in 50µl sterile dH_2O and incubated in a water bath at 60°C for 15 minutes, before being stored at -70°C.

2.5.3 DNase treatment

Removal of genomic DNA from RNA was performed using DNase I and RiboLock RNase Inhibitor from Thermo by adding the following components to an RNase-free tube:

Total RNA of each sample	1µg
10x reaction buffer with $MgCl_2$	1µl
DNase I	1µl
RiboLock RNase Inhibitor	0.5µl
Sterile dH_2O	to 10µl

Total volume 10µl

The above reaction was run according to the following program:

37°C 30 minutes*

65°C 10 minutes

*Note that the program was paused, tubes were immediately transferred on ice and 1µl of 50mM EDTA was added. The program continued to reach 65°C, then was paused again and tubes were placed back into the thermal cycler.

2.5.4 Plasmid extraction

2.5.4.1 *E. coli* small-scale plasmid extraction

Colonies of *E. coli* obtained after transformation were grown overnight at 37°C and shaking at 200rpm by inoculating them in LB broth supplemented with the appropriate antibiotic/reagents as indicated at Table 2.1. Plasmid extraction for Level 2i-1, 2, M and P was performed using the NucleoSpin® Plasmid kit by Macherey-Nagel following the manufacturers' protocol for high-copy plasmid DNA isolation from *E. coli.*

2.5.4.2 *E. coli* alkaline lysis small-scale plasmid extraction

Plasmid extraction of the initial Level 0 and Level 1 constructs was conducted using a modified alkaline lysis based protocol, using homemade buffers (Birnboim & Doly, 1979). According to this protocol, the liquid culture was centrifuged in 1.5ml Eppendorf tube 2-3 times. After discarding all the supernatant, the pellet was resuspended in 300µl P1 Buffer (50mM Tris/ 10mM EDTA, pH 8.0) supplemented with RNase A (3mg/ml or 3µl per sample of 10mg/ml stock RNase A (#EN0531, Thermo Scientific, UK) and was vigorously shaken until it resuspended. Then, 300µl

P2 Buffer (200mM NaOH/ 1% (w/v) SDS) were added and the tube was inverted gently until suspension became clear. Next, 300µl P3 Buffer (3M Potassium acetate/~10% (v/v) Glacial acetic acid/pH 5.5) were added, the tube was inverted again and left on ice for 10 minutes. The cell debris, proteins and chromosomal DNA were pelleted by centrifugation at full speed for 10 minutes. The supernatant was transferred into a clean 1.5ml Eppendorf tube, 600µl Isopropanol were added and the tube was centrifuged at full speed for 15 minutes for plasmid DNA precipitation. After spinning, the supernatant was carefully discarded, and the DNA pellet was washed with 700µl of 70% ethanol. After centrifugation at full speed for 10 minutes, the ethanol was carefully removed, and the tubes were incubated at 37°C for 10 minutes to accelerate the evaporation of any residual ethanol. Finally, the pellet was resuspended in 20µl sterile deionized H_2O.

2.5.4.3 *E. coli* large-scale plasmid extraction

Higher concentrations of the plasmids were needed for the PEG-mediated transformation of *P. patens* protoplasts. The NucleoBond®Xtra Midi kit from Macherey-Nagel was used in this case, according to manufacturers' protocol using a starter culture of 100ml and OD_{600} =4.

2.5.4.4 *A. tumefaciens* plasmid extraction

Plasmid extraction from *A. tumefaciens* was performed using Nucleospin®Plasmid by Macherey-Nagel kit for low-copy plasmids, according to a supplementary protocol provided by the manufacturers. The initial liquid culture was inoculated with one unique colony for screening in 4ml of YEB medium (5g/l tryptone, 1g/l yeast extract, 5g/l nutrient broth, 5g/l sucrose, 0.49g/l $MgSO_4 \cdot 7H_2O$) supplemented with rifampicin/streptomycin and kanamycin or carbenicillin for 36-48 hours at 28°C. The liquid culture was centrifuged in 2ml tubes at 14,000 x g for 1 minute and, then,

resuspended in 1ml Wash Buffer (1M NaCl). The mixture was centrifuged at 14,000 x g for 1 minute, cells were resuspended in 200µl Lysis Buffer (25Mm Tris-HCl, 10mM EDTA, pH 8.0, 50mM glucose, 50mg/ml lysozyme) and were shaken for 30 minutes at 37°C, for total digestion of the cell wall. The tube was filled to a total volume of 500µl with Resuspension Buffer A1 provided by the kit and the protocol for low-copy plasmids continued from cell lysis step.

2.5.5 Restriction Digest

The restriction enzymes used in this project were provided by Thermo Scientific, UK, and are listed below:

Table 2.10 Restriction enzymes used in digest for screening of the plasmids isolated. All were in the FastDigest® edition by Thermo, using the 10X FastDigest Green Buffer provided.

Restriction Enzyme
*Bam*HI
*Bpi*I (*Bbs*I)
*Bsa*I (*Eco*31I)
*Eco*RI
*Eco*RV (*Eco*32I)
*Hind*III
*Kpn*I
*Mls*I (*Msc*I)
*Nco*I
*Pml*I (*Eco*72I)

The reaction below was incubated at 37°C for 30 minutes before gel electrophoresis:

10X FastDigest Green Buffer	2µl
FastDigest enzyme	1µl
Plasmid DNA	1µl (up to 1µg)
Sterile H_2O	16µl
Total volume	**20µl**

2.5.6 Polymerase Chain Reaction (PCR)

PCRs for screening the presence of the genes were performed using the DreamTaq Green DNA Polymerase (#EP0711, Thermo Scientific, UK) by adding the following components for each 50µl reaction:

10x DreamTaq Green Buffer (20mM $MgCl_2$)	5µl (1x)
10mM dNTPs	1 (0.2mM of each)
Forward primer	1.0 µM
Reverse primer	1.0 µM
Template DNA	~10pg for plasmid DNA/ ~200ng for plant gDNA
DreamTaq DNA Polymerase	0.025U/µl
Sterile dH_2O	to 50µl
Total volume	**50µl**

The above reaction was run for 35 cycles, according to the following program:

95°C	2 minutes	
95°C	30 seconds	x35
50-60°C*	30 seconds	
72°C	1 minute	
72°C	10 minutes	
10°C	Final storage	

*Note that for the primer annealing step the T_a (annealing temperature) was calculated typically 5°C to 8°C below T_m (melting temperature) of each primer.

The primers used for the 7 genes of the pathway, plus the selective marker are listed below:

Table 2.11 Primers used for amplification of gene fragments. FF, forward primer; RR, reverse primer; reg, regular.

Primer Name	Sequence (5' → 3')
regNPTII_FF	AGTGACAACGTCGAGCACAG
regNPTII_RR	AGACAATCGGCTGCTCTGAT
regGGS_FF	CTTCGCGACGACTACATCAA
regGGS_RR	AGCGATCCTGTCTCTTGCAT
regCYC_FF	CGCTCAGCTCCCTTTATGAC
regCYC_RR	ATGGGTGGTTGAGAACTTGC
regP450-1_FF	CCGGTATACAGAAGGCCTGA
regP450-1_RR	GTGCAGGAGTAGCGACATCA
regP450-2_FF	GCCAAGACTGCTGAAAGACC
regP450-2_RR	AGCTCCTTCATCAGCACGAT
regP450-3_FF	CAACTCTTCAAACCCCGGTA
regP450-3_RR	AAGGACAGCTTTCTCGACCA
regSDR_FF	CAAATGATGGAAGGCAAGGT
regSDR_RR	CGATTCTCTCGCTTCCAAAG

regATF_FF	ATATTACCGCATGGCTCCTG
regATF_RR	TGTTTTCCTGGGGCTGATAG

PCRs for amplification of the *nptII* coding sequence from pICSL70004 and of the homologous regions from wild-type *P. patens* DNA samples were conducted using the Phusion Green High-Fidelity DNA Polymerase (#F-534L, Thermo Scientific, UK), according to the following 50µl reaction:

5x Phusion Green HF Buffer (1.5mM $MgCl_2$)	10µl (1x)
10mM dNTPs	1 (0.2mM of each)
Forward primer	1.0 µM
Reverse primer	1.0 µM
Template DNA	~10pg for plasmid DNA/ ~200ng for plant gDNA
Phusion DNA Polymerase	0.02U/µl
Sterile H_2O	to 50µl
Total volume	**50µl**

This reaction was run based on a modified version of Touchdown PCR (Bounce PCR V.3) that facilitates the amplification when using primer-extension sequences (Mugford & Hogenhout, 2018):

98°C	2 minutes		
98°C	20 seconds	x15	x35
68°C	15 seconds / 1.0°C decrease		
72°C	1 minute		
98°C	20 seconds	x25	
53°C	15 seconds / 0.6°C increase		
72°C	1 minute		
72°C	10 minutes		
10°C	Final storage		

All the PCR reactions were conducted in the thermal cycler PCR max Version 2.41 or the BioRad T100.

2.5.7 Quantitative Reverse Transcription PCR (RT-qPCR)

Relative expression levels of the 7 genes in *M. polymorpha* were compared to empty vector control samples. For normalization, *actin7* expression levels were also analyzed. Luna® Universal One-Step RT-qPCR kit from New England BioLabs was used, which combines *in silico* reverse transcription (RT), using the Luna WarmStart Reverse Transcriptase (cDNA synthesis) and then amplification, using the Hot Start *Taq* DNA polymerase. For quantification after each PCR cycle, SYBR Green I was used as a double-stranded DNA binding dye.

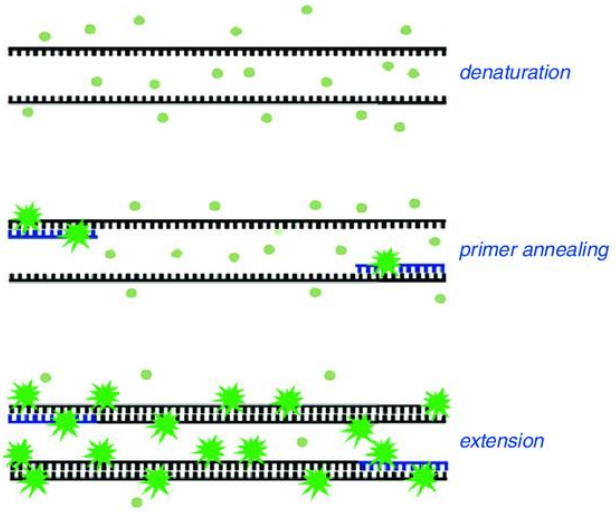

Figure 2.8 SYBR Green Dye during amplification. Fluorescence increases 100 to 200-fold when bound to double-stranded DNA (Fraga et al., 2008).

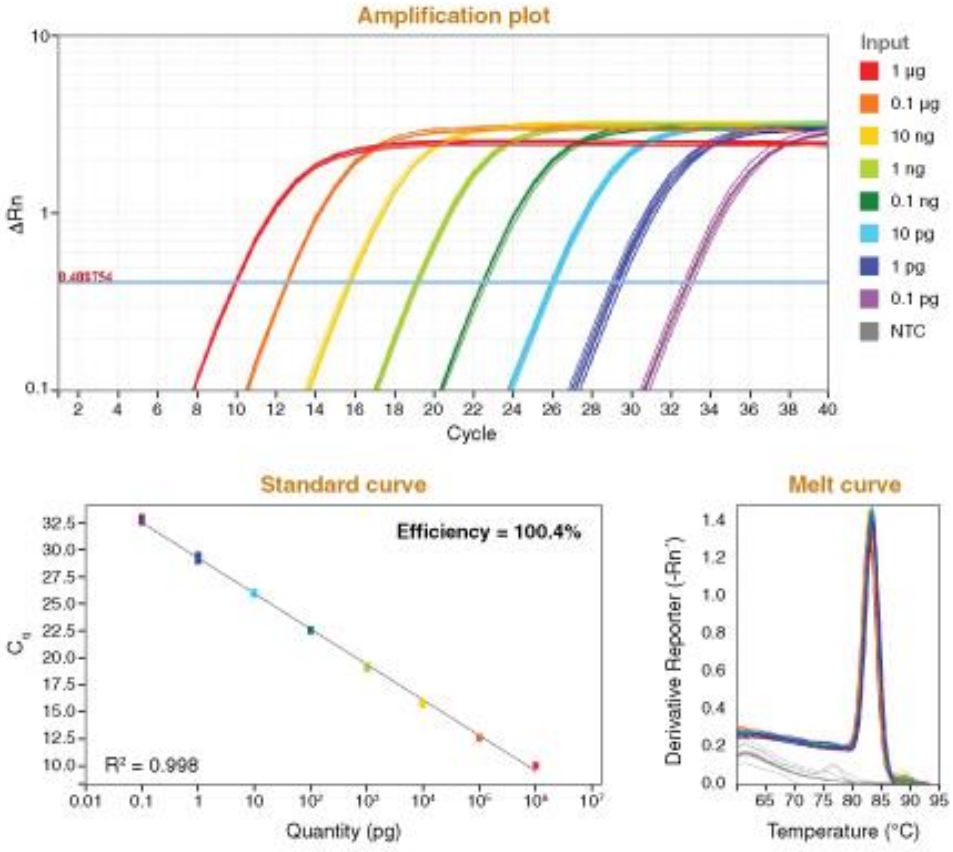

Figure 2.9 Graph of the amplification plot, standard curve and melt curve of th RT-qPCR using Luna® kit. The horizontal line of the amplification plot indicates the threshold line where fluorescence signal is produced. The threshold cycle (Ct) demonstrates the amplification cycle where fluorescence

exceeds the baseline. The cycle of quantification value (Cq) is the PCR cycle which the sample intersects the threshold line. A range of input concentrations was used (0.1pg-1μg) with 8 replicates of each concentration. NTC used as a non-template control. Melt curve shows the change in fluorescence when double-stranded DNA dissociates to single-stranded DNA due to temperature rise (product # E3000L, adapted from NEB.com).

Relative expression levels were calculated using Microsoft® Excel 2007 according to the ΔΔCt method (Zhang et al., 2015), using the following equation:

$$\text{Amount of target or } \mathbf{REU^*} = 2^{-\Delta\Delta Ct}$$

Average Test Ct value	**Average Test Ct value**	**Average Control Ct value**	**Average Control Ct value**
TE	HE	TC	HC
ΔCt value (Test)		**ΔCt value (Control)**	
TE-HE		TC-HC	

ΔΔCt = ΔCt value (Test) - ΔCt value (Control)

*REU stands for Relative Expression Units that were displayed as fold change relative to control samples. TE is the average Ct value for the gene being tested and HE for the housekeeping gene, both under experimental conditions. TC is the average Ct value for the gene being tested and HC for the housekeeping gene, both under control conditions.

The Luna® reaction was conducted using the CFX Connect Real-Time PCR Detection System by Bio-Rad and data were obtained using the CFX Maestro Software. The components of the RT-qPCR reaction were the following:

Reaction mix (2x)	5µl (1x)
WarmStart reverse transcriptase	0.5µl
Forward primer	0.4µl
Reverse primer	0.4µl
Template RNA	≤1µg
Sterile dH_2O	to 10µl
Total volume	**10µl**

The primers used are listed in Table 2.12. The above reaction was run according to the following program:

55°C	10 minutes	x1
95°C	1 minute	
95°C	10 seconds	x40
60°C	30 seconds	
60°C to 95°C	increment 0.5°C for 0.05	x1

Table 2.12 Primers used for qPCR and sequencing. FF, forward primer; RR, reverse primer; q, qPCR; seq, sequencing.

Primer Name	Sequence (5' → 3')
seq/q_GGS_FF	AAGATGAGTCTGCCCTCCG
seq/q_GGS_RR	ACCTGTTTTCATGCCAAGGTC
seq/q_CYC_FF	TCGAGATCGTATGGTCGCTC
seq/q_CYC_RR	GACACCTTTTCCTGCCACAA
seq_NPTII_FF	GCTCCTGCCGAGAAAGTATC
seq_NPTII_RR	GGCTTCCATCCGAGTACGTG

seq/q_P450-1_FF	GACTACATCCCTCGCGGTTT
seq/q_P450-1_RR	TCAAGCCAGCTACGACCATC
seq/q_P450-2_FF	GCTCTAATTCCTTGGCTCGC
seq/q_P450-2_RR	TACGCCAGCTTCCATTCTCT
seq/q_SDR_FF	ACTCAACATCTGCGACAAGG
seq/q_SDR_RR	TGTCCCATACATCGTCCTCG
seq/q_ATF_FF	TATTACCGCATGGCTCCTGT
seq/q_ATF_RR	ACCGCCTAACGGTATAAGCA
seq/q_P450-3_FF	AATGCGAGGTCATGCGTACT
seq/q_P450-3_RR	AGTCGTATCAGCACCAGCAA
q_*MpACT7*FF	GTGCCGAAAGATTCAGGTGC
q_*MpACT7*RR	TTTCCCTGGTCATACGCTCG

2.5.8 Gel electrophoresis

Agarose gels 1% (w/v) in TAE were used for visualising DNA using a UV transilluminator. Agarose powder was solved in 1x TAE Buffer (50x TAE: Tris-acetate 40mM/ pH 7.5, glacial acetic acid 20mM, Na_2EDTA 1mM/ pH 8.0), including Midori Green Advance DNA stain (Nippon Genetics, Europe GmbH), heated in a microwave and poured into a mould with appropriately spaced combs to form sample wells. Where needed, samples were mixed with 1x Loading Dye (6x DNA Loading Dye: glycerol 50% (v/v), 50x TAE 2% (v/v), bromophenol blue 0.25% (w/v), xylene cyanol 0.25% (w/v), RNA Loading Dye: formamide 95% (v/v), SDS 0.025% (w/v), 0.5mM EDTA, bromophenol blue 0.025% (w/v), xylene cyanol 0.025% (w/v)), loaded on gel lanes and run at 120V in Bio-Rad horizontal gel tanks. Results were obtained with the Bio-Rad ChemiDoc XRS+® or Gel Doc EZ®, using the ImageLab® software. 1kb Plus DNA Ladder (2-log DNA Ladder) from New England BioLabs was used as a marker (Figure 2.10).

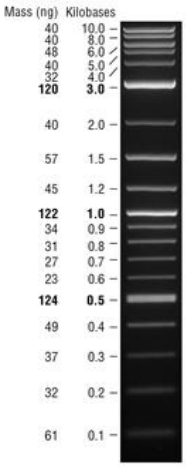

Figure 2.10 5µl of 1kb Plus DNA Ladder visualised by ethidium bromide staining on a 1% (w/v) TBE agarose gel (product #N3200S, adapted from NEB.com).

2.5.9 PCR product purification

NucleoSpin® Gel and PCR Clean-up kit from Macherey-Nagel was used for removal of salts, enzymes and primer dimers from PCR reactions following the manufacturers' protocol.

2.5.10 Gel extraction

The desired bands were cut from 1% (w/v) agarose gels which were run at 60V for 25 minutes in order to lower the temperature during electrophoresis and the UV exposure was applied at the longest wavelength possible to avoid damaging the DNA. NucleoSpin® Gel and PCR Clean-up kit from Macherey-Nagel was used following the manufacturers' protocol.

2.5.11 DNA sequencing

DNA sequencing was conducted by Source BioScience in Cambridge, UK. The primers used for sequencing of the genes are listed at Table 2.12 and the primers used for the old *nptII* Level 1 plasmid are listed below:

Table 2.13 Primers used for amplification of the old *nptII* Level 1 transcription unit. FF, forward primer; RR, reverse primer; seq, sequencing.

Primer Name	Sequence (5' → 3')
seq_L1P3FNPTII_p1FF	ccaaccacgtctacaaagca
seq_L1P3FNPTII_p2RR	TGTCGATCAGGATGATCTGG
seq_L1P3FNPTII_p3FF	CGGCCATTTTCCACCATGAT
seq_L1P3FNPTII_p4RR	gcgggactctaatcataaaaacc

2.5.12 Quantification of nucleic acids

The purity and concentration of isolated nucleic acids was estimated using the NanoPhotometer® N60/N50 provided by Implen.

2.6 Preparation of competent bacterial cells

2.6.1 Chemically competent E.coli **(''Ultra-competent'' cells by Inoue method)**

(Im et al., 2011; Inoue et al., 1990)

a) Preparation of cells

Inoue transformation buffer (10.88g/l $MnCl_2.4H_2O$, 2.2g/l $CaCl_2.2H_2O$, 18.65g/l KCl, 0.5M PIPES/ pH_{KOH} 6.7, H_2O to 1l) was filter sterilised and chilled before use. A single bacterial colony was picked from a freshly streaked plate and grown at 37°C into 25ml of LB Broth in a 250ml flask for 6-8 hours. Three 1L flasks were inoculated with the starter culture, each containing 250ml of LB broth. The first was inoculated with 2ml, the second with 4ml and the third with 10ml. All three flasks were incubated overnight at 20°C and shaking at 100rpm. The following morning the OD_{600} was measured every 45 minutes until one of the cultures reached OD=0.55. This culture was immediately transferred into an ice-cold water bath for 10 minutes. The culture was poured into 50ml Falcon® tubes and centrifuged at 2,500 x g

for 10 minutes at 4°C. After complete removal of the medium, the cells were resuspended in 80ml of ice-cold Inoue transformation buffer, mixed gently in the cold room (4°C) and harvested by centrifugation at 2,500 x g for 10 minutes at 4°C.

b) Freezing of competent cells

After the last centrifugation the supernatant was discarded and the cell pellet was resuspended in 20ml of ice-cold Inoue transformation buffer. Then, 1.5ml of DMSO was added into the suspension, the bacterial cells were mixed and then incubated on ice for 10 minutes. Finally, the bacterial suspension was dispensed into aliquots of 50µl, immediately snap-frozen in a bath of liquid nitrogen and stored at -70°C until needed.

2.6.2 Electro-competent *E. coli*

A single colony was picked from a streaked plate and grown in 5ml LB broth overnight at 37°C and 200rpm. The next day the 5ml culture was transferred into 100ml liquid LB broth at the same conditions until OD_{600} reached 0.4-0.6. The culture was poured into two 50ml centrifuge tubes and placed on ice for 10 minutes. The cells were pelleted at 4,000 x g for 10 minutes at 4°C and resuspended in pre-chilled sterile H_2O. At this step 15ml H_2O were added to each tube and the content of both tubes was merged. The one tube containing both cell pellets was filled up to 50ml with H_2O and the cells were resuspended. The cells were centrifuged at 4,000 x g for 10 minutes at 4°C and the previous resuspension step was repeated. After the second centrifugation, the supernatant was removed and the cells were resuspended in pre-chilled glycerol solution 10% (w/v) (4ml per tube) and centrifuged at the same

conditions. The final pellet was resuspended again in pre-chilled glycerol solution 10% (w/v) (250µl per tube), dispensed in 40µl aliquots, flash-frozen in liquid nitrogen and stored at -70°C until use.

2.6.3 Chemically competent *A. tumefaciens*

One single colony was inoculated in 5ml YM broth containing the appropriate antibiotics. The next day, 2ml of the overnight culture were added to 50ml YM Broth in a 200ml flask and grew until OD_{600} reached 0.6. The culture was left on ice for 15 minutes and centrifuged at 3,000 x g at 4°C for 5 minutes. The cells were resuspended in 1ml of 20mM $CaCl_2$ solution and dispensed in 100µl aliquots into pre-chilled tubes. Finally, the tubes were flash-frozen into liquid N_2 and stored at -80°C until use (An et al., 1988).

2.6.4 Electro-competent *A. tumefaciens*

LBA4404 *A. tumefaciens* glycerol stock was streaked on a plate with YM media, supplemented with 20µg/ml rifampicin and 100µg/ml streptomycin (Table 2.1). After 2-3 days growth on plates, 5ml of YM liquid media was inoculated with one single colony containing the appropriate antibiotics and incubated at 28°C with agitation at 200rpm. Six hours later three 150ml cultures were inoculated with 1ml each of the 5ml culture and grown for 30-40 hours. When OD_{600} reached 0.8-1.0 the cultures were put on ice for 15 minutes. All next steps were performed on ice. Cultures were distributed to 8x50ml tubes and centrifuged at 4,000 x g for 30 minutes at 4°C. The pellets were washed with 10ml sterile ice cold dH_2O and filled up to 50ml with dH_2O. The above centrifugation step was repeated and pellets were washed again with 10 ml ice cold dH_2O. The solutions were combined into 4x50ml tubes and filled

up with dH_2O to 50ml. Another centrifugation step was conducted and pellets were dissolved in 10ml ice cold dH_2O, combined to 2x50ml tubes and filled up to 50ml with dH_2O. The tubes were centrifuged again and the pellets were resuspended with 10ml ice cold dH_2O, and then combined to 1x50ml tube. A final centrifugation step was performed, the cell pellet was resuspended in 4.5ml ice cold 10% glycerol, dispensed into 80µl aliquots, flash-frozen in liquid N_2 and stored at -80°C until use.

2.7 Transformation of bacterial cells

2.7.1 Chemical transformation of *E.coli*

Into each aliquot of competent cells, 5-10ul of ligation reaction or plasmid were added, and the tube was flicked and left on ice for 40 minutes. A heat-shock treatment at 42°C was applied for 60 seconds and cells were recovered by short incubation on ice then addition of 1ml prewarmed LB broth without antibiotics. The tubes were incubated for 1 hour at 37°C to allow the cells with the new plasmid to express resistance and then plated into LB plates containing the appropriate antibiotics.

2.7.2 Electroporation of *E. coli*

Aliquots of electro-competent cells were thawed on ice and 1-2µl of ligation reaction or plasmid was added. The mixture was loaded into a pre-chilled 0.2cm cuvette and 2.5kV electric pulse was applied for 5msec using the MicroPulser Electroporator by BioRad (Setting ‘’Ec2’’). Immediately after electroporation, 1ml of pre-warmed LB broth was added and the cuvette content was transferred back to the tube and the tubes were incubated at 37°C for 1 hour before plating on selective LB media.

2.7.3 Chemical transformation of *A. tumefaciens*

Agrobacterium aliquots were thawed on ice and up to 10µl plasmid (100-1000ng) were added. The tube was mixed, kept on ice for 5 minutes and then transferred into liquid N_2 for 5 minutes. The tubes were incubated for 5 minutes in a water bath of 37°C. Then, 1ml LB medium was added and the tubes were left at 28°C for 3 hours for cells to recover, before plating them on selective YM media.

2.7.4 Electroporation of *A. tumefaciens*

Plasmid DNA (0.1-0.5µl) was added to an 80µl *Agrobacteria* aliquot, the tube was mixed and loaded into a 0.1cm cuvette. A pulse of 2.2kV was delivered using the MicroPulser Electroporator by BioRad (Setting ‘’Agr’’) and immediately 500µl SOC media (For 100ml SOC: 99ml SOB, 1ml 2M glucose solution; SOB: 0.5g/l NaCl, 20g/l Tryptone, 5g/l Yeast Extract) were added into the cuvette. The mixture after being transferred back to the tube, was incubated for 2-3 hours at 28°C, before plating on selective YM media.

2.8 Agro-infiltration of *Nicotiana tabacum* (Li, 2011)

a) Preparation of *Agrobacterium* culture

After streaking *Agrobacteria* glycerol stocks on YM plates and incubation at 28°C for 2-3 days, a single colony was used to inoculate 5ml YM Broth medium with 20µg/ml rifampicin, 100µg/ml streptomycin and 50µg/ml kanamycin (pL2.2, pL2.5, pL2.7) or 75µg/ml carbenicilin (pL1empty) and incubated overnight at 28°C with agitation at 200rpm. The next day, 1ml of the starter culture was used to inoculate 25ml LB with the same antibiotics, plus 20µM acetosyringone and grown overnight. The third day, the OD_{600} of the culture was measured and the culture was centrifuged

at 5,000 x g for 15 minutes. The pelleted cells were resuspended in Resuspension Solution (10mM $MgCl_2$, 10mM MES-K/ pH 6.6 with KOH, with filter-sterilized 100µM acetosyringone added after autoclaving of the solution and immediately before use) to reach a final OD_{600} of 0.4. The cells were stored at room temperature for 2-3 hours before infiltration.

b) Infiltration of *N. tabacum*

Leaves of approximately 5-week-old *N. tabacum* were used for infiltration, while the same leaf was infiltrated for each technical replicate to achieve the same developmental stage. Using a 5ml syringe without needle, the mixture containing the transformed *Agrobacteria* was infiltrated by placing the syringe on the underside of the leaf and applying a counter-pressure to the upper side of the leaf with the gloved fingers. Successful filling of the apoplastic spaces with the bacterial solution became visible by a dark-green pattern (‘’wetting’’ area). After infiltration, the plants were grown for a week post-infiltration in a plant incubator at 25°C, 16hr light/ 8hr dark, 60% humidity and 100µmol/m^2s light intensity, and leaves were harvested for screening, 3, 5 and 7 days post-infection (d.p.i).

2.9 Stable transformation of *Marchantia polymorpha*

Transformation of *M. polymorpha* was performed by following an *Agrobacterium*-mediated transformation protocol using regenerating thalli (Kubota et al., 2013). According to this protocol, 14-day-old thalli were cut across the apical-basal axis, about 2-3mm from the tip, including the meristem. Thallus regeneration was accomplished by incubating cut thalli on a half strength Gamborg’s B5 medium supplemented with 1% (w/v) sucrose for 3-7 days under normal growth conditions

(Section 2.2.2). In the meantime, *A. tumefaciens* strain LBA4404 harboring each plasmid (Section 2.4.4) was inoculated in a starter culture of 5ml 2 days before co-cultivation. On the day of co-cultivation, the bacterial cells were harvested by centrifugation, resuspended in 5 volumes of 0M51C medium (Table 2.14) supplemented with 100μM acetosyringone, and incubated for 6 hours at 28°C and 200 rpm. After 6 hours, approximately 20 regenerating plantlets and 1ml of *Agrobacterium* culture, as described, were co-cultivated in 50ml of 0M51C medium supplemented with 2% (w/v) sucrose and 100μM acetosyringone into 200ml flasks for 3 days under normal growth conditions (Section 2.2.2) and agitation at 130rpm. Next, the thalli were washed 5-6 times with sterile dH_2O and left to soak in sterile dH_2O containing 1g/l cefotaxime to prevent *Agrobacterium* growth. After 30 minutes, the plantlets were transferred into half strength Gamborg's B5 medium supplemented with 1% (w/v) sucrose, 100mg/l cefotaxime and 5mg/l G418 (Geneticin®, Santa Cruz Biotechnology, USA). Geneticin-resistant thalli became distinct 15 days after transfer to the selective media, whereas the original cut thalli became necrotic. Isogenic lines were obtained after 2 cycles of transplantation of gemmae (G2 generation), which were used for analyses (Figure 2.11).

Table 2.14 0M51C medium used for *M. polymorpha* transformation. 10x stock was autoclaved without B5- micro components or B5-vitamin, which were filter sterilised and added after autoclaving. L-glutamine, casamino acids, sucrose and acetosyringone were also filter sterilised and added before use.

0M51C medium (1l pH 5.5 with 1N KOH)	
10x 0M51C stock	100ml
0.03% (w/v) L-glutamine	0.3g
0.1% (w/v) casamino acids	1g

10x 0M51C stock (4l store at -20°C)	
KNO_3	80g
NH_4NO_3	16g
$MgSO_4.7H_2O$	14.8g
$CaCl_2.2H_2O$	12g
KH_2PO_4	11g
EDTA-NaFe(III)	1.6g
B5-micro components	40ml
B5-vitamin	40ml
KI solution (750mg/100ml)	4ml
B5-micro components (100ml store at -20°C)	
$NaMoO_4.2H_2O$	25mg
$CuSO_4.5H_2O$	2.5mg
$CoCl_2.6H_2O$	2.5mg
$ZnSO_4.7H_2O$	200mg
$MnSO_4.7H_2O$	1g
H_3BO_3	300mg
B5-vitamin (100ml store at -20°C)	
Inositol	10g
Nicotinic acid	100mg
Pyridoxine-HCL	100mg
Thiamine-HCL	1g

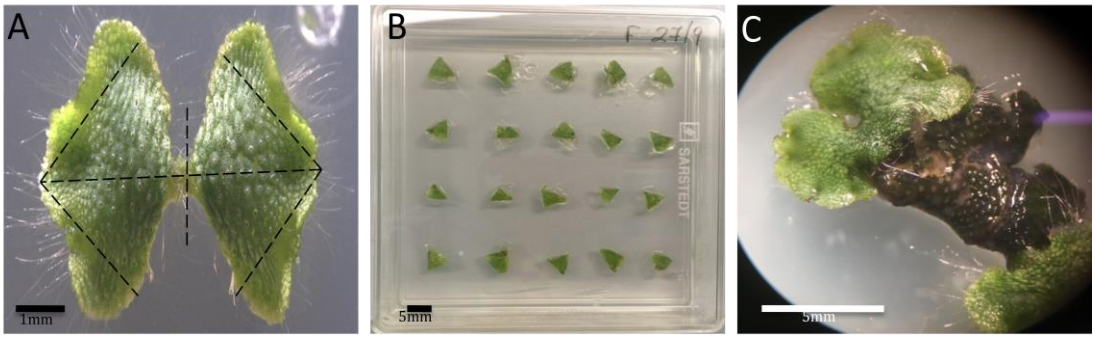

Figure 2.11 Transformation of *M. polymorpha* regenerating thalli. (A) A 14-day-old thallus indicated by the parts that are being cut. **(B)** Fragments after thallus cutting on half strength Gamborg's B5 supplemented with 1% (w/v) sucrose. **(C)** After 3-7 days of regeneration, thalli were co-cultivated with *Agrobacterium* in 0M51C medium containing 100µM acetosyringone for 3 days. Two weeks later, resistant thalli became distinct while the original thalli became necrotic. Scale bars represent 1mm (A) and 5mm (B-C).

2.10 Stable transformation of *Physcomitrella patens* (Schaefer et al., 1991)

a) DNA preparation

Plasmid DNA was isolated using the NucleoBond®Xtra Midi kit from Macherey-Nagel. 100µg plasmid DNA was digested using 100u (or 10µl) *Pml*I enzyme (Thermo Scientific, UK). The cut plasmid was precipitated, cleaned and dissolved in 100µl dH_2O, with a final minimum concentration of 500ng/µl.

b) Tissue preparation

Tissue was prepared by culturing *P. patens* plant homogenised with the T10 basic ULTRA-TURRAX® homogeniser, IKA, UK, in sterile dH_2O onto 2 BCD-AT plates overloaded with cellophane disks. After growing for 5 days, tissue from each

plate was passaged again and split onto 2 plates. This procedure was repeated 3 times, every 4-5 days.

c) Protoplast isolation

250mg Driselase® (Sigma, UK) was dissolved in 25ml 8.5% (w/v) mannitol, mixed by shaking for 20 minutes and filter sterilised into a new falcon tube. The tissue was collected from 4-6 cellophane plates and added into the previous 25ml solution. The mixture was placed in the dark for 30 minutes with gentle mixing every 5-7 minutes, and filtered through a sterile cell strainer 70µm (Fisherbrand, UK) into a new sterile petri dish. The mixture was filtered again into a second petri dish and then transferred into a sterile test tube 100x16mm with a cap (VWR, UK). The cells were pelleted by centrifugation at 600xg for 5 minutes, resuspended into 10ml 8.5% (w/v) mannitol and centrifuged again. Previous resuspension and centrifugation steps were repeated two more times.

d) Protoplast PEG-mediated transformation

Using a haemocytometer, protoplasts were counted and resuspended to a concentration of $1.6x10^6$/ml in MMM solution (Table 2.15). 10-15µg DNA in maximum 30µl dH_2O was dispensed in each new transformation tube. 300µl protoplasts in MMM solution were added and mixture was mixed gently. Next, another 300µl PEG solution was added and heat-shock at 45°C for 5 minutes was applied. The tubes were left for 5 minutes at room temperature before adding 1ml of protoplast liquid media. The tubes were set for 5 minutes and 2ml of protoplast liquid media were added. After waiting a further 5 minutes, 3ml of protoplast liquid media were added and mixture was poured into small petri dishes, wrapped in foil, sealed with micropore tape and kept overnight at growth chamber. The next day, the

protoplasts were centrifuged at 600xg for 5 minutes and resuspended into 8ml PRM/T. These 8ml were then plated out onto 4 regeneration plates PRM/B with cellophane discs and sealed with micropore tape. After growing in chamber for 7 days the protoplasts that had survived were transferred to selection plates containing 25mg/l G-418. After 10 days the resistant colonies were then transferred onto plates without selection for further 10 days and finally a small amount of tissue was propagated back onto selective plates.

Table 2.15 Solutions used for the PEG-mediated transformation of *P. patens* protoplasts. Solutions B, C, D, AT and TES detailed in Table 2.2.

Transformation solutions		
MMM solution (20ml)	1M $MgCl_2$	300µl
	1% (w/v) MES/ pH_{KOH} 5.6	2ml
	mannitol	1.7g
PEG solution (10ml)	8.5% (w/v) mannitol	8.2ml
	1M $Ca(NO_3)_2$	1ml
	1M Tris/ pH 7.2	100µl
	molten PEG 6000	3.5g
Protoplast liquid media (100ml)	stock A*, B, C, AT	1ml
	mannitol	6.6g
	glucose	0.5g
	*A: 118g.l $Ca(NO_3)_2.4H_2O$, 1.25g/l $FeSO_4.7H_2O$	
PRM/B (500ml)	stock B, C, D, AT	5ml
	1x TES	500µl
	mannitol	30g

	$CaCl_2.2H_2O$	0.935g
	Agar	4g
PRM/T (100ml)	stock B, C, D, AT	1ml
	1x TES	100µl
	mannitol	8g
	$CaCl_2.2H_2O$	0.145g
	Agar	0.7g

2.11 Metabolite extraction from plant material

The plant tissue was snap-frozen in liquid nitrogen and ground to a fine powder. When tobacco leaves were harvested, the leaf midvein was discarded. The ground tissue was transferred to 2ml tubes and 1.5ml of 40% aqueous methanol (MeOH), containing 0.5% acetic acid was added. The tubes were mixed vigorously for 2-3 minutes and were sonicated for 20 minutes. After centrifugation at 12,000xg and 4°C for 15 minutes, the supernatant was transferred into a glass vial, vacuum dried and pellet was resuspended in 100µl acetonitrile.

2.12 LCMS analysis

LCMS analyses were run using a Waters system, with a Waters 2767 autosampler, Waters 2545 pump system and a Phenomenex Kinetex column. The Diode Array detector between 200 and 600nm was by Waters 2998. ES+ and ES- were operating by a Waters 2424 ELSD and Waters SQD-2 mass detector between 100 *m/z* and 800 *m/z* (de Mattos-Shipley et al., 2018). Data were visualized using the Waters MassLynx V4.2 SCN982 software. Solvents were a linear 5%-95% gradient of acetonitrile (in water), 20min.

2.13 Bioinformatics software

For the visualization of construct maps, digestion profiles and sequencing data Benchling® and SnapGene® were used. Known sequences were downloaded from the National Center for Biotechnology Information (NCBI) library. BLAST® (Basic Local Alignment Search Tool) and primer design tool were also conducted on NCBI site. Sequences of the genes and the final plasmids are shown in FASTA format in Appendix A.

2.14 Microscopic observation and image processing

Observation of plants was performed with LEICA® M205 C, LEICA® DMLB and GX® stereo microscope XTC series, using the GX Capture software. Photos were taken using a Canon® PowerShot A3300 IS, image processing and analyzing was developed with Image J® (Fiji), Adobe® Illustrator CS6 and Adobe® Photoshop CC.

Chapter 3: Construction of plasmids

3.1 Aims

In order to build the pleuromutilin biosynthetic gene cluster in different plant species, the genes of the pathway were cloned using the Golden Gate system, using promoters and terminators that are functional in the several plant species (see Section 2.4). The empty vector construct contains only the plant selectable marker gene of neomycin phosphotransferase II (*nptII*), which provides resistance to geneticin, kanamycin or neomycin. The construct containing the first 2 genes of the pathway, *geranylgeranyl pyrophosphate synthetase* (*ggs*) and *cyclase* (*cyc*) also contains the *nptII* marker. The 5-gene construct consists of *ggs*, *cyc*, two *cytochrome P450s* (*p450-1*, *p450-2*), a *short-chain dehydrogenase/ reductase* (*sdr*), and the plant selectable marker *nptII*. The complete gene cluster construct, encoding all seven enzymes of the pleuromutilin pathway, contains the genes *ggs*, *cyc*, *p450-1*, *p450-2*, *p450-3*, *sdr*, an *acetyltransferase* (*atf*) and the *nptII* marker. For *P. patens* homologous recombination, the same combination of genes was used and the homologous regions from locus *Pp*108.1 from *P. patens* genome were cloned bilaterally between the transcription units.

3.1.1 Level 0 plasmids

Prior to commencing this research, level zero plasmids containing cDNA of each of the coding sequences of all seven genes of pleuromutilin pathway and *nptII* were generated by Suphattra Sangmalee a previous student within the group. These

had also been modified to remove all internal *Bsa*I/*Bpi*I sites as these would interfere with the Golden Gate cloning system.

Prior to their use, the L0 plasmids were confirmed by restriction digests with *Bsa*I (Figure 3.1). In all cases the expected digest pattern was obtained confirming that they were correct and that the internal *Bsa*I sites had indeed been removed. Specific compatible sets of Level 0 modules were ligated into a complete functional transcription unit (TU), giving each Level 1 module. All Level 1 vectors are able to promote a known position and orientation for TUs.

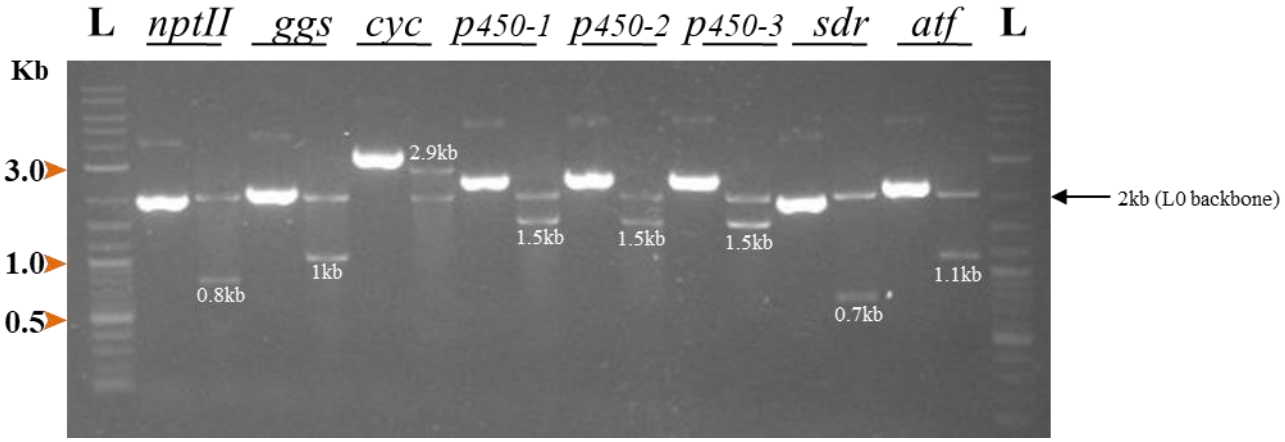

Figure 3.1 Agarose gel (1% w/v) of Level 0 plasmids, paired lanes of undigested DNA and DNA cut with *Bsa*I. **L** indicates the 1kb Plus DNA Ladder (2-log DNA Ladder) from New England BioLabs. The approximate expected band sizes are: for the plant selectable marker (*nptII)* 2kb and 0.8kb, for *geranylgeranyl pyrophosphate synthetase* (*ggs)* 2kb and 1kb, for *cyclase* (*cyc)* 2.9kb and 2kb, for *p450-1* 2kb and 1.5kb, for *p450-2* 2kb and 1.5kb, for *p450-3* 2kb and 1.5kb, for *short-chain dehydrogenase/ reductase (sdr)* 2kb and 0.7kb, for *acetyltransferase* (*atf)* 2kb and 1.1kb.

3.1.2 Level 1 plasmids

Having shown the level 0 cDNA plasmids were correct, two approaches were followed in order to create L1 (TU; Transcription Unit) plasmids; the first consisting

of the same promoter (CaMV 35S) and terminator (nopaline synthase) throughout all the TUs and the second using a diversity of transcriptional-regulatory elements, shown in Figure 3.3 A & B, and Table 2.8. In each case, the level 0 vector, the donor for the promoter region, terminator regions and the L1 acceptor vector were all digested with *Bsa*I. Digests were mixed together with ligase and rescued into *E. coli* based on selection of carbenicillin-resistance and white colonies on X-gal (20µg/ml) and IPTG (100µM). Plasmid construction was confirmed by restriction digest with *Bpi*I to show that the transcriptional unit has been correctly assembled. Indicative schematics of Level 0 and Level 1 plasmids are shown in Figure 3.2 (For all Level 0 and Level 1 plasmid maps see Appendix A). The restriction digest profiles of Level 1_35S and Level 1_D (Diverse promoters) are depicted in Figures 3.3.

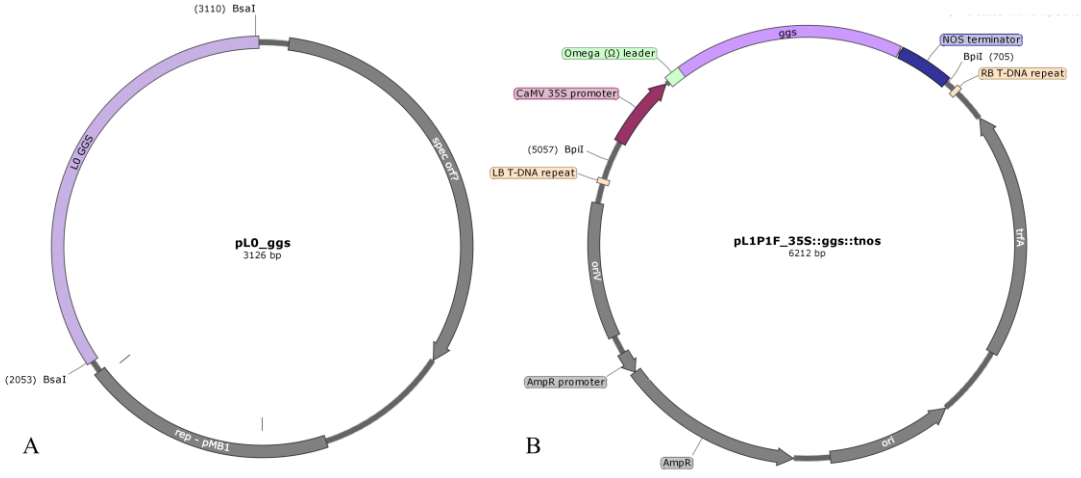

Figure 3.2 Plasmids of Level 0 (A) and Level 1 (B) of the *ggs* gene. All plasmids contain an antibiotic resistance gene for *E. coli* (spectinomycin for Level 0 and carbenicillin for Level 1 plasmid), Left and Right Borders for plant transformation via T-DNA transfer. For Level 0 and Level 1 restriction digests the enzymes *Bsa*I and *Bpi*I were used, respectively, and are shown in this figure.

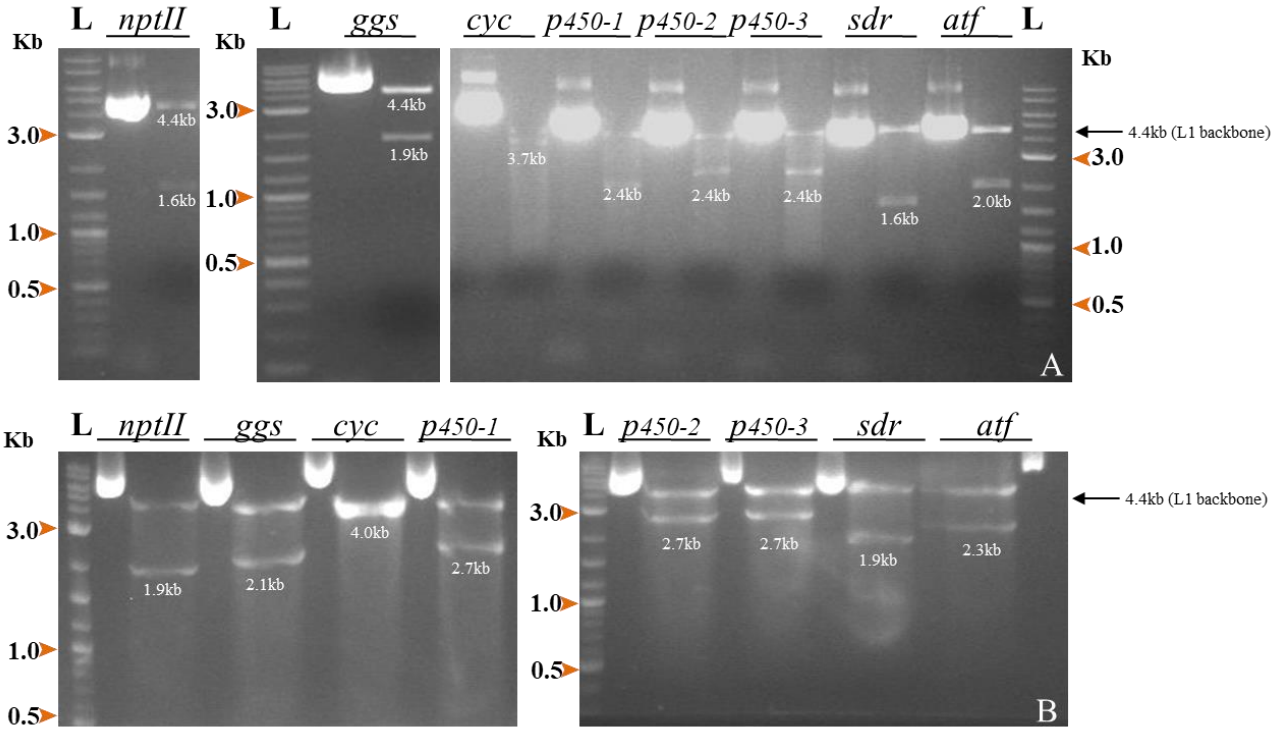

Figure 3.3 Agarose gel (1% w/v) of Level 1 TU plasmids, paired lanes of undigested DNA and DNA cut with *Bpi*I, **(A)** containing the same promoter (CaMV 35S) and terminator (nopaline synthase) for all the TUs and **(B)** using a diversity of transcription elements for the different TUs. **L** indicates the 1kb Plus DNA Ladder (2-log DNA Ladder) from New England BioLabs, which was used as a marker. The approximate expected band sizes are: **(A)** for *nptII* 4.4kb and 1.6kb, for *ggs* 4.4kb and 1.9kb, for *cyc* 4.4kb and 3.7kb, for *p450-1* 4.4kb and 2.4kb, for *p450-2* 4.4kb and 2.4kb, for *p450-3* 4.4kb and 2.4kb, for *sdr* 4.4kb and 1.6kb, for *atf* 4.4kb and 2kb and **(B)** for *nptII* 4.4kb and 1.9kb, for *ggs* 4.4kb and 2.1kb, for *cyc* 4.4kb and 4kb, for *p450-1* 4.4kb and 2.7kb, for *p450-2* 4.4kb and 2.7kb, for *p450-3* 4.4kb and 2.7kb, for *sdr* 4.4kb and 1.9kb, for *atf* 4.4kb and 2.3kb.

To confirm that the 35S cassette would work in both *M. polymorpha* and *P. patens*, a 35S::*gfp*::tnos was also made in the same way. Its digest profile is shown in Figure 3.4.

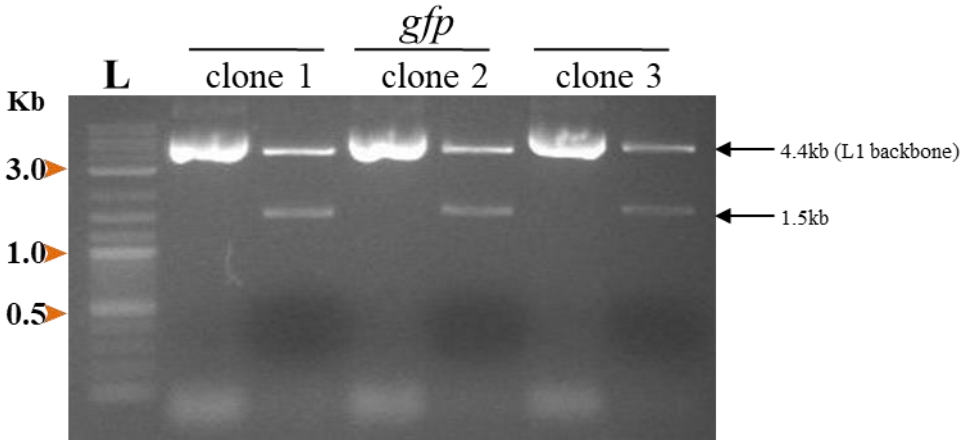

Figure 3.4 Agarose gel (1% w/v) of Level 1 35S::*gfp*::tnos, paired lanes showing plasmids undigested DNA and DNA cut with *Bpi*I. **L** indicates the 1kb Plus DNA Ladder (2-log DNA Ladder) from New England BioLabs, which was used as a marker. The approximate expected band sizes are: 4.4kb and 1.5kb.

Transformation of *P. patens* is more efficient if vectors include a region of host DNA, the usual locus being *Pp108*. Therefore the *Pp108* locus was amplified from *P. patens* (see section 2.3.4). As a vector backbone, pICH41331 was used, which consists of a Level 0 acceptor (TU vector) for complete gene modules. The digest profiles, PCR amplicons and the PCR gel used in gel extraction are depicted in Figure 3.5.

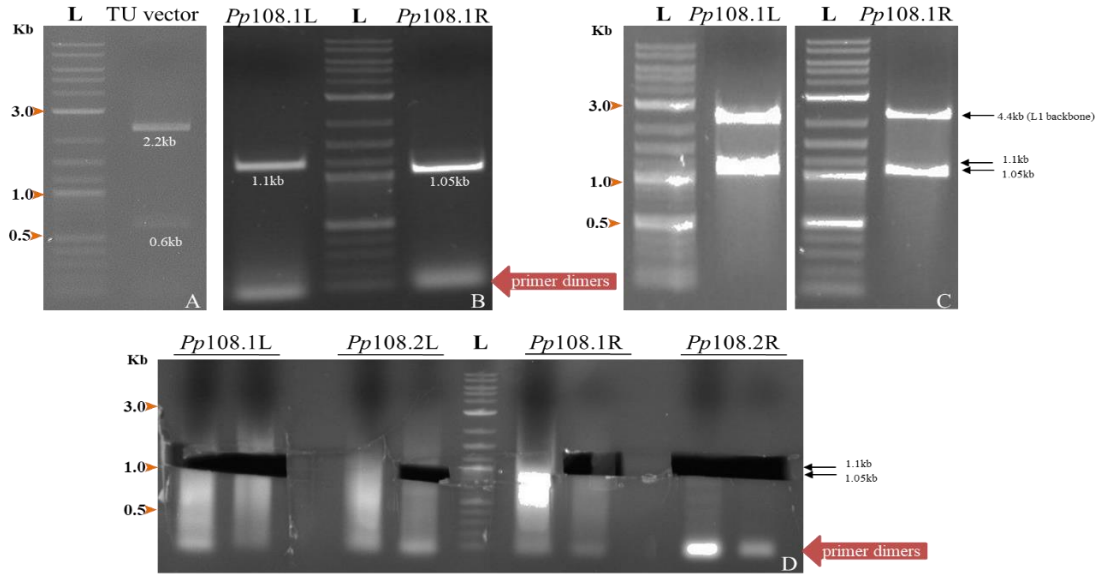

Figure 3.5 Agarose gel (1% w/v) of Level TU vector and *Pp108.1* locus amplicons, where **L** indicates the 1kb Plus DNA Ladder (2-log DNA Ladder) from New England BioLabs, which was used as a marker. **(A)** TU vector loaded cut with *Bsa*I and the approximate expected bands are: 2.2kb and 0.6kb. **(B)** PCR amplicons of *Pp*108.1L and *Pp*108.1R, with products at 1.1kb and 1.05kb, respectively. **(C)** Level 1 of *Pp*108.1L and *Pp*108.1R loaded cut with *Bpi*I and approximate expected bands are: for *Pp*108.1L 4.4kb and 1.1kb, for *Pp*108.1R 4.4kb and 1.05kb. **(D)** Cut gel after gel extraction in order to ligate the initial Pp108.1 and *Pp*108.2 loci into the TU vector, with products at 1.1kb for *Pp*108.1L and *Pp*108.2L and 1.05kb for *Pp*108.1R and *Pp*108.2R.

3.1.3 Level 2, M and P plasmids

In order to proceed to Level 2 (multigene constructs), Level 1, Level M for position 6 and Level M for position 7 vectors, as well as the end-linker pELB-4 were digested using *Bpi*I to confirm they were the correct starting material (Figure 2.6; Figure 3.6).

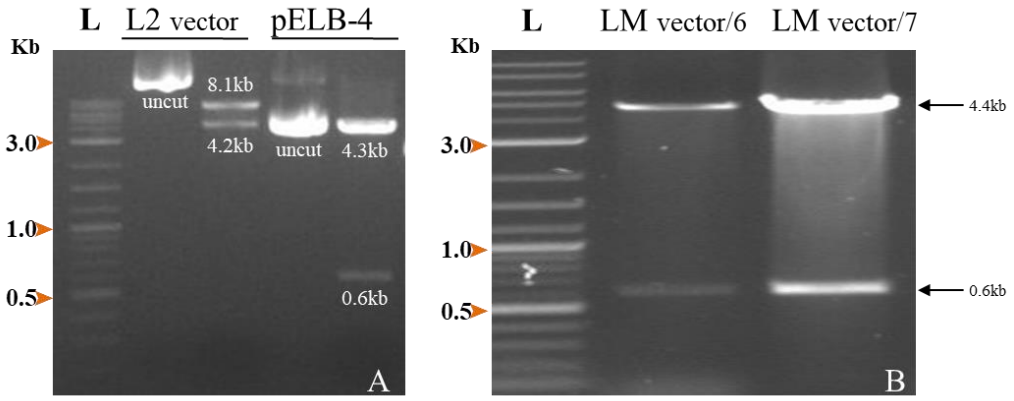

Figure 3.6 Agarose gel (1% w/v) of Level 2, Level M no6, Level M no7 and end-linker pELB4 vectors, where **L** indicates the 1kb Plus DNA Ladder (2-log DNA Ladder) from New England BioLabs, which was used as a marker. **(A)** L2 vector loaded uncut and cut with *Bpi*I, with expected bands at 8.1kb and 4.2kb and vector pELB-4 loaded uncut and cut with *Bsa*I, with expected bands at 4.3kb and 0.6kb. **(B)** LM no6 and LM no7 vectors loaded cut with *Bpi*I, with expected bands at 4.6kb and 0.6kb for both vectors.

The initial scheme was to make plasmids containing four genes: *ggs*, *cyc*, *p450-1* and *nptII*. Two versions were planned, one with all genes under control of 35S promoter and the other with diverse promoters. The plasmid maps of Level 2.4_D and Level 2.4_35S are shown in Figure 3.9. According to the Golden Gate scheme, ligation of the first four genes into the L2 vector should have given blue and red colonies only, where blue colonies have plasmids which had incorporated the end-linker and accordingly would be the ones selected for screening. However, apart from blue and red colonies, the reaction also led to a high proportion of white colonies. These were unexpected and might have been an indication of contamination or perhaps were the result of partial/incorrect ligation, thus giving unexpected byproducts (Figure 3.7). Therefore in order to eliminate any issues regarding *E. coli* cells or the transformation protocol, transformation efficiency, along with a negative control was checked (Figure 3.8).

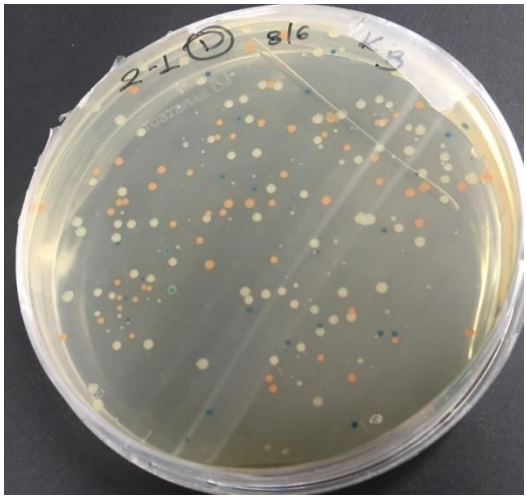

Figure 3.7 Transformation after ligation with Level 2.4 vector, containing the first four genes. Blue colonies have the *lacZ* end-linker, red have received the empty Level 2 vector containing the red colour selectable marker CRed and white colonies are probably partially ligated (byproducts).

Two different protocols were conducted, using a heat-shock period of 30 or 50 seconds, with the rest of the protocol steps staying the same. In the 30sec protocol 130 colonies were obtained, whereas the 50sec protocol gave 70 colonies (Figure 3.9). As a result, transformation efficiency in the first case was $\frac{130\text{cfu}}{0.05\text{ng}} = 2.6 \times 10^6\text{cfu/}\mu\text{gDNA}$ and in the second $\frac{70\text{cfu}}{0.05\text{ng}} = 1.4 \times 10^6\text{cfu/}\mu\text{gDNA}$, where cfu stands for colony-forming units. This is a low efficiency of transformation for golden-gate cloning methods, which recommends efficiencies of $>5\text{x}10^7$ cfu/μg DNA. The negative control gave no colonies, showing the cells were free of any contamination. Also, the *E. coli* TOP10 competent cells were plated onto LB with spectinomycin, carbenicillin or kanamycin, and none of these yielded any colonies, again confirming the cells were not contaminated.

Lab stocks of *E. coli* DH5α were also tested to see if they might perform better. On plating onto LB, the morphology of the colonies was unexpected (spreading and slimy). In addition transformation with the control plasmid pUC19 gave satellite colonies, which indicates that the cells may not be transformed but are resistant to ampicillin through secreted β-lactamase. The stock of DH5α was disposed of, and only the TOP10 strain was used onwards (Figure 3.8).

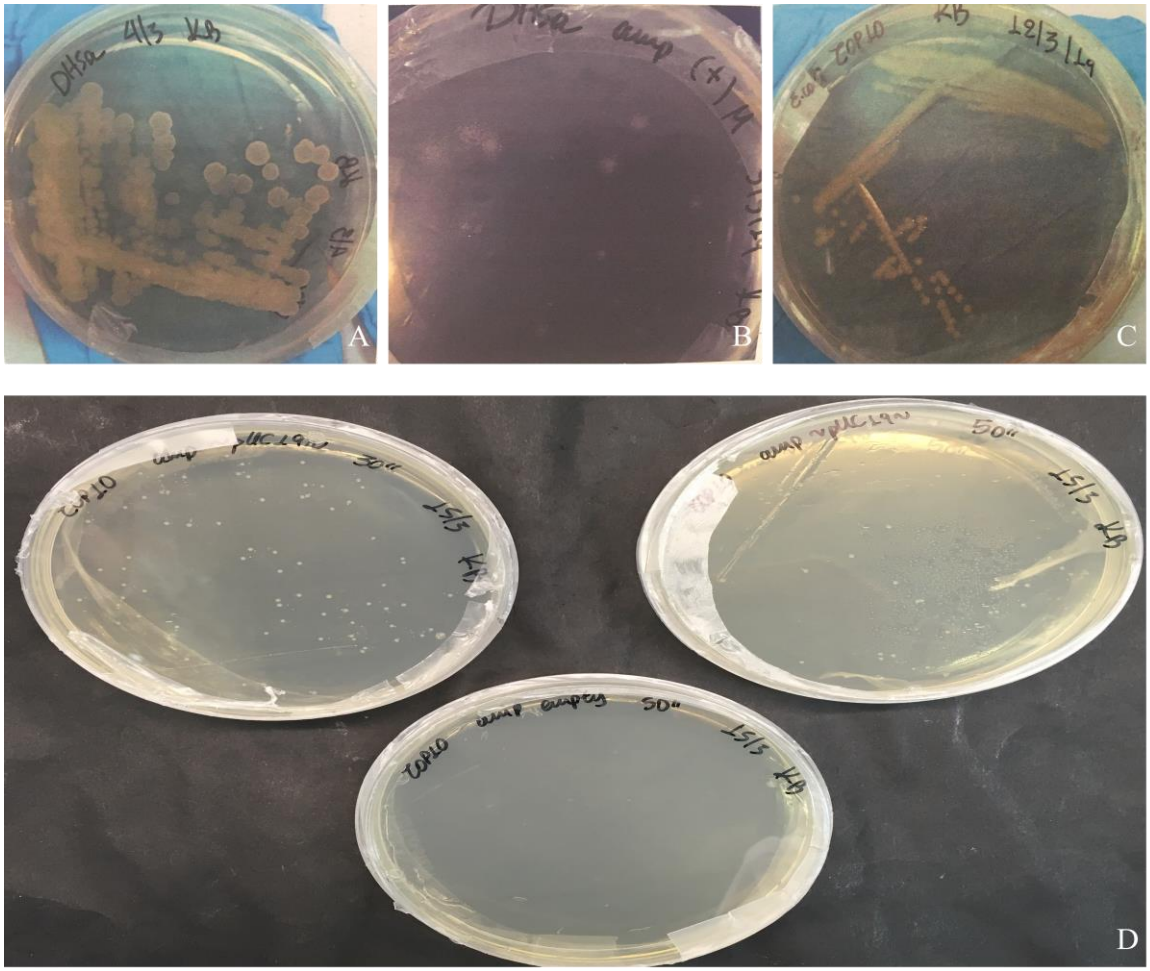

Figure 3.8 *E. coli* strains DH5α and TOP10, streaked on LB agar plates. (A) DH5α streaked on LB agar without antibiotics **(B)** DH5α transformed with pUC19 plasmid on LB agar with ampicillin **(C)** TOP10 streaked on LB agar without antibiotics **(D)** TOP10 transformed with pUC19 and 30sec heat-shock (up-left), 50sec heat-shock (up-right) and a negative control (bottom).

Unfortunately after screening some of the blue colonies, via plasmid extraction and restriction digestion, the wrong digest profiles were obtained, demonstrating that the *lac*Z cassette was incorporated but not all of the first four genes (Figure 3.10).

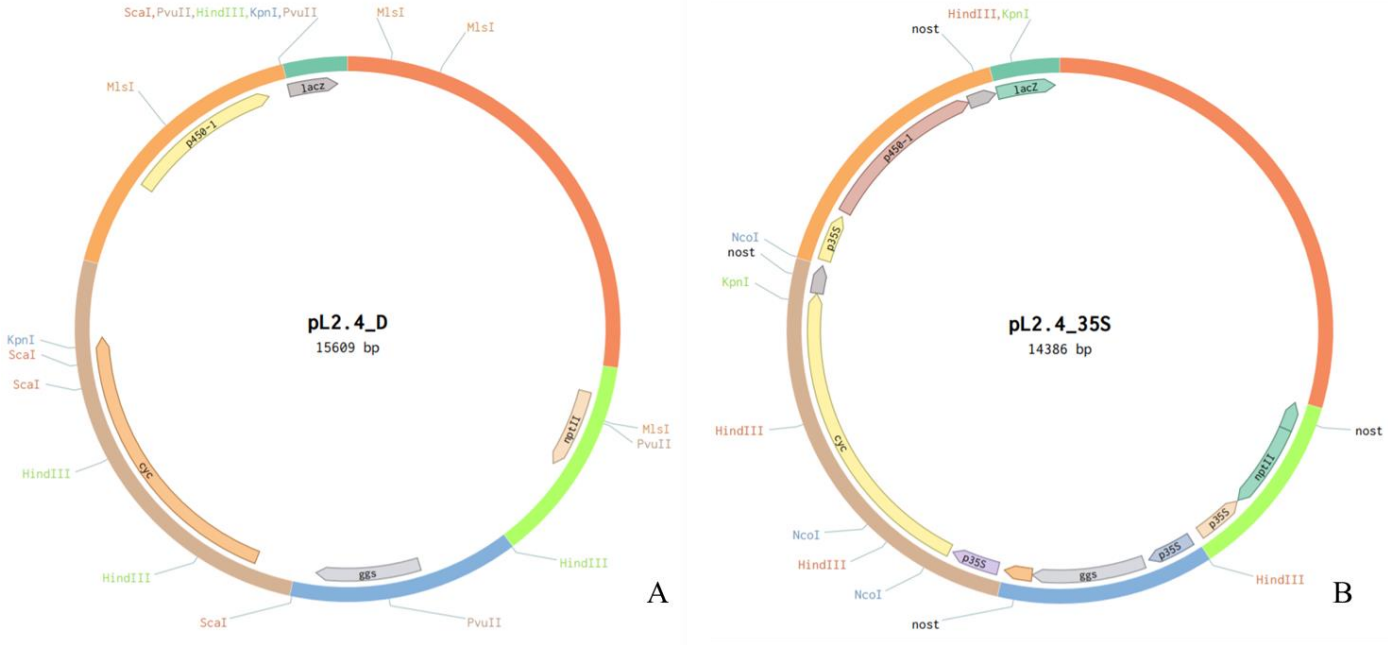

Figure 3.9 Predicted Plasmid maps of Level 2.4_D (A) and Level 2.4_35S (B).

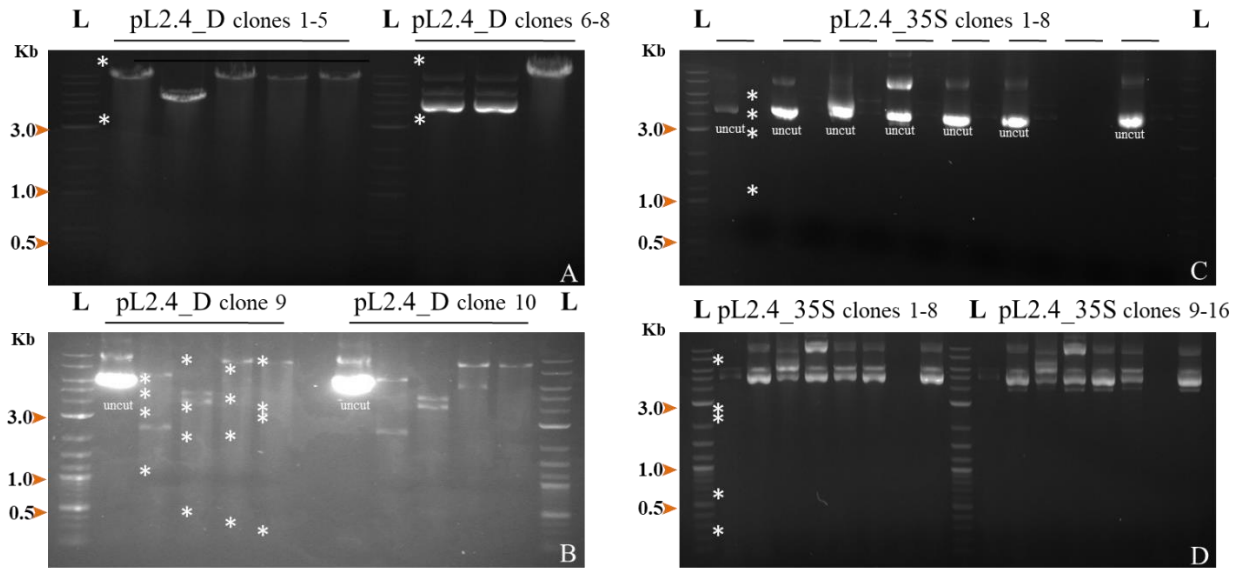

Figure 3.10 Agarose gel (1% w/v) of potential Level 2.4_D and Level 2.4_35S plasmids, uncut and/or cut with various restriction enzymes. L indicates the 1kb Plus DNA Ladder (2-log DNA Ladder) as a marker. Expected bands are shown using asterisks. (A) pL2.4_D clones 1-8 cut with *Kpn*I, with expected bands approximately at 11.9kb and 3.7kb (B) pL2.4_D clone 9 and 10, where each first line is loaded with uncut plasmid following cut with *Hind*III, *Msc*I, *Pvu*II and *Sca*I, respectively, where expected bands are at 6.5kb, 4.7kb, 3kb, 1.2kb for *Hind*III, 9kb, 3.8kb, 2,2kb, 0.5kb for *Msc*I, 7.6kb, 5kb, 2.6kb, 0.3kb for *Pvu*II, 9kb, 3.5kb, 3kb, 0.2kb for *Sca*I (C) pL2.4_35S clones 1-8 uncut and cut

with *Hind*III, with expected bands at 6.3kb, 4kb, 2.9kb, 1.2kb (D) pL2.4_35S clones 1-16 cut with *Kpn*I and *Nco*I with expected bands at 8.8kb, 2.6kb, 2.1kb, 0.6kb, 0.3kb.

The Level 1 plasmids which deliver each cassette had not previously been digested with these enzymes so there was a possibility that the predicted maps were incorrect, therefore the first four Level 1 transcription units were digested with *Hind*III and/or *Msc*I. This did give the expected profile (Figure 3.11), showing that the predicted maps were accurate and what had been obtained from the ligation was incorrect. Consequently, the troubleshooting was then focused on the dig-lig reaction conditions, contents and proportions. After testing multiple protocols, the final protocol that seemed to work best consisted of a double cycle number (50 cycles instead of 26), the addition of the 10x Buffer G, containing 0.1 mg/ml BSA, provided by Thermo and the T4 ligase, also provided by Thermo instead of the T4 ligase by New England Biolabs which was initially used (see section 2.3.3). This approach led to an increased number of colonies, eliminating colonies with the wrong colour and after screening nearly all chosen colonies depicted the correct digestion profile.

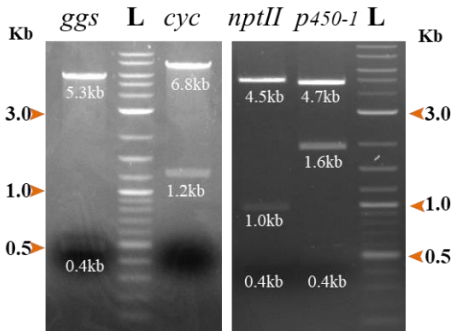

Figure 3.11 Agarose gel (1% w/v) of Level 1 and plasmids for the first four genes, cut with various restriction enzymes. **L** indicates the 1kb Plus DNA Ladder (2-log DNA Ladder) from New England BioLabs, which was used as a marker. 1st lane: pL1_pact2::ggs::t35S cut with *Hind*III and *Msc*I with expected bands at 5.3kb, 0.4kb, 3rd lane: pL1_pmas::cyc::tosc cut with *Hind*III with expected bands at 6.8kb, 1.2kb, 4th lane: pL1_p35S2x::nptII::tnos cut with *Msc*I with expected bands at

4.5kb, 1kb, 0.4kb, 5th lane: pL1_pact2::p450-1::t35S cut with *Msc*I with expected bands at 4.7kb, 1.6kb, 0.4kb.

After altering the dig-lig reaction protocol, the correct digest profiles were obtained (Figure 3.12, for plasmid maps see Appendix A). The separate dig-lig reactions were set as shown in Figure 2.6 and blue/white selection determined the isolation of the correct colour from each reaction/ plate. From this stage only the same 35S promoter approach continued. The pL2.3 plasmid, containing the genes *nptII*, *ggs* and *cyc* was isolated from white colonies, the pL2.4 plasmid containing the genes *nptII*, *ggs*, *cyc* and *p450-1* was isolated from blue colonies and the pL2.6 plasmid, containing the genes *nptII*, *ggs*, *cyc*, *p450-1*, *p450-2*, and *sdr* was also isolated from blue colonies.

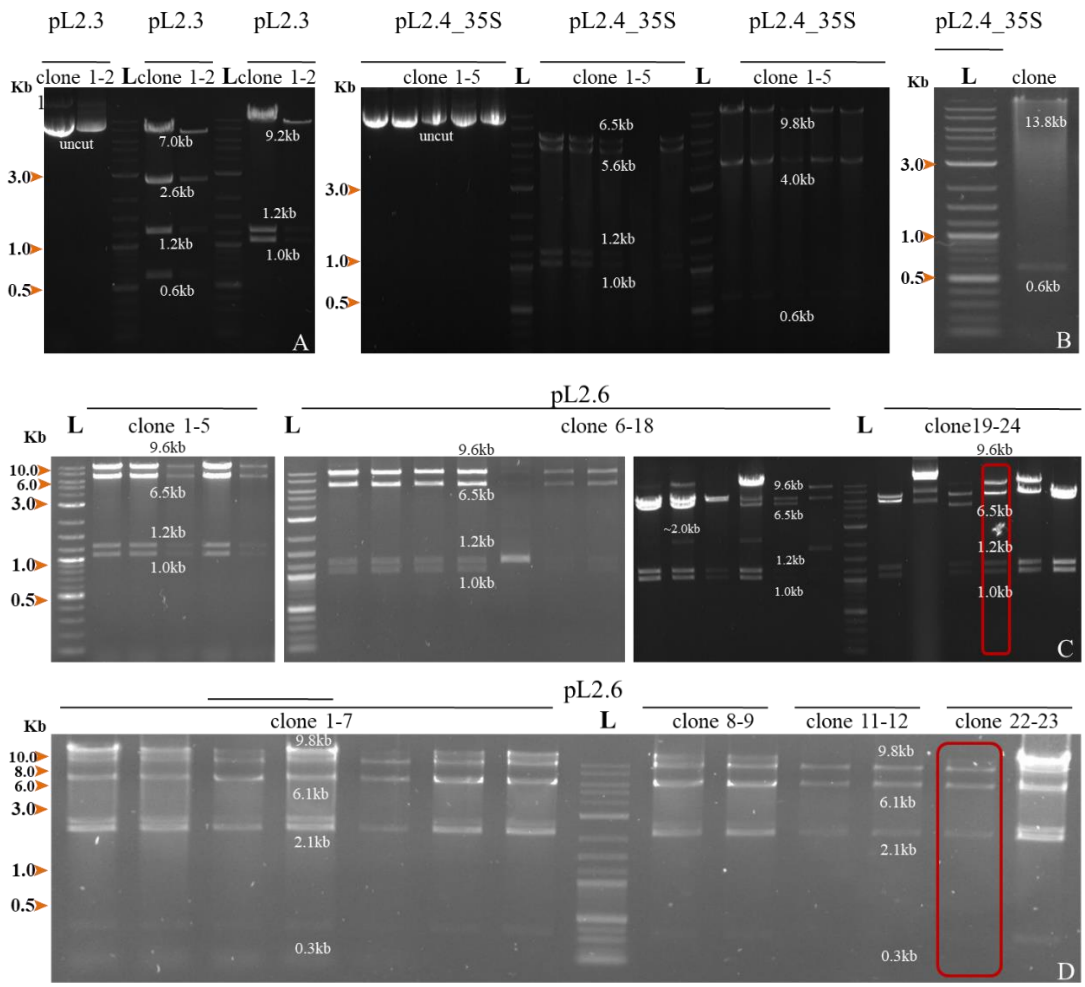

Figure 3.12 Agarose gel (1% w/v) of Level 2.3, 2.4 and 2.6 plasmids, cut with various restriction

enzymes. **L** indicates the 1kb Plus DNA Ladder (2-log DNA Ladder) from New England BioLabs, which was used as a marker. **(A)** pL2.3, containing the genes *ggs, cyc*, *nptII* uncut (lanes1,2) and cut with *Bam*HI (lanes 4, 5) with expected bands at 7kb, 2.6kb, 1.2kb, 0.6kb or *Hind*III (lanes 7, 8) with expected bands at 9.2kb, 1.2kb, 1kb, **(B)** pL2.4, containing the genes *ggs, cyc, nptII, p450-1* uncut (lanes 1-5) and cut with *Hind*III (lane 6-10) with expected bands at 6.5kb, 5.6kb, 1.2kb, 1kb, *Nco*I (lanes 12-16) with expected bands at 9.8kb, 4kb, 0.6kb or *Bsa*I (lane 18) with expected bands at 13.8kb, 0.6kb, **(C)** pL2.6, containing the genes *ggs, cyc, nptII, p450-1, p450-2, sdr* cut with *Hind*III throughout the gel with expected bands at 9.6kb, 6.5kb, 1.2kb, 1kb, **(D)** pL2.6, containing the genes *nptII, ggs, cyc, p450-1, p450-2, sdr* cut with *Kpn*I throughout the gel with expected bands at 9.8kb, 6.1kb, 2.1kb, 0.3kb. Clone 1, for pL2.3 and pL2.4, and clone 22 (red box) for pL2.6 were used in further experiments.

The first plasmid that was used for establishing *Agrobacterium*-mediated transformation of *M. polymorpha* within the lab was the one indicated as pL2.6 clone 22, shown in the red box in Figure 3.12. Despite repeated attempts with the transformation protocol for *M. polymorpha,* only necrotic thalli were generated with no successful geneticin-resistant lines. Careful scrutiny of the initial Level 0 coding sequence of the *nptII* gene (made by previous workers in the lab) led to the realization that its anti-sense form was cloned, thus resulting in a dysfunctional transcription unit. This assumption was also confirmed by sequencing. The correct orientation was therefore cloned into the Level 0 acceptor vector, *pICH41308*, amplified from the plasmid *pICSL70004*, using specific primers (see section 2.3.4; Figure 3.13). Level 0 plasmid was used to clone *nptII* into a Level 1 vector containing the 35S promoter and nopaline synthase terminator, and then used to make new Level 2 plasmids as detailed in Figure 3.14. When these correct constructs were used in transformation of *M. polymorpha*, geneticin-resistant thalli were successfully produced.

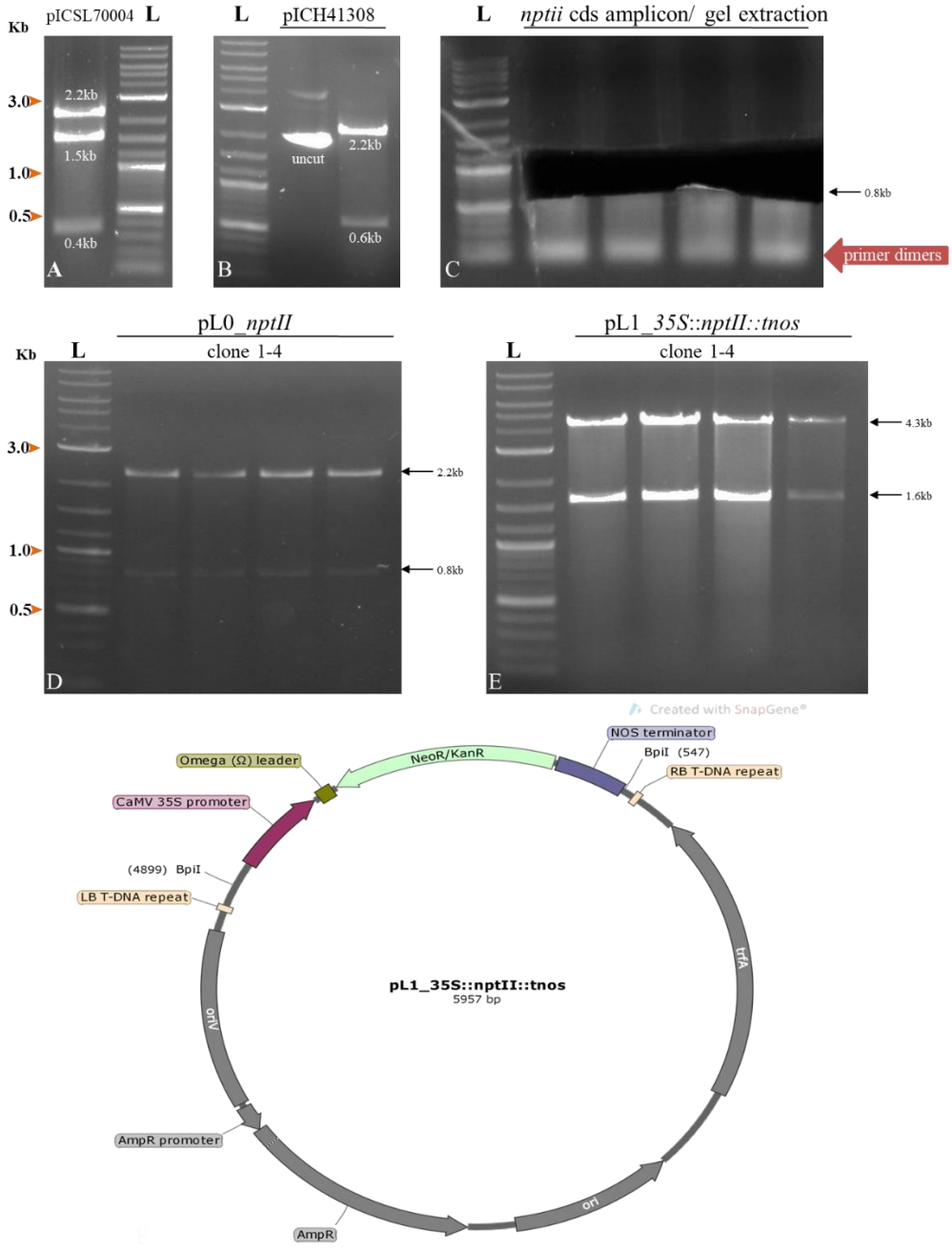

Figure 3.13 Agarose gel (1% w/v) of pICH41308, pICSL70004, *nptII* amplicon, Level 0 and Level 1, and initial Level 1 *nptII*. L indicates the 1kb Plus DNA Ladder. **(A)** pICSL70004 that contains the *nptII* coding sequence cut with *Bsa*I and *Nco*I, with expected bands at 2.2kb, 1.5kb, 0.4kb, **(B)** pICH41308 loaded uncut and cut with *Bsa*I, with expected bands at 2.2kb, 0.6kb, **(C)** PCR product of *nptII* with special flanking sites at 0.8kb and gel extraction, **(D)** pL0_nptII cut with *Bsa*I with expected bands at 2.2kb, 0.8kb, **(E)** pL1_35S::nptII::tnos cut with *Bpi*I with expected bands at 4.3kb, 1.6kb, **(F)** initial pL1_35S::nptII::tnos map where the antisense coding sequence is visible.

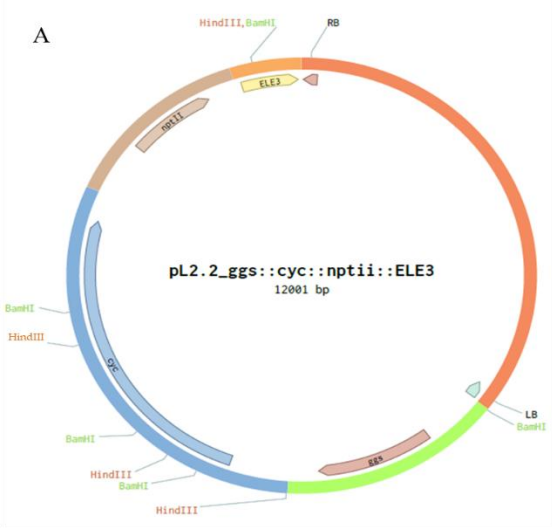
A
HindIII,BamHI
RB
ELE3
nptII
pL2.2_ggs::cyc::nptii::ELE3
12001 bp
BamHI
HindIII
cyc
BamHI
HindIII
BamHI
LB
BamHI
HindIII

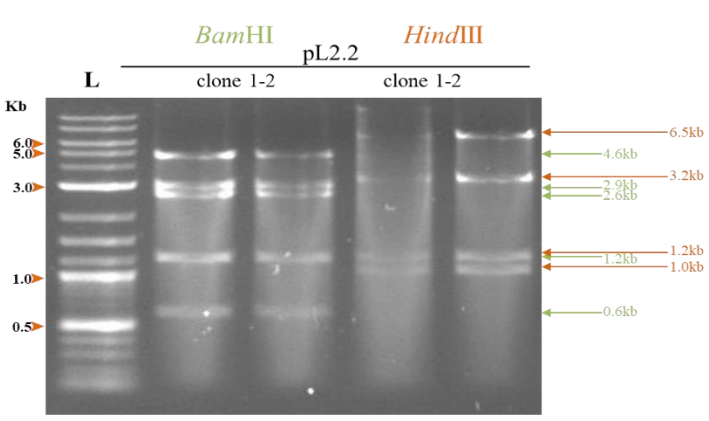
B
BamHI
HindIII
pL2.2
L
clone 1-2
clone 1-2
Kb
6.0
5.0
3.0
1.0
0.5
6.5kb
4.6kb
3.2kb
2.9kb
2.6kb
1.2kb
1.2kb
1.0kb
0.6kb

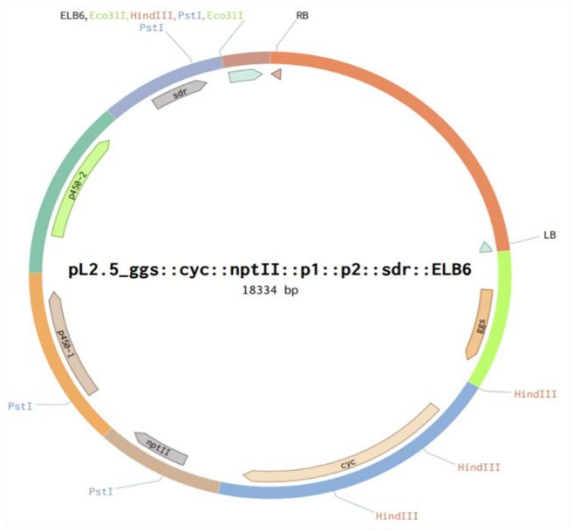
C
ELB6,Eco31I,HindIII,PstI,Eco31I
PstI
RB
sdr
p450-2
pL2.5_ggs::cyc::nptII::p1::p2::sdr::ELB6
18334 bp
LB
ELB6
p450-1
PstI
nptII
cyc
HindIII
HindIII
PstI
HindIII

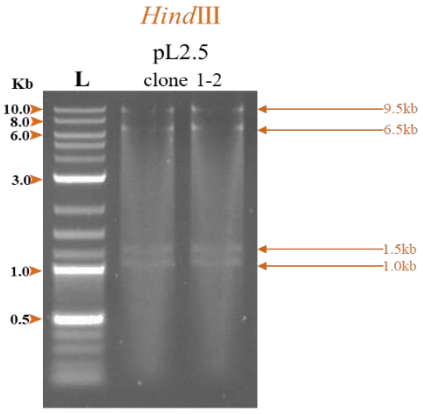
D
HindIII
pL2.5
Kb
L
clone 1-2
10.0
8.0
6.0
3.0
1.0
0.5
9.5kb
6.5kb
1.5kb
1.0kb

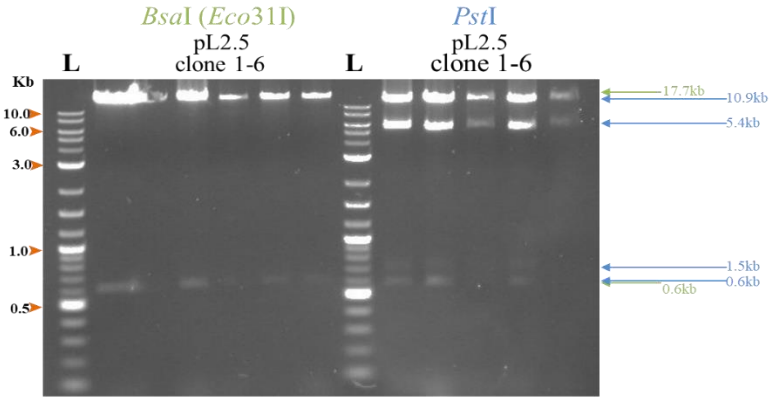
BsaI (Eco31I)
pL2.5
L
clone 1-6
PstI
pL2.5
L
clone 1-6
Kb
10.0
6.0
3.0
1.0
0.5
17.7kb
10.9kb
5.4kb
1.5kb
0.6kb
0.6kb

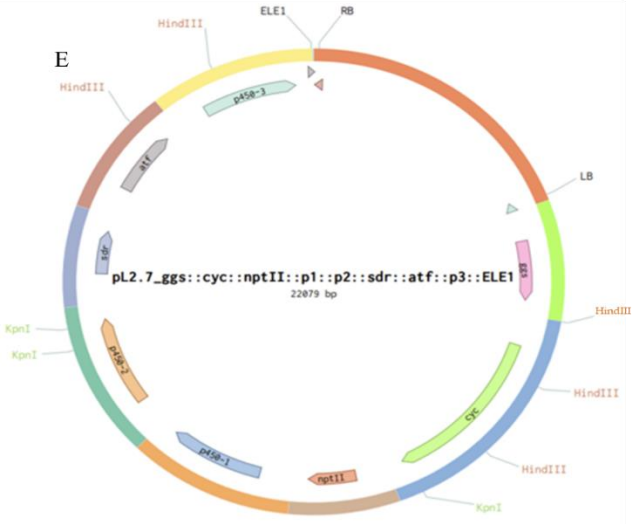
E
HindIII
ELE1
RB
HindIII
p450-3
atf
sdr
pL2.7_ggs::cyc::nptII::p1::p2::sdr::atf::p3::ELE1
22079 bp
ELE1
LB
HindIII
KpnI
KpnI
p450-2
HindIII
cyc
p450-1
nptII
HindIII
KpnI

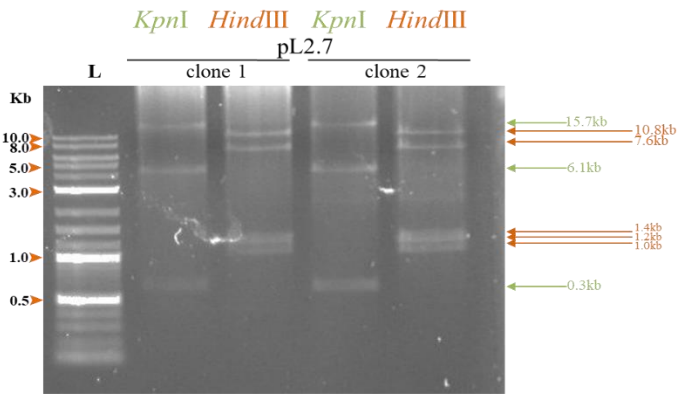
F
KpnI
HindIII
KpnI
HindIII
pL2.7
L
clone 1
clone 2
Kb
10.0
8.0
5.0
3.0
1.0
0.5
15.7kb
10.8kb
7.6kb
6.1kb
1.4kb
1.2kb
1.0kb
0.3kb

Figure 3.14 Agarose gel (1% w/v) of pL2.2, pL2.5 and pL2.7, all units containing the 35S promoter. L indicates the 1kb Plus DNA Ladder. **(A)** pL2.2_ggs::cyc::nptII::ELB3 map, **(B)** pL2.2, containing the genes *ggs*, *cyc*, *nptII* cut with *Bam*HI (lanes 2, 3) with expected bands at 4.6kb, 2.9kb, 2.6kb, 1.2kb, 0.6kb (green arrows) or *Hind*III (lanes 4, 5) with expected bands at 6.5kb, 3.2kb, 1.2kb, 1kb (orange arrows), **(C)** pL2.5_ggs::cyc::nptII::p1::p2::sdr::ELB6 map, **(D)** pL2.5, containing the genes *ggs*, *cyc*, *nptII*, *p450-1*, *p450-2*, *sdr* cut with *Hind*III (lanes 2, 3) with expected bands at 9.5kb, 6.5kb, 1.2kb, 1kb (orange arrows), *Bsa*I (lanes 2-7) with expected bands at 17.7kb, 0.6kb (green arrows), or *Pst*I (lanes 9-13) with expected bands at 10.9kb, 5.4kb, 1.5kb, 0.6kb (blue arrows), **(E)** pL2.7_ggs::cyc::nptII::p1::p2::sdr::atf::p3::ELE1 map, **(F)** pL2.7, containing the genes *ggs*, *cyc*, *nptII*, *p450-1*, *p450-2*, *sdr*, *atf*, *p450-3* cut with *Kpn*I (lanes 2,4) with expected bands at 15.7kb, 6.1kb, 0.3kb (green arrows) or *Hind*III (lanes 3,5) with expected bands at 10.8kb, 7.6kb, 1.4kb, 1.2kb, 1kb (orange arrows).

Table 3.1 Final plasmids made and used in transformation of *M. polymorpha* and *Agro*-infiltration of tobacco.

	pL1Empty	pL2.2	pL2.5	pL2.7
T-DNA	empty vector	2-gene vector	5-gene vector	7-gene vector
Coding sequences/ genes	*nptII*	*nptII*, *ggs*, *cyc*	*nptII*, *ggs*, *cyc*, *p450-1*, *p450-2*, *sdr*	*nptII*, *ggs*, *cyc*, *p450-1*, *p450-2*, *sdr*, *atf*, *p450-3*

Chapter 4: Assessing host-plant sensitivity to mutilins and other antibiotics

4.1 Aims

This chapter describes a series of investigations to determine whether the target plant hosts were susceptible to mutilin antibiotics. If they were sensitive, this might limit the utility as hosts for heterologous expression. To achieve this, the moss *P. patens* and liverwort *M. polymorpha* were grown in media as described in section 2.2.2, supplemented with a dilution series of antibiotics that cover a wide range of mechanisms of action, including pleuromutilin derivative, tiamulin, and mutilin, such as the pleuromutilin derivative, tiamulin, and a precursor of pleuromutilin, mutilin. Denagard® (tiamulin hydrogen fumarate) was used as a semi-synthetic pleuromutilin derivative. In addition, the antibiotics chloramphenicol, kanamycin and nalidixic acid were used in both plant growth assays, while ampicillin was also tested in *M. polymorpha*. These additional assays were carried out as positive controls, as there has been relevant work in the literature (Kasten & Reski, 1997; Katayama et al., 2003; Tounou et al., 2002). Detailed preparation of antibiotics is shown in Table 2.3. All antibiotics were supplemented in the media at concentrations of: 0µg/ml (untreated), 1µg/ml, 5µg/ml, 10µg/ml, 50µg/ml, 100µg/ml, 200µg/ml, 250µg/ml and 500µg/ml. Untreated plants were mock treated using solvent as indicated in Sections 2.2.2 and 2.3.

4.1.1 Effect of antibiotics on growth of *P. patens* and *M. polymorpha*

The pleuromutilin derivative, tiamulin, appears to affect the growth of both plants, causing a reduction in size. *P. patens* was viable when grown in up to 10µg/ml

tiamulin (Figure 4.1), but a reduction in moss colony diameter was observed with concentrations higher than1μg/ml. At concentrations higher than 10μg/ml there was no growth. *M. polymorpha* was more tolerant and could generate a thallus when grown in up 50μg/ml, although there was a visible effect on thallus growth at concentrations above 1 μg/ml tiamulin (Figure 4.2). Complete inhibition of growth was observed at concentrations higher than 50mg/ml.

Mutilin is a pathway precursor of pleuromutilin. When tested with *P. patens*, this still supported a colony diameter of 0.3cm at 250μg/ml. At concentrations higher than 250mg/ml, there was no growth. This means that mutilin needed an approximate 25-fold increase in antibiotic concentration to deliver the same level of growth inhibition when compared to tiamulin. In *M. polymorpha*, a similar outcome was observed, with an average of $0.1cm^2$ thallus area produced at the highest concentration of 500μg/ml mutilin (Figures 4.3 and 4.4), indicating a 10-fold greater tolerance to mutilin compared to tiamulin.

When supplemented with chloramphenicol, moss colony diameter showed a moderate decrease in growth, where at 50μg/ml this decrease was readily observed, while at concentrations greater than 100μg/ml the inoculum did not grow. In contrast, *Marchantia* thalli were not notably affected at low concentrations, yet showed a dramatic reduction in growth at 50μg/ml, indicating a tolerance threshold. At higher concentrations gemmae did not generate thalli (Figures 4.5 and 4.6).

The treatment of *P. patens* with kanamycin had little effect at concentrations up to 10μg/ml, but there was a considerable decrease in colony diameter between 50 and 100μg/ml and no growth at higher concentrations. In *M. polymorpha* a similar result was observed, with little effect of kanamycin at low concentrations, but a sharp

decline in thallus area above 50µg/ml. There were some occasions where growth of thalli up to 250µg/ml was observed (Figures 4.7 and 4.8).

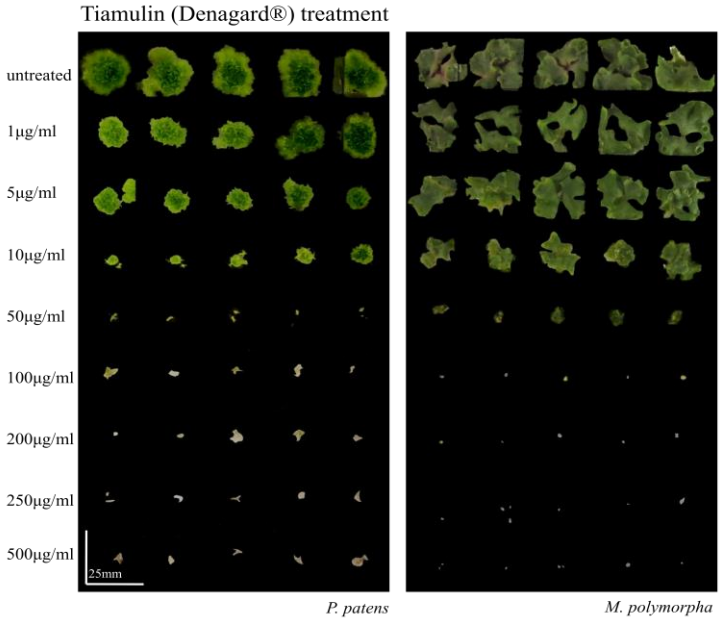

Figure 4.1 Tiamulin treatment assay for *P. patens* (left) and *M. polymorpha* (right), grown on tiamulin concentrations ranging from 1 to 500µg/ml. Mock assays were treated using solvent (untreated). Each assay consisted of 3 technical replicates (representative images shown above with additional replicates in Appendix B, for *P. patens* n=15 and for *M. polymorpha* n=15). Scale bar is at 25mm.

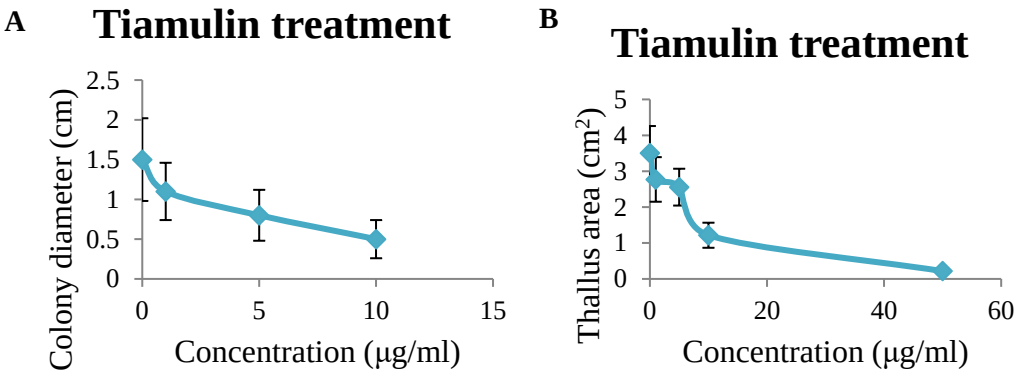

Figure 4.2 Tiamulin treatment assay for *P. patens* (A) and *M. polymorpha* (B), grown on tiamulin concentrations ranging from 1 to 500µg/ml. Mock assays were treated using solvent (untreated). Values are the average ±SD measurements of colony diameter of *P. patens* **(A)** and thallus area of *M.*

polymorpha **(B)**, respectively. Each assay consisted of 3 technical replicates, measured according to Figure 3.15 and the other replicates (shown in Appendix B, for *P. patens* n=15 and for *M. polymorpha* n=15).

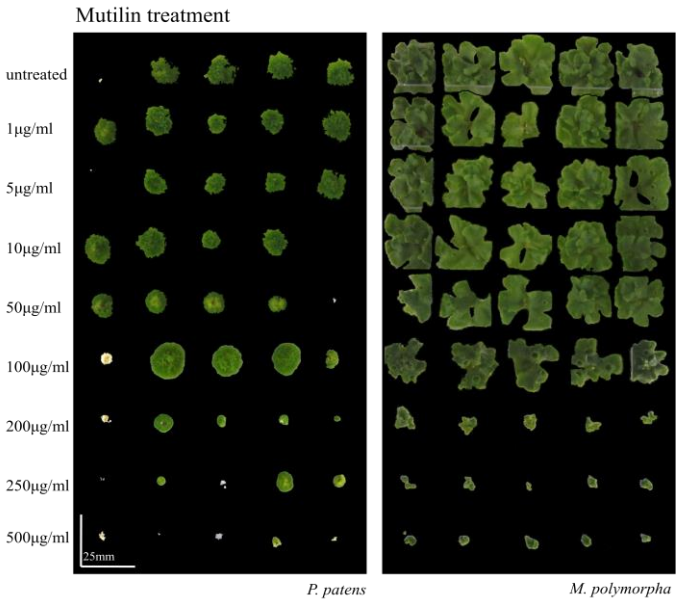

Figure 4.3 Mutilin treatment assay for *P. patens* (left) and *M. polymorpha* (right), grown on mutilin concentrations ranging from 1 to 500µg/ml. Mock assays were treated using solvent (untreated). Each assay consisted of 3 technical replicates (representative images shown above with additional replicates in Appendix B, for *P. patens* n=10 and for *M. polymorpha* n=15). Scale bar is at 25mm.

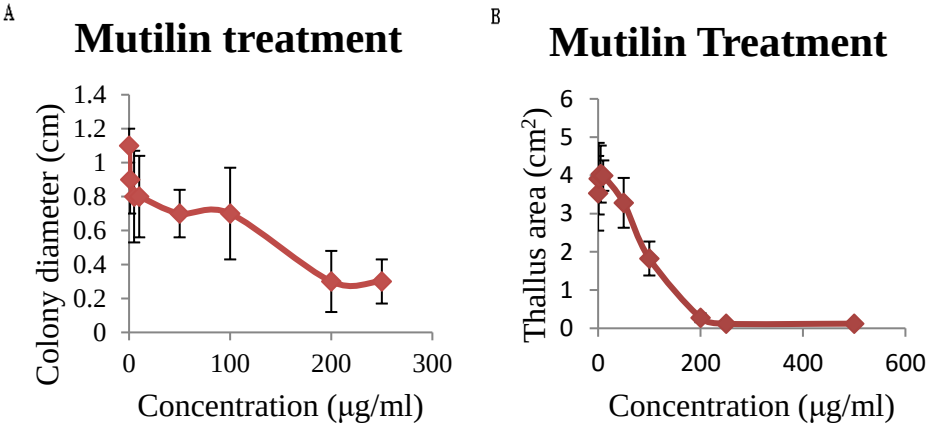

Figure 4.4 Mutilin treatment assay for *P. patens* (A) and *M. polymorpha* (B), grown on mutilin concentrations ranging from 1 to 500µg/ml. Mock assays were treated using solvent (untreated). Values

are the average ±SD measurements of colony diameter of *P. patens* **(A)** and thallus area of *M. polymorpha* **(B)**, respectively. Each assay consisted of 3 technical replicates, measured according to Figure 3.17 and the other replicates (shown in Appendix B, for *P. patens* n=10 and for *M. polymorpha* n=15).

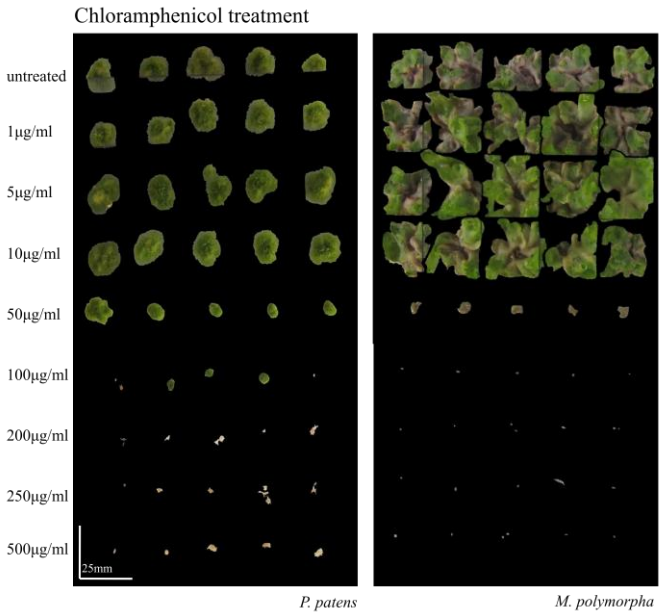

Figure 4.5 Chloramphenicol treatment assay for *P. patens* (left) and *M. polymorpha* (right), grown on media containing chloramphenicol concentrations ranging from 1 to 500µg/ml. Mock assays were treated using solvent (untreated). Each assay consisted of 3 technical replicates (representative images shown above with additional replicates in Appendix B, for *P. patens* n=15 and for *M. polymorpha* n=10). Scale bar is at 25mm.

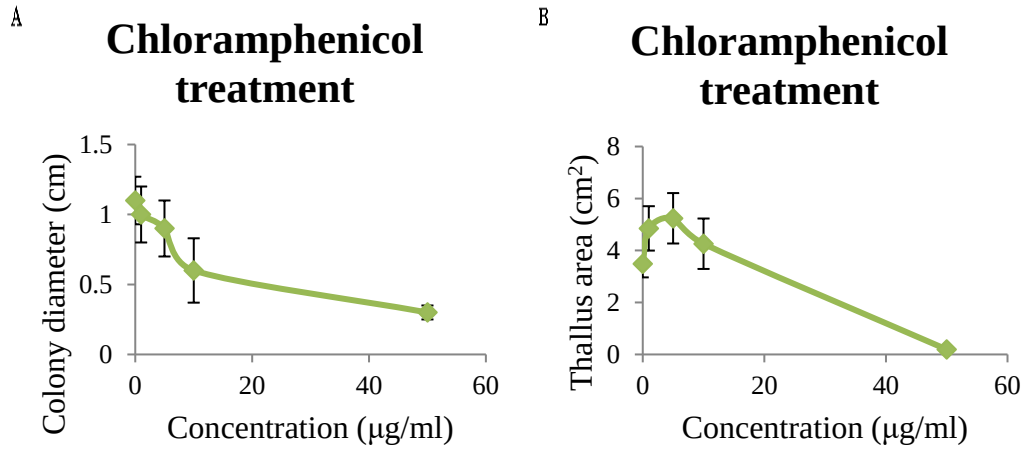

Figure 4.6 Chloramphenicol treatment assay for *P. patens* (A) and *M. polymorpha* (B), grown on chloramphenicol concentrations ranging from 1 to 500µg/ml. Mock assays were treated using solvent (untreated). Values are the average ±SD measurements of colony diameter of *P. patens* **(A)** and thallus area of *M. polymorpha* **(B)**, respectively. Each assay consisted of 3 technical replicates, measured according to Figure 3.19 and the other replicates (shown in Appendix B, for *P. patens* n=15 and for *M. polymorpha* n=10).

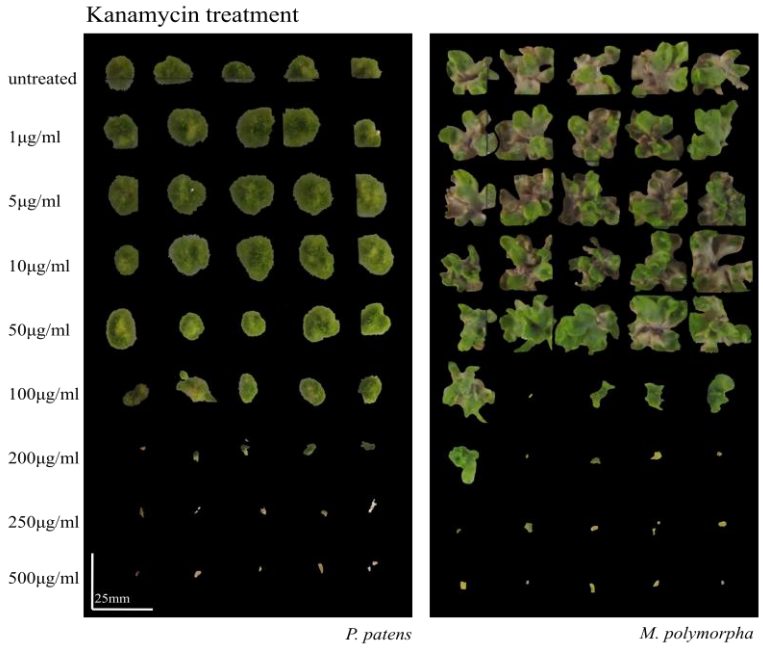

Figure 4.7 Kanamycin treatment assay for *P. patens* (left) and *M. polymorpha* (right), grown on kanamycin concentrations ranging from 1 to 500µg/ml. Mock assays were treated using solvent (untreated). Each assay consisted of 3 technical replicates (representative images shown above with additional replicates in Appendix B, for *P. patens* n=15 and for *M. polymorpha* n=15). Scale bar is at 25mm.

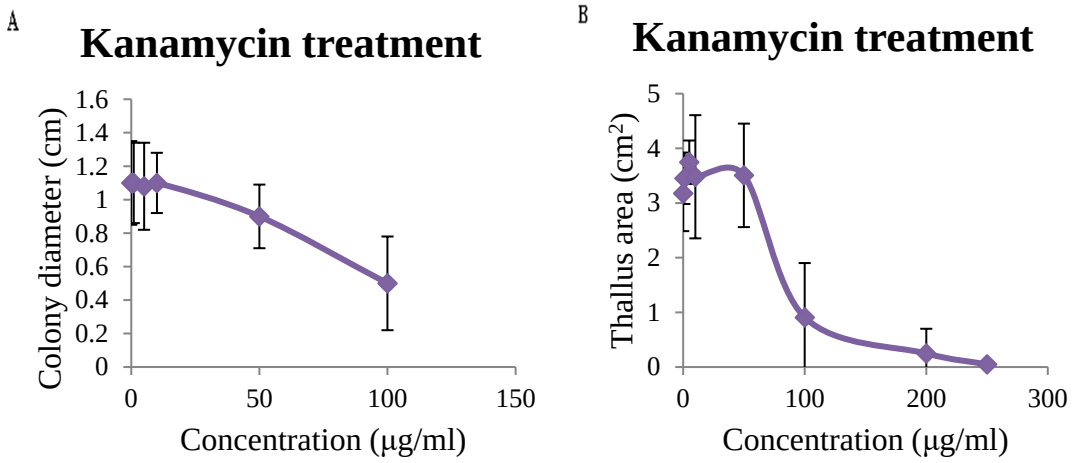

Figure 4.8 Kanamycin treatment assay for *P. patens* (A) and *M. polymorpha* (B), grown on kanamycin concentrations ranging from 1 to 500µg/ml. Mock assays were treated using solvent (untreated). Values are the average ±SD measurements of colony diameter of *P. patens* **(A)** and thallus area of *M. polymorpha* **(B)**, respectively. Each assay consisted of 3 technical replicates, measured according to Figure 3.21 and the other replicates (shown in Appendix B, for *P. patens* n=15 and for *M. polymorpha* n=15).

Treatment of moss with nalidixic acid gave a decline in growth starting from the treatment of 1µg/ml, while at concentrations higher than 10µg/ml there was total inhibition of growth. It is worth mentioning that a considerable decrease in size was observed in untreated samples. Additionally, when supplemented in *M. polymorpha* media, nalidixic acid repressed growth at concentrations above 5µg/ml, with only rare instances of thalli growth at 5µg/ml (Figures 4.9 and 4.10).

As far as the treatment with ampicillin is concerned, *M. polymorpha* thalli only showed a small reduction in growth at concentrations over 100µg/ml (Figures 4.11 and 4.12) so can be considered tolerant of ampicillin.

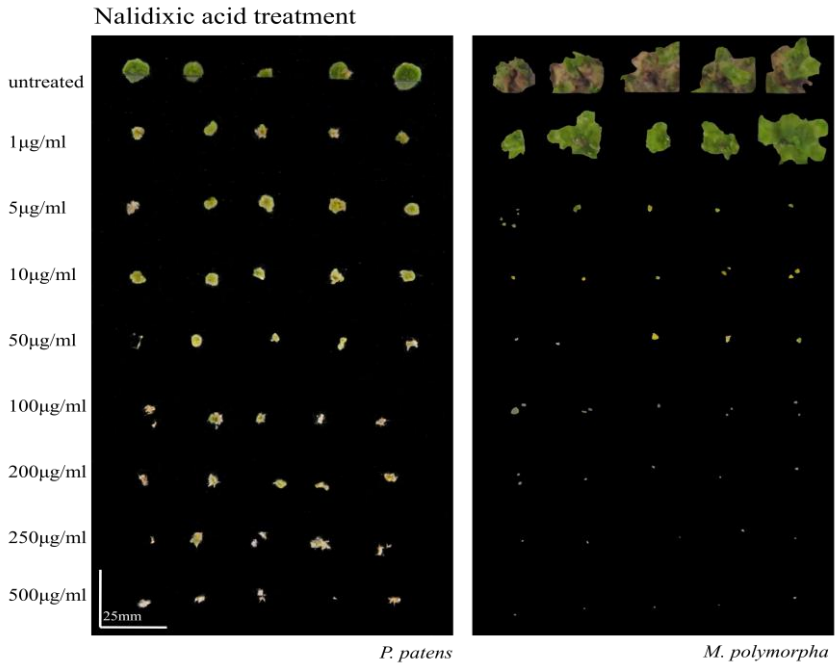

Figure 4.9 Nalidixic acid treatment assay for *P. patens* (left) and *M. polymorpha* (right), grown on nalidixic acid concentrations ranging from 1 to 500µg/ml. Mock assays were treated using solvent (untreated). Each assay consisted of 3 technical replicates (representative images shown above with additional replicates in Appendix B, for *P. patens* n=15 and for *M. polymorpha* n=15). Scale bar is at 25mm.

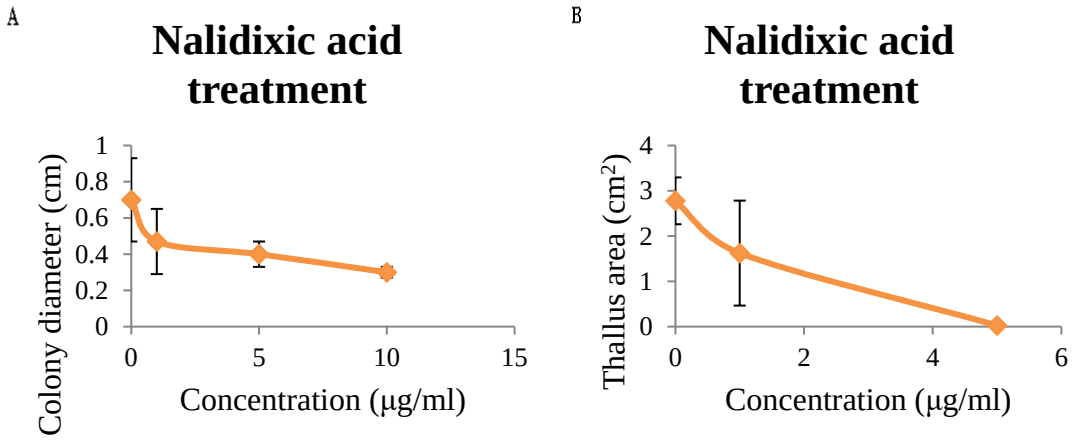

Figure 4.10 Nalidixic acid treatment assay for *P. patens* (A) and *M. polymorpha* (B), grown on nalidixic acid concentrations ranging from 1 to 500µg/ml. Mock assays were treated using solvent (untreated). Values are the average ±SD measurements of colony diameter of *P. patens* **(A)** and thallus area of *M. polymorpha* **(B)**, respectively. Each assay consisted of 3 technical replicates, measured

according to Figure 3.23 and the other replicates (shown in Appendix B, for *P. patens* n=15 and for *M. polymorpha* n=15).

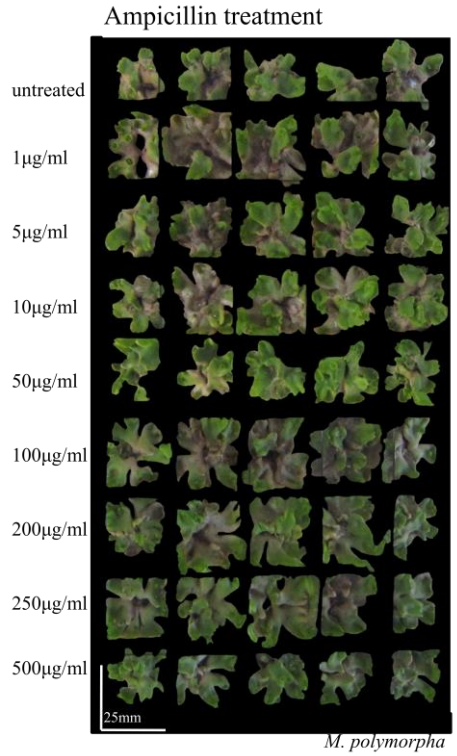

Figure 4.11 Ampicillin treatment assay for *M. polymorpha*, grown on ampicillin concentrations ranging from 1 to 500µg/ml. Mock assays were treated using solvent (untreated). The assay consisted of 3 technical replicates (representative images shown above with additional replicates in Appendix B, for *M. polymorpha* n=15). Scale bar is at 25mm.

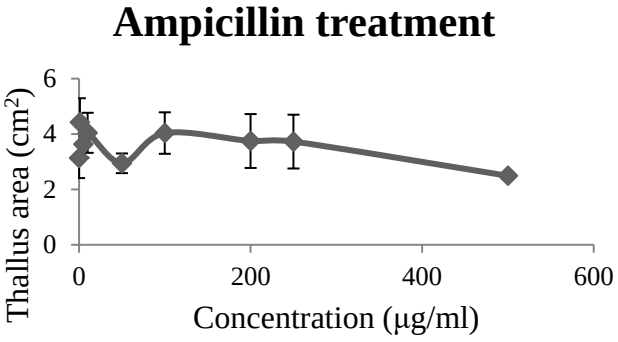

Figure 4.12 Ampicillin treatment assay for *M. polymorpha*, grown on ampicillin concentrations ranging from 1 to 500µg/ml. Mock assays were treated using solvent (untreated). Values are the average ±SD measurements of thallus area of *M. polymorpha*. The assay consisted of 3 technical

replicates, measured according to Figure 3.25 and the other replicates (shown in Appendix B, for *M. polymorpha* n=15).

4.1.2 Effect of antibiotics on the morphology of *P. patens* and *M. polymorpha*

Treatment using different antibiotics led to the appearance of different characteristic phenotypes. Untreated moss had a colony morphology consisting of filaments and covered with leafy gametophores as shown in Figure 4.13. Treatment with mutilin at a concentration above 50µg/ml led to compact colonies with filamentous protonemata and reduced number of leafy gametophores (Fig 4.13 B) or solely filamentous protonemata at concentrations higher than 100µg/ml (Fig 4.13 C). This latter morphology was also observed with chloramphenicol treatment at the concentration of 50µg/ml and kanamycin treatment at the concentration of 100µg/ml.

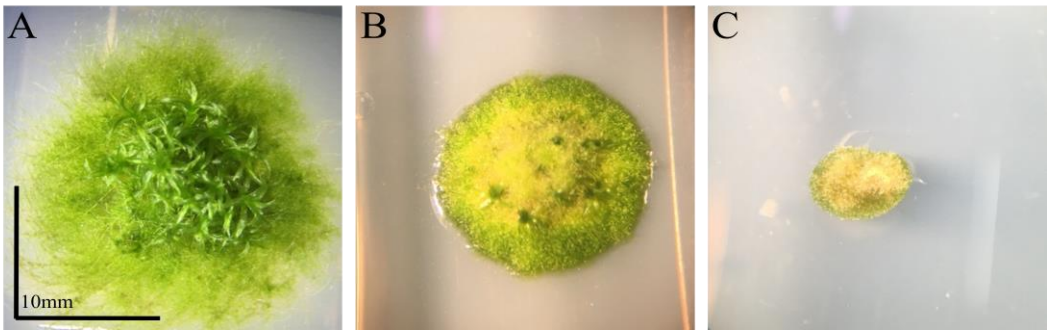

Figure 4.13 Developmental effects of antibiotics on *P. patens*. (A) Untreated colonies grown in solvent, **(B)** mutilin at 50µg/ml and **(C)** mutilin at 100µg/ml or above. Similar effects were seen in plants gnown on media containing chloramphenicol at 50µg/ml or above, or kanamycin at 100µg/ml or above. Scale bar is at 10mm.

Untreated *M. polymorpha* thalli demonstrate a dorsiventral pattern with gemma cups, where gemmae are produced as shown in Figure 4.14. When plants were

grown on concentrations equal or higher than: 10µg/ml pleuromutilin, 100µg/ml mutilin, 100µg/ml kanamycin and 1µg/ml nalidixic acid, the "intermediate phenotype" was produced with a hyponastic curvature of the thallus, a reduced size and reduced dorsiventrality, but still producing rhizoids (Fig 4.14 B). Gemma cups are non-existent in this figure, but thalli eventually are capable of developing a few gemma cups, days or weeks later than untreated cultures. Treatments with kanamycin above 100µg/ml gave a severe impact on morphology which appeared as an undifferentiated mass, (Fig 4.14 C).

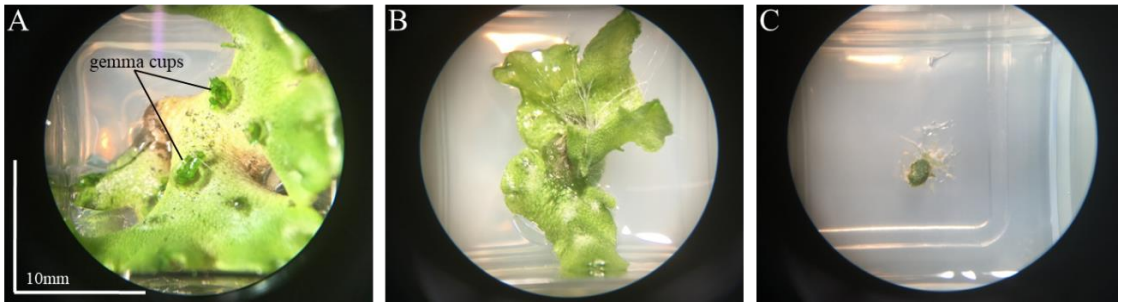

Figure 4.14 Developmental effects of antibiotics on *M. polymorpha*. (A) Untreated colonies grown in solvent, **(B)** pleuromutilin, mutilin, kanamycin or nalidixic acid and **(C)** kanamycin. Scale bar is at 10mm.

Along with the macro-morphology of moss colonies, filamentous protonemata were observed under the microscope in order to evaluate the impact of the antibiotics on chloroplast numbers and locations. Pleuromutilin (5µg/ml) and mutilin (100µg/ml) had no obvious impact on either protonemata morphology or chloroplasts as shown in Figure 4.15, apart from reduction of protonemata perimeter observed in Figure 4.1 and 4.3, respectively. In contrast, chloramphenicol (100µg/ml), kanamycin (100µg/ml) and nalidixic acid (10µg/ml) led to a degraded appearance of protonemata and a yellowing chlorotic tint of chloroplasts.

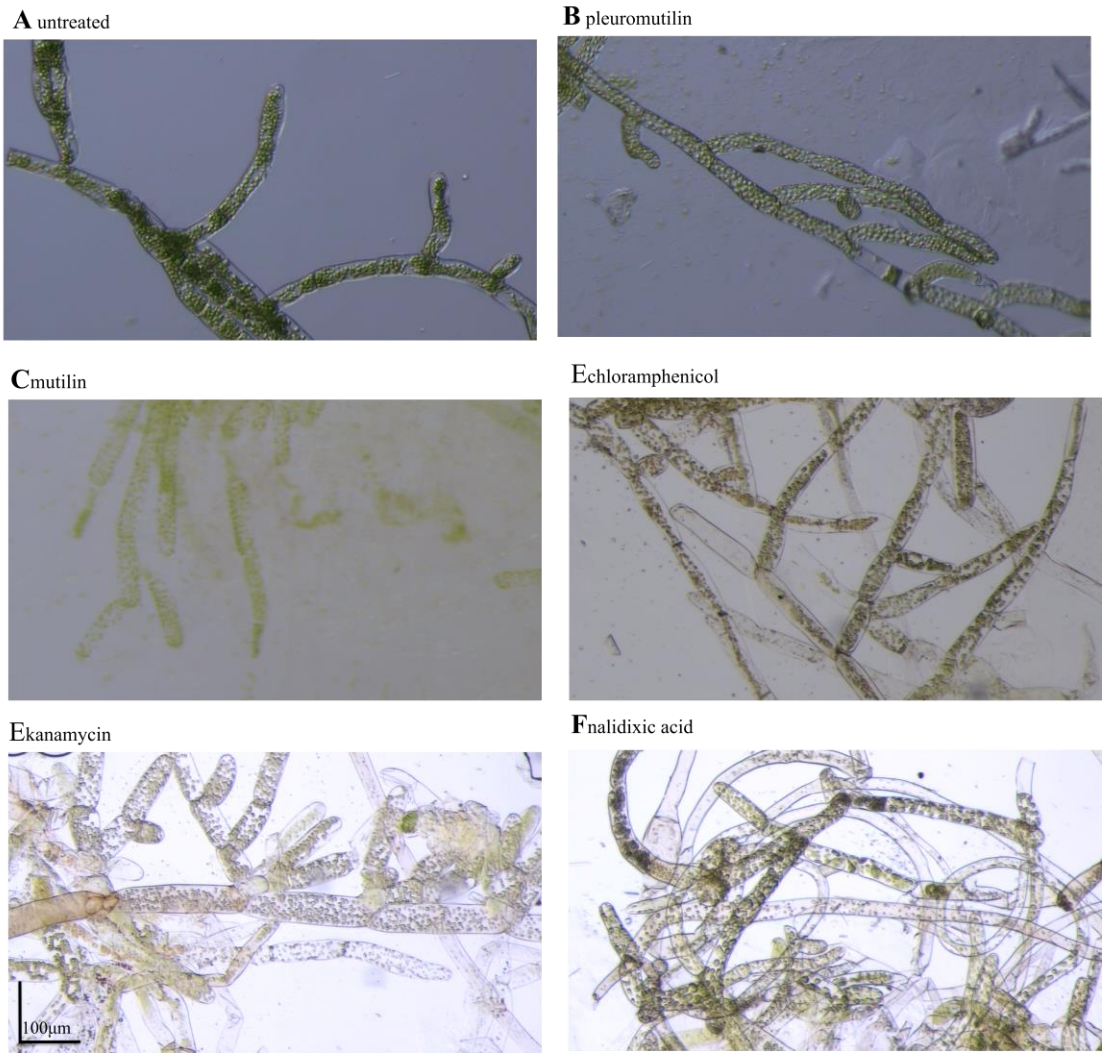

Figure 4.15 Effects of antibiotics on *P. patens* protonemata. (A) Untreated colonies grown in solvent, **(B)** pleuromutilin (5µg/ml), **(C)** mutilin (100µg/ml), **(D)** chloramphenicol (100µg/ml), **(E)** kanamycin (100µg/ml) and **(F)** nalidixic acid (10µg/ml). Scale bar is at 100µm.

The sensitivity of *M. polymorpha* and *P. patens* appeared to be sufficiently low for mutilin but relatively high for the pleuromutilin derivative, tiamulin. However, without having fine-tuned the heterologous expression *in planta*, it was possible that the hosts would be producing quite low concentrations of the compounds, resulting in mild or no toxicity.

Chapter 5: Heterologous plant hosts for expression of the pleuromutilin biosynthetic pathway

5.1 Aim

The aim of this chapter was to obtain *M. polymorpha* transformants, analyse gene expression and detect metabolites. The pleuromutilin derivative, tiamulin, caused a reduction in size of *P. patens* colonies diameter at 10μg/ml tiamulin (Figure 4.1), with a smaller reduction at 1μg/ml, and no growth at concentrations higher than 10μg/ml. *M. polymorpha* was more tolerant and could generate a thallus when grown in up to 50μg/ml, although growth was affected in concentration of 1μg/ml tiamulin (Figure 4.2), while total inhibition of growth was observed at concentrations higher than 50mg/ml. Due to these observations, the 2-gene and 5-gene construct were used in order to study three critical steps in pleuromutilin pathway, the cyclization of GGPP to 3-deoxo-11-dehydroxy-mutilin (2-gene construct) and the dehydrogenation of 3,11-dihydroxy premutilin to mutilin (5-gene construct) and the hydroxylation of 14-O-acetylmutilin to pleuromutilin.

5.1.1 *Agrobacterium*-infiltration of tobacco led to chlorotic leaves

Leaves of approximately 5-week-old tobacco were infiltrated with the empty vector, the 2-gene vector, the 5-gene vector or the 7-gene vector in the underside of the third leaf from the shoot apical meristem leaving a dark-green area (‘’wetting’’ area). The leaves were observed and harvested 3, 5 and 7 days post-infection (d.p.i.). The tobacco leaves shown in Figure 5.1 demonstrate a characteristic chlorotic tint, which became more visible at later days. This was more severe in the expression vectors where there was typically severe necrosis observed in the infiltrated regions,

particularly with vectors 2.5 and 2.7. Tissue was ground into a fine powder, which was used for metabolite extraction and HPLC analysis.

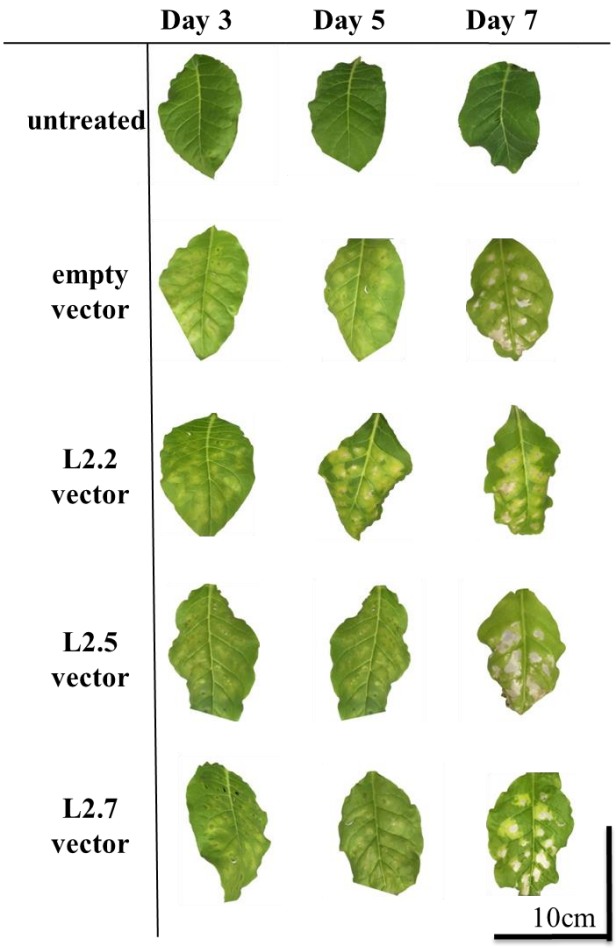

Figure 5.1 Tobacco leaves *Agrobacterium*-infiltration with the different plasmids, 3, 5 and 7 days post-infection. Untreated or WT leaves (1st row), empty vector leaves that were infiltrated using an empty vector (2nd row), leaves infiltrated using *Agrobacteria* transformed with the 2-gene construct (3rd row), 5-gene construct (4th row) and 7-gene construct (5th row).

5.1.2 HPLC analysis of extracts from infiltrated leaves

In an attempt to search for pleuromutilin and pleuromutilin precursor production, extracts from infiltrated tobacco leaves were analyzed through HPLC. The leaves were harvested 3, 5 and 7 days post-infection and as control sample the empty vector leaves were used. Three different leaves were harvested for each timepoint and vector and independently assessed as technical replicates. Overall, 3 individual leaves-samples per d.p.i. were analyzed, derived from 4 categories of infiltrated leaves with: an empty vector, the 2-gene, 5-gene and 7-gene construct detailed in Section 2.4.4.

Representative samples are shown in HPLC chromatograms in Figure 3.34. Despite careful analysis there were no apparent peaks with the same retention as the previously purified and characterized mutilin for the 5-gene construct or pleuromutilin for the 7-gene constructs at retention time (Rt) 12.24 at with mass 366 in the ES- spectrum and at Rt 11.97 at with mass 423 in the ES- spectrum, respectively. As a pleuromutilin indicator (positive control), pleuromutilin (≥95% purity) from Sigma-Aldrich was used. Furthermore, the 2-gene construct hypothetically leading to the production of the first cyclised compound, 3-deoxy-11-dehydroxy-mutilin, was expected to be observed with the mass 289 in the ES- spectrum and no such signal could be identified.

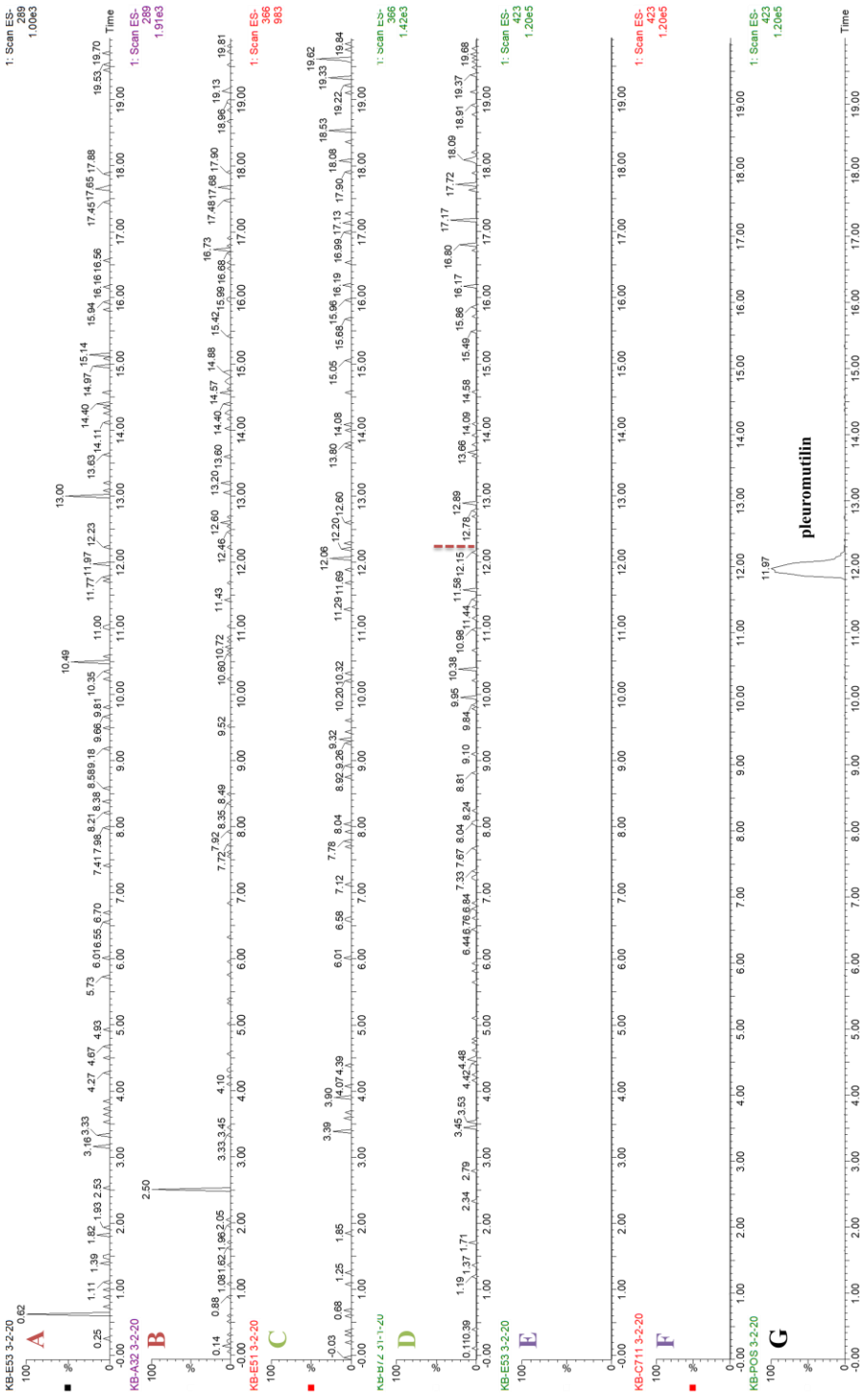

Figure 5.2 HPLC analysis of tobacco leaf extracts; extracted ion chromatographs for 289 (A, B), 366 (C, D) and 423 (E, F, G) in the ES- spectrum. (A) Extract from tobacco leaves infiltrated with *Agrobacteria* harbouring an empty vector for 289 in the ES- spectrum. **(B)** Extract from tobacco leaves infiltrated with *Agrobacteria* harbouring the 2-gene construct for 289 in the ES- spectrum. **(C)** Extract from tobacco leaves infiltrated with *Agrobacteria* harbouring an empty vector for 366 in the ES- spectrum. **(D)** Extract from tobacco leaves infiltrated with *Agrobacteria* harbouring the 5-gene vector

for 366 in the ES- spectrum. Rt should be observed at 12.24 (red dashed line) **(E)** Extract from tobacco leaves infiltrated with *Agrobacteria* harbouring an empty vector for 423 in the ES- spectrum. **(F)** Extract from tobacco leaves infiltrated with *Agrobacteria* harbouring the 7-gene vector for 423 in the ES- spectrum. Rt should be observed at 11.97 as shown in positive control. **(G)** Positive control of pleuromutilin ≥95% for 423 in the ES- spectrum.

5.2.1 *Marchantia* transformation using cut thalli

In order to observe in detail the growth of the wild-type *Tak-1* line, the development of gemmalings was observed for 14 days (Figure 5.3). Transformation protocols recommend thalli of 8-12mm, therefore transformation of *M. polymorpha* was conducted using 14-day old cut thalli. All transformations were performed using co-cultivation with *Agrobacterium LBA*4404, harboring the construct under study each time.

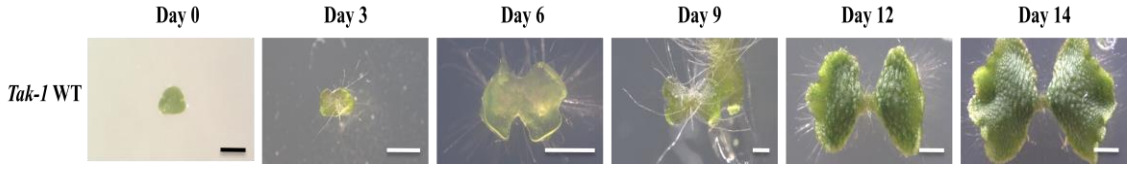

Figure 5.3 Time-course observation of *Tak-1* WT thalli. 14-day old thalli were used in the transformation protocol described at Section 2.8. Black scale bar (Day 0) is at 0.5mm. White scale bar (Day 3-14) is at 2mm.

The 14-day old thalli were cut in four fragments each and left to recover under normal conditions for 7 days prior to transformation (Figure 5.4, A). These typically were able to reform the characteristic apical notches (Figure 5.4, A). After co-cultivation for 3 days with *Agrobacteria* containing the construct under study, plantlets were transferred onto half strength Gamborg's B5 medium supplemented with 1% (w/v) sucrose, cefotaxime and Geneticin® (Figure 5.4, B). Geneticin-

resistant thalli were apparent 15 days after transfer to the above selective media, while the original cut thalli became necrotic (Figure 5.4, D; Figure 5.5, C). Isogenic lines were obtained after 2 cycles of transplantation of gemmae (G2 generation), which were used for further analyses.

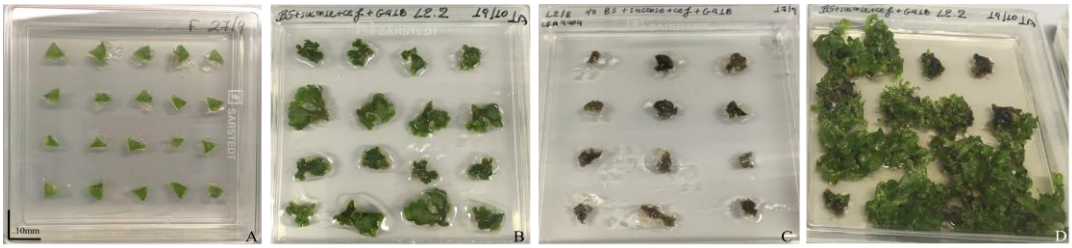

Figure 5.4 *Marchantia* transformation protocol workflow. (A) Cut thalli on half strength Gamborg's B5 supplemented with 1% (w/v) sucrose. **(B)** After 3 days of co-cultivation with *Agrobacteria*, the thalli were transferred into half strength Gamborg's B5 medium supplemented with 1% (w/v) sucrose, cefotaxime and geneticin® (selection media) **(C)** Necrotic thallus that derived from *Agrobacterium*-mediated transformation, harbouring a plasmid that contained a non-functional selection marker gene *nptII*. **(D)** Two weeks after transfer to selective media geneticin-resistant thalli were observed. For those transformed with a functional *nptII*. Scale bar is at 10mm.

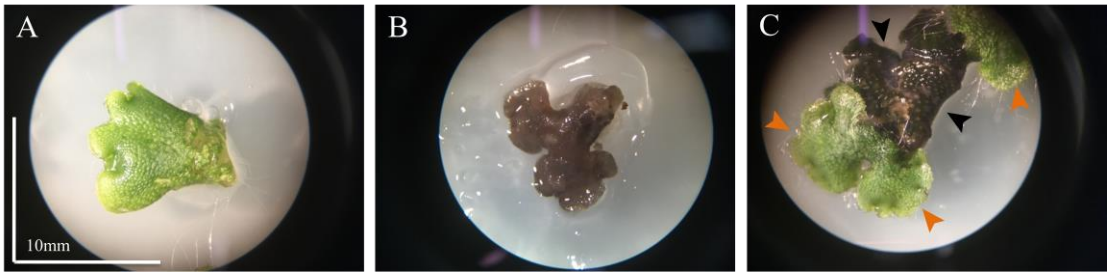

Figure 5.5 Characteristic morphology of *Marchantia* thalli during transformation. (A) 7-day healthy thallus growing under normal conditions after being cut and prior to transformation (see Section 2.8). **(B)** Necrotic thallus that derived from untransformed or negative control/ failed transformants on exposure to geneticin. **(C)** Geneticin-resistant thalli were observed 15 days after transfer to the selective media (orange arrows), while original cut thalli became necrotic (black arrows). Scale bar is at 10mm.

It is worth mentioning that the plantlets transformed with the initial plasmids, (harbouring the anti-sense and therefore non-functional *nptII* selection gene) did not lead to regenerated thalli, indicating that were not any geneticin-resistant thalli (Figure 5.4, C; Figure 5.5, B).

Table 5.1 Different groups/ lines of *Marchantia* transformed with individual constructs detailed in Section 2.4.4. All transcription units had the 35S promoter and nos terminator.

	Group E	Group A	Group B	Group C
T-DNA Coding sequences/ genes	empty vector *nptII*	2-gene vector *nptII, ggs, cyc*	5-gene vector *nptII, ggs, cyc, p450-1, p450-2, sdr*	7-gene vector *nptII, ggs, cyc, p450-1, p450-2, sdr, atf, p450-3*

5.2.2 HPLC analysis of *Marchantia* tissue

Extracts from *Marchantia* tissue were analyzed through HPLC for any trace of pleuromutilin or pleuromutilin precursors. The control sample was *Marchantia* transformed with an empty vector. Overall, 8 individual samples per vector were analyzed, derived from 4 categories of transformed *Marchantia* with: an empty vector, the 2-gene, 5-gene and 7-gene construct detailed in Section 2.4.4.

Representative samples are shown in HPLC graphs in Figure 5.6, where the peaks with the same retention as the previously purified and characterized mutilin for the 5-gene construct and pleuromutilin for the 7-gene constructs, with peaks expected

in HPLC at retention time (Rt) 12.24 at mass 366 in the ES- spectrum and at Rt 11.97 at mass 423 in the ES- spectrum, respectively. As a pleuromutilin indicator (positive control), pleuromutilin ≥95% from Sigma-Aldrich was used. Furthermore, the 2-gene construct hypothetically leading to the production of the first cyclised compound, 3-deoxy-11-dehydroxy-mutilin, was expected to be observed for the mass 289 in the ES- spectrum. The peak at retention time (Rt) 12.24 with mass 366 in the ES- spectrum was observed in two different samples, indicating the possibility of heterologous production of the precursor mutilin. Those samples belong to the 3rd group (group B), transformed with the 5-gene construct leading to the production of mutilin. Both analyses of samples B3 and B4 are shown in Figure 5.6 E and D, respectively.

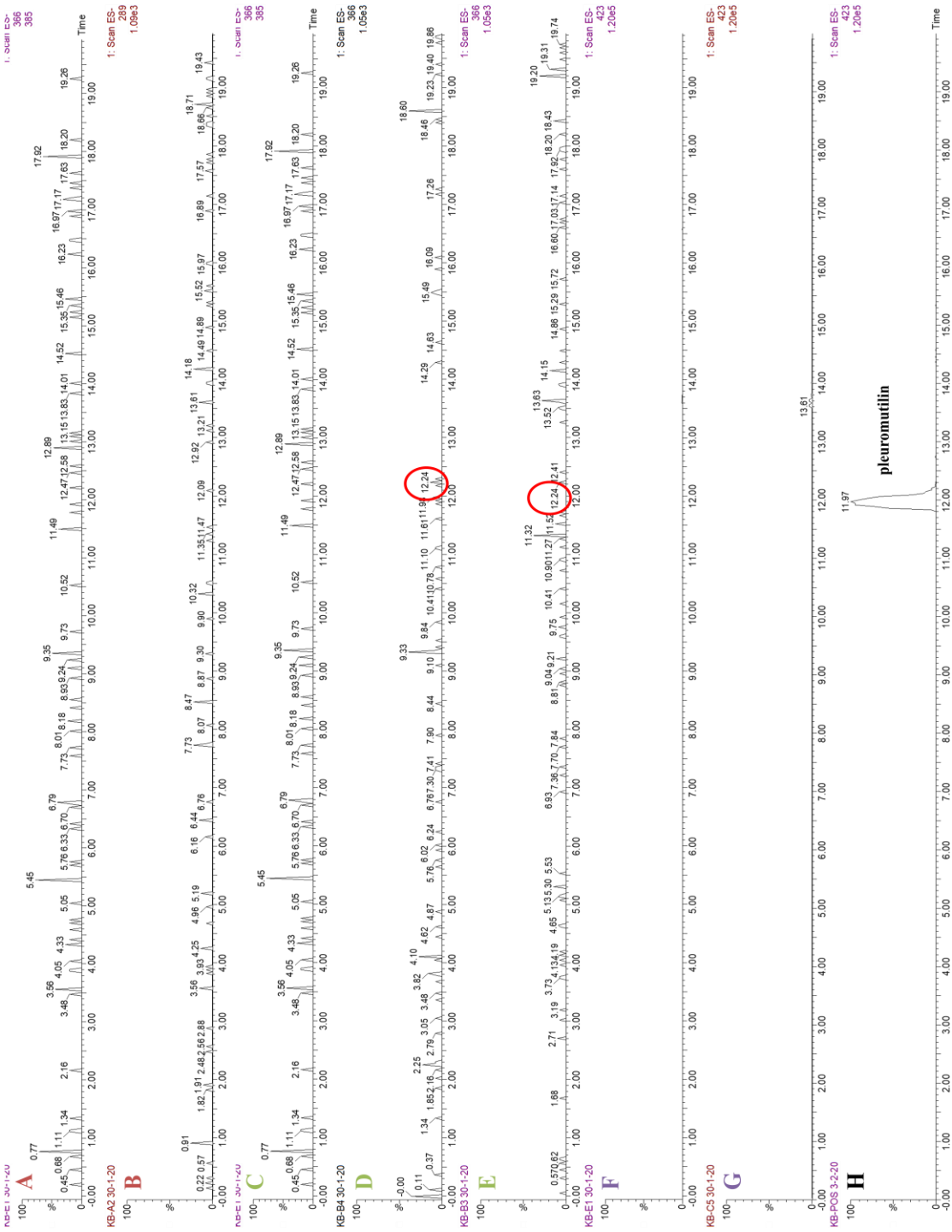

Figure 5.6 HPLC analysis of *M. polymorpha* tissue extracts for 289 (A, B), 366 (C, D) and 423 (E, F, G, H) in the ES- spectrum. (A) Extract from *M. polymorpha* harbouring an empty vector T-DNA for 289 in the ES- spectrum. **(B)** Extract from *M. polymorpha* harbouring the 2-gene construct T-DNA for 289 in the ES- spectrum. **(C)** Extract from *M. polymorpha* harbouring an empty vector T-DNA for 366 in the ES- spectrum. **(D)** Extract from *M. polymorpha* B4 harbouring the 5-gene T-DNA for 366 in the ES- spectrum. Rt should be observed at 12.24. **(E)** A second sample extract from *M. polymorpha*

B3 harbouring harbouring the 5-gene T-DNA for 366 in the ES- spectrum. Rt should be observed at 12.24. **(F)** Extract from *M. polymorpha* harbouring an empty vector T-DNA for 423 in the ES- spectrum. **(G)** Extract from *M. polymorpha* harbouring the 7-gene construct vector T-DNA for 423 in the ES- spectrum. Rt should be observed at 11.97 as shown in positive control. **(H)** Positive control of pleuromutilin ≥95% for 423 in the ES- spectrum.

5.2.3 Expression analysis of the genes under study in *M. polymorpha*

In order to examine the expression levels of each gene of the biosynthetic pathway of pleuromutilin, tissue from *Marchantia* transformants was ground into a fine powder and total RNA was isolated. Successful RNA isolation was confirmed by gel electrophoresis showing the presence of 28S, 18S and 5S ribosomal RNA (rRNA (Figure 5.7). Residual genomic DNA removal was conducted for each sample and the protocol for Luna® Universal one-step RT-qPCR was followed, with each sample being run in triplicate (n=3).

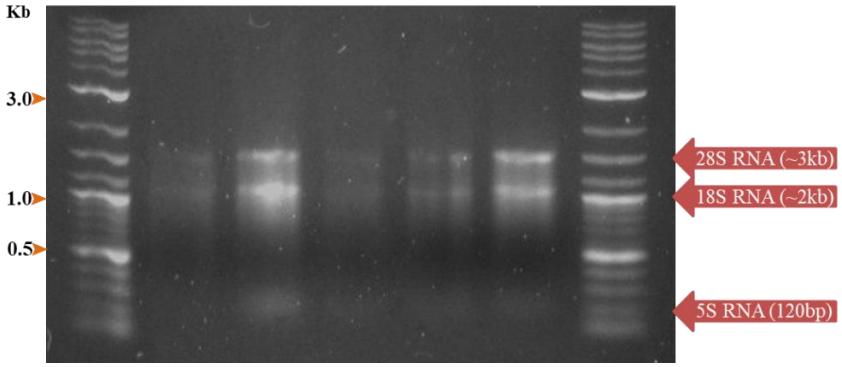

Figure 5.7 0.8% agarose gel of RNA samples after total RNA purification and genomic DNA removal from *Marchantia polymorpha.* Successful isolation of RNA is indicated by the observation of the 3 distinctive bands at 3kb, 2kb and 120bp, representing 28S, 18S and 5S ribosomal RNA (rRNA), respectively.

Expression levels of the different genes in *Marchantia* were evaluated by the relative quantification of the respective mRNA transcripts using specific primers. The

expression levels from the endogenous house-keeping gene *actin7* were used as the reference for normalization of qPCR data. *Actin7* transcription levels are reported to be constant during diverse biological states such as abiotic stress, hormone treatment and different developmental stages (Saint-Marcoux et al., 2015).

Whilst *Agrobacterium*-mediated transformation tends to result in single-copy insertion of constructs in *Marchantia,* the site of insertion will vary and so some lines may have inserts in chromatin regions that are poorly expressed compared to other lines. qPCR was performed to determine the plant lines in which the genes are incorporated into transcriptionally active regions, resulting in heterologous expression. In the following figures, expression levels of each gene in transformant groups A, B and/or C are shown compared to the expression levels of the empty vector group E that was used as a control. As expected, in control lines or empty vector lines, no heterologous expression of the genes was apparent.

For group A (2-gene, GGS and cyclase transformants) *GGPP synthase* gene heterologous expression was readily evident in lines **A2** and **A8**, with the lines **A6** and **A7** showing low expression (Figure 5.8). *Terpene cyclase* gene illustrates a similar expression pattern with clear heterologous expression in lines **A2** and **A8** (Figure 5.9).

In group B (5-gene transformants; GGS, cyclase, P450-1, P450-2 , SDR), lines **B3** and **B6** has obvious expression for *GGPP synthase* with weak expression in **B4** and **B5** (Figure 5.8). The *terpene cyclase* showed a similar pattern with strong expression for lines **B3** and **B6,** but weak expression only for **B4** (Figure 5.9).

In group C, line **C7** had good expression for both and (Figures 5.8 & 5.9). Line **C5** has good expression for *GGPP synthase* but is weak for *terpene cyclase*.

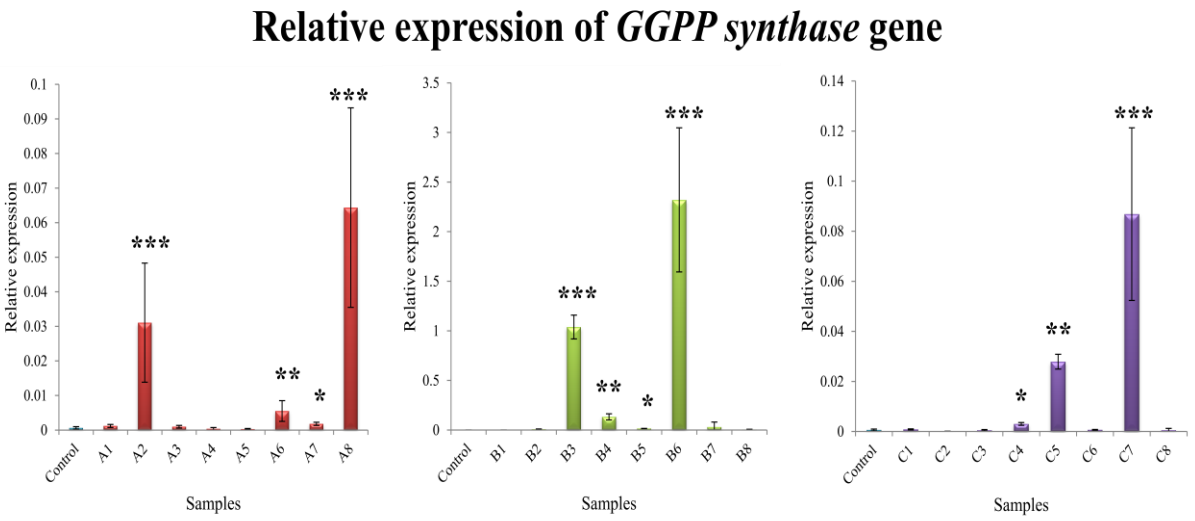

Figure 5.8 qPCR data analysis of the *GGPP synthase* gene in control (transformed with an empty vector) and transformed with the gene under study (*ggs*) lines of *M. polymorpha*. A1-A8 samples were transformed with the 2-gene plasmid, B1-B8 samples were transformed with the 5-gene plasmid and C1-C8 samples were transformed with the 7-gene plasmid. Asterisks indicate 3 different groups of heterologous expression, (*): low/medium expression, (**): medium/high expression, (***): highest expression group. In each sample, values depict the mean ±SD where n=3.

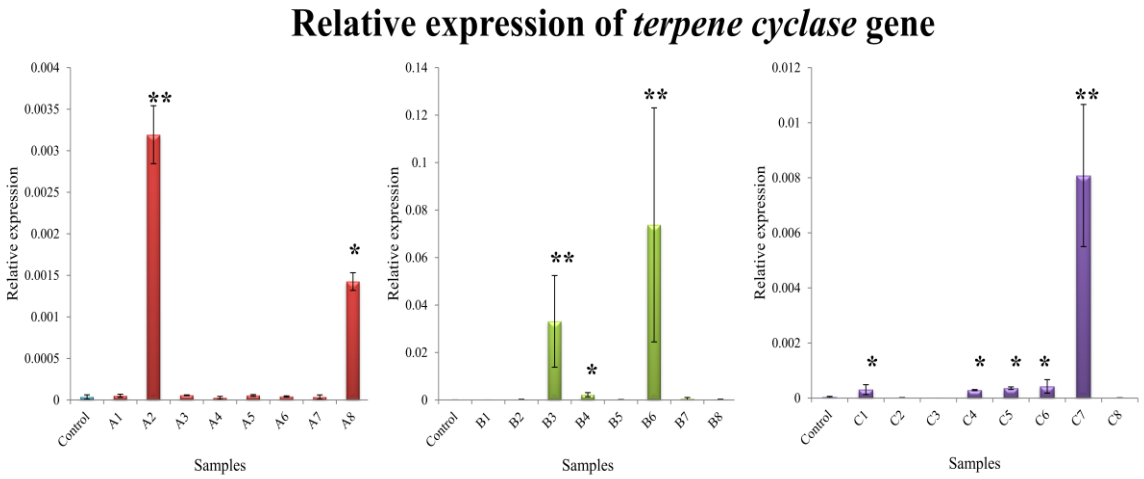

Figure 5.9 qPCR data analysis of the *terpene cyclase* gene in control (transformed with an empty vector) and transformed with the gene under study (*cyc*) lines of *M. polymorpha*. A1-A8 samples were transformed with the 2-gene plasmid, B1-B8 samples were transformed with the 5-gene plasmid and C1-C8 samples were transformed with the 7-gene plasmid. Asterisks indicate 2 different groups of

heterologous expression, (*): low/medium expression, (**): highest expression group. In each sample, values depict the mean ±SD where n=3.

As far as the relative expression of the *cytochrome p450-1* is concerned, **B8** had high expression levels, **B1**, **B7**, demonstrated weak heterologous expression of *p450-1* gene, while B2-B6 gave no apparent signal (Figure 5.10). Heterologous expression of *P450-1* was also observed in lines with the 7-gene construct, strongly in **C5**, and weakly in **C1**, **C2**, **C4**, **C6** (Figure 5.10)**.**

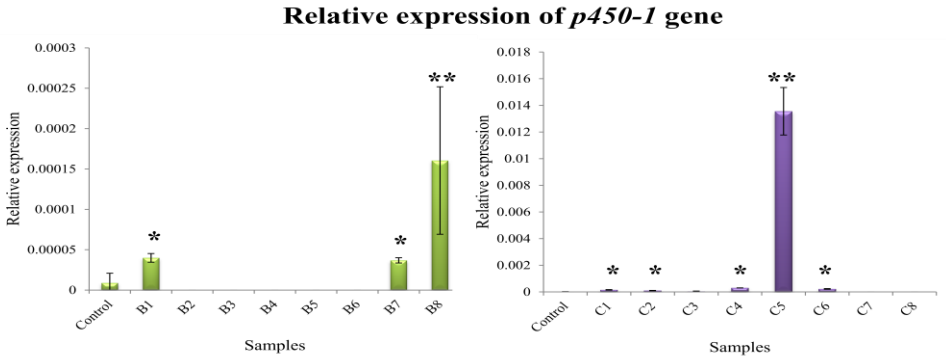

Figure 5.10 qPCR data analysis of the *cytochrome p450-1* gene in control (transformed with an empty vector) and transformed with the gene under study (*p450-1*) lines of *M. polymorpha*. B1-B8 samples were transformed with the 5-gene plasmid and C1-C8 samples were transformed with the 7-gene plasmid. Asterisks indicate 2 different groups of heterologous expression, (*): low/medium expression, (**): highest expression group. In each sample, values depict the mean ±SD where n=3.

The gene *p450-2* is also expressed in lines **B3**, **B4**, **B6** (Figure 5.11) and **C4**, **C5**, **C6**, **C7**, **C8** (Figure 5.11)**.**

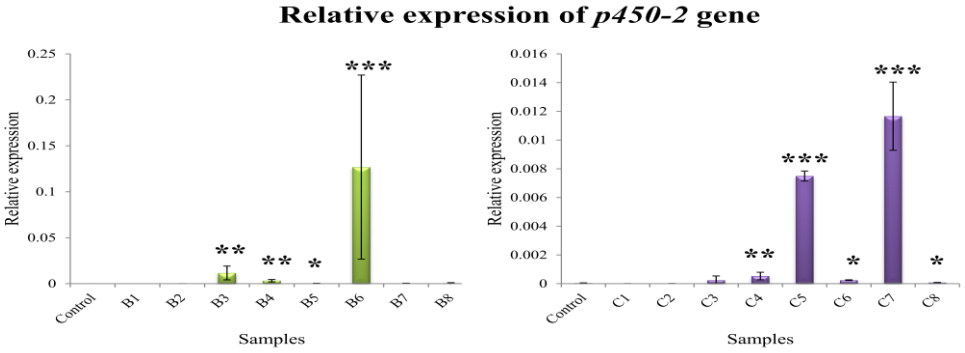

Figure 5.11 qPCR data analysis of the *cytochrome p450-2* gene in control (transformed with an empty vector) and transformed with the gene under study (*p450-2*) lines of *M. polymorpha*. B1-B8 samples were transformed with the 5-gene plasmid and C1-C8 samples were transformed with the 7-gene plasmid. Asterisks indicate 3 different groups of heterologous expression, (*): low/medium expression, (**): medium/high expression, (***): highest expression group. In each sample, values depict the mean ±SD where n=3.

Short-chain reductase mRNA levels were noticeable in samples **B3**, **B4**, **B6**, while in the group C samples all lines **C1-C7**, apart from C8, show relative expression compared to the empty vector control samples (Figure 5.12).

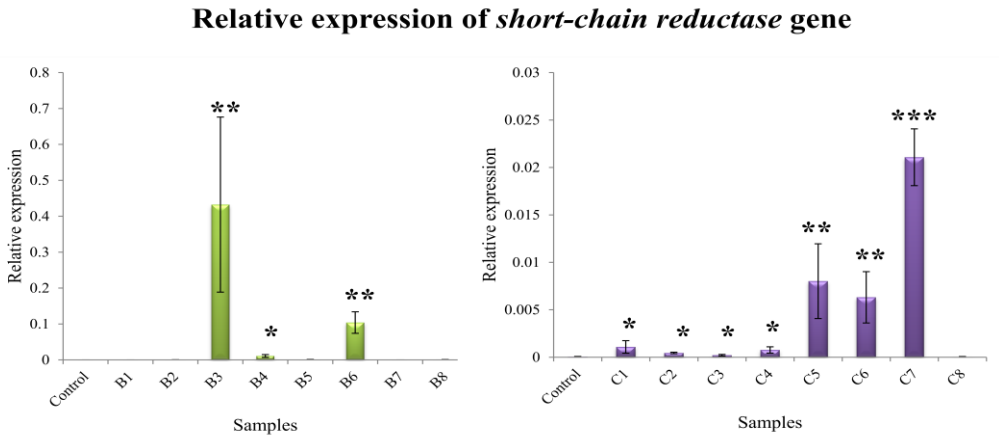

Figure 5.12 qPCR data analysis of the *short-chain reductase* gene in control (transformed with an empty vector) and transformed with the gene under study (*sdr*) lines of *M. polymorpha*. B1-B8 samples were transformed with the 5-gene plasmid and C1-C8 samples were transformed with the 7-gene plasmid. Asterisks indicate 3 different groups of heterologous expression, (*): low/medium expression, (**): medium/high expression (or highest for the left graph), (***): highest expression group. In each sample, values depict the mean ±SD where n=3.

In the group C of the 7-gene construct transformants, *acetyltransferase* expression is apparent in lines **C1**, **C5**, **C6** and **C7** (Figure 5.13, left graph). The final gene of the

pleuromutilin 7-gene construct, *p450-3*, is heterologously expressed in samples **C3**, **C5**, **C6**, **C7 and C8** (Figure 5.13, right graph).

However, it is clear that there are differences in fold expression between some individual genes or between different groups of the same gene. It was also noticeable that some lines were expressing some of the genes even though no expression was detected for some other genes of the same line/construct. This was expected as the Ct where signal was observed for the reference gene was at around 18-20 cycles, for Group B genes at around 24-26 cycles, while for Group A and C at around 29-31 cycles.

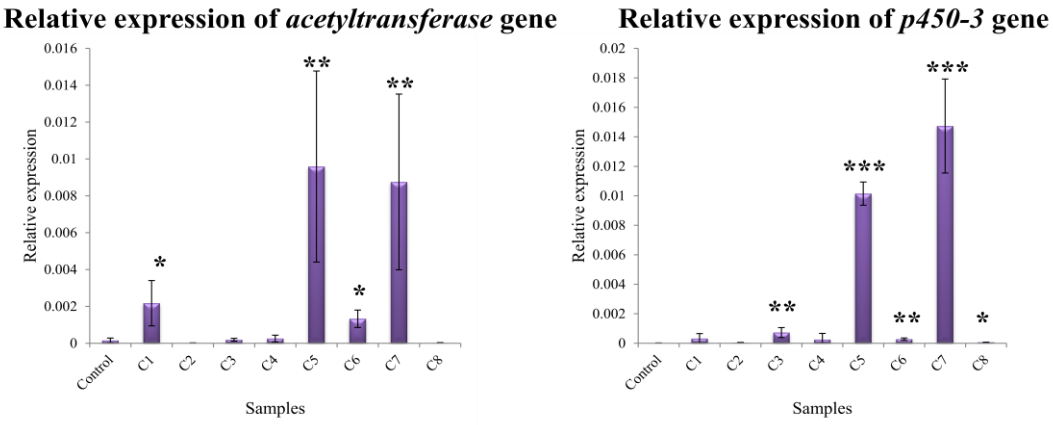

Figure 5.13 qPCR data analysis of the acetyltransferase (left) and cytochrome p450-3 (right) genes in control (transformed with an empty vector) and transformed with the genes under study (atf or p450-3) lines of *M. polymorpha*. C1-C8 samples were transformed with the 7-gene plasmid. Asterisks indicate 3 different groups of heterologous expression, (*): low/medium expression, (**): medium/high expression (or highest for the left graph), (***): highest expression group. In each sample, values depict the mean ±SD where n=3.

According to the aforementioned, it is essential to screen more plant lines to acquire sufficient overexpression of the cluster, since the lines analysed did not highly express all genes at the same time. Further optimization of gene expression is needed to result in lines expressing all seven genes of the pathway. The relative expression is summarised in Figure 5.14.

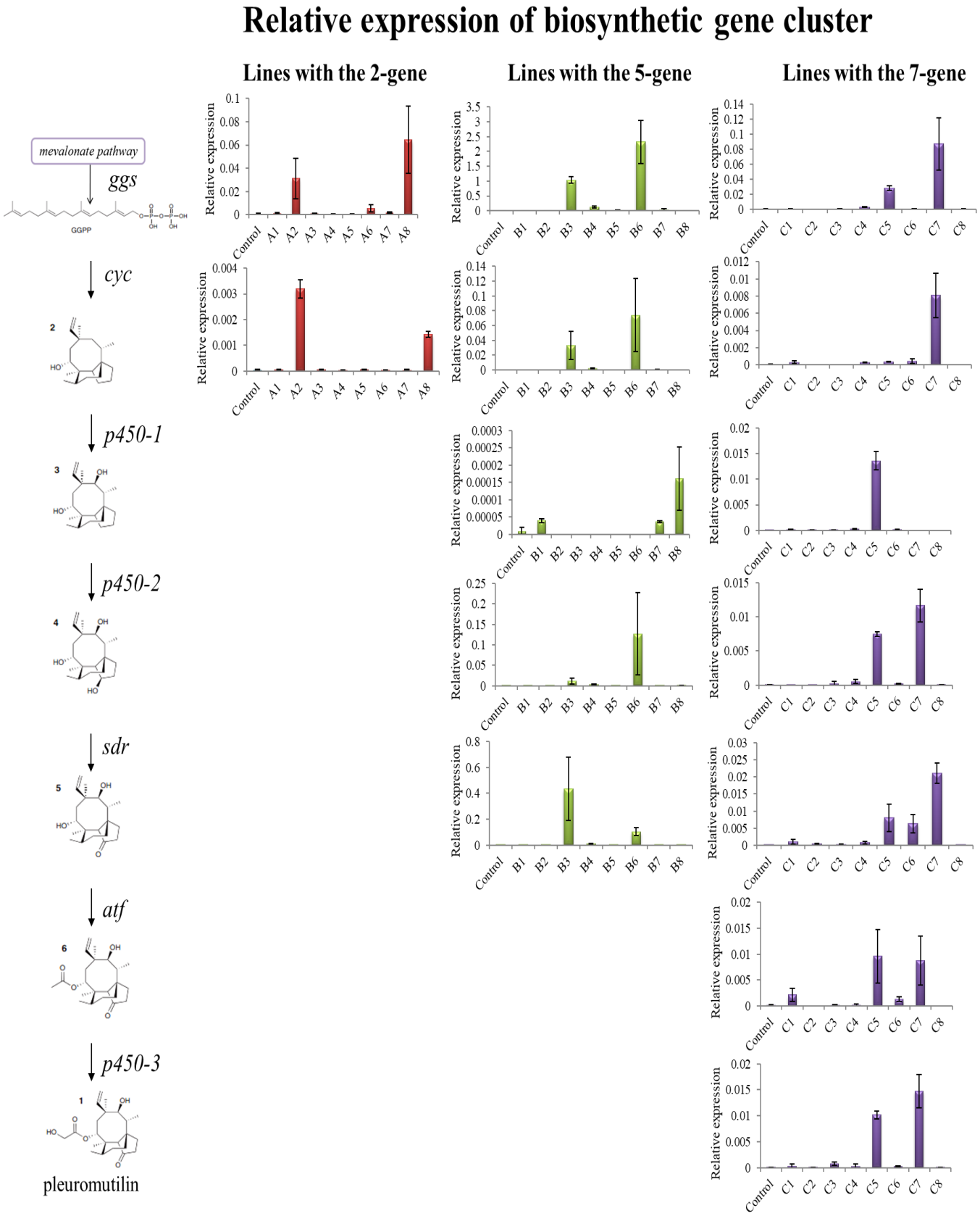

Figure 5.14 Summary illustration of the pleuromutilin gene cluster with every *M. polymorpha* line and their respective gene expression levels.

Chapter 6: Discussion and Further work

Until very recently the pleuromutilins were regarded as a niche class of antibiotic with few practical uses in medicine due to lack of oral availability, or toxicity issues, however this has changed with the discovery of Lefamulin. With this being usable in both tablet and IV injection, this version has the potential to become an antibiotic in high demand, particularly given its unique mechanism of action, which involves tight binding to the conserved peptidyl transferase centre, resistance to pleuromutilin is slow to be developed while it has minimal cross-resistance with other antibiotics (Davidovich et al., 2007; Paukner & Riedl, 2017). Conventional fermentation of pleuromutilin is not very efficient as the producing fungus is not very amenable to large-scale fermentation or to conventional strain improvement, so if it is to be produced in high-yield, a biotechnological solution to its production is needed. The pathway of pleuromutilin production has been identified by Bailey et al. (2016) and pathway intermediates have been elucidated by Alberti et al. (2017) by step-wise heterologous expression of the pathway genes in *A. oryzae*. The Alberti paper confirmed the expression of the partial pathway, where different intermediates could be isolated. These could be further chemically modified to obtain the end-metabolite. This approach also led to the development of bio-conversion chassis, as feeding chemically modified analogues could be converted to semi-synthetic pleuromutilin derivatives. Despite their work however, yields from heterologous production in a fungus were still comparatively low and so alternative expression platforms may be desirable.

This thesis explored the feasibility of producing pleuromutilins in bryophytes, showing that the host plants were tolerant to mutilin, the key precursor used in industry for conversion to medically relevant antibiotics. Plasmid vectors were made

to support expression of the necessary genes for expression of the biosynthetic pathway. Moss and liverwort hosts were screened for susceptibility to pleuromutilin. This work has shown that pleuromutilin, mutilin and a diverse selection of antibiotics impact on growth and development of *P. patens* and *M. polymorpha,* when supplemented into growing media. Interestingly, mutilin showed a 25- and a 10-fold antibiotic concentration tolerance of survival compared to tiamulin (pleuromutilin derivative) when tested in media growing *P. patens* or *M. polymorpha,* respectively. Both plant hosts also demonstrated some characteristic phenotypic changes when growing media were supplemented with some of the antibiotics under study, including mutilin for *P. patens* and tiamulin or mutilin for *M. polymorpha.*

This project also consists of the first attempt of building the pleuromutilin pathway into different plant hosts. Initially, the multigene constructs used in transformation were made, consisting of the CaMV 35S promoter and nopaline synthase terminator. Successful transformants of *M. polymorpha* obtained geneticin-resistant thalli, while plantlets transformed with the non-functional *nptII* selection marker plasmid became necrotic. Moreover, two out of eight *Marchantia* lines depicted the desirable peak of Rt 12.24 at 366 in the ES- spectrum in HPLC, indicating a possibility of mutilin production. Expression analysis was carried out to validate the heterologous expression of the genes. Whilst not definitive, these findings suggest that this might be a feasible approach for production if gene expression could be optimized.

6.1 Antibiotic assays

Subcellular organelles, such as mitochondria and chloroplasts are believed to have originated from endosymbiotic α-proteobacteria and cyanobacteria-like prokaryotes, respectively. However, in higher plants they are shown to have diverged

considerably from these ancestral origins, although bacteria-like ribosomes are present in both organelles (Kasten & Reski, 1997). Interestingly, inhibition of chloroplast division was observed in suspension cultures of *P. patens* but not in the dicot *Lycopersicon esculentum* (tomato) when treated with the β-lactam antibiotics ampicillin, cefotaxime and penicillin, and also led to macrochloroplast formation in *P. patens.* This study concluded that prokaryotes and moss chloroplasts may share a common component in their division mechanisms (Kasten & Reski, 1997). However, with moss chloroplasts lacking a peptidoglycan wall it is unclear how β-lactam antibiotics would act. In bacteria the penicillin-binding protein FtsI when binding to β-lactam antibiotics, cannot support FtsZ tubule formation, leading to undivided bacteria, and ,presumably, a FtsI homolog in moss could have a similar effect (Kasten & Reski, 1997; Miyagishima et al., 2014). Similarly, suspension cultures of *M. polymorpha* treated with the β-lactam antibiotic ampicillin were reported to show a decrease in chloroplast number, also demonstrating inhibition of chloroplast division (Tounou et al., 2002). There is a possibility that either the bacteria-like ribosomes, present in chloroplasts or mitochondria are responsible for the effect tiamulin (pleuromutilin derivative) has on growth and morphology of both *P. patens* and *M. polymorpha*. Support for this is the observation that mutilin showed a milder effect on growth and development of the two plant hosts. This is also seen in bacteria and is likely due to the role of the C-14 sidechain which is important for full activity, indeed this region is the part of the molecule that is then modified during semisynthesis to further improve the efficiency of derivatives such as Lefamulin. Whilst the susceptibility to pleuromutilin might prevent production of the mature compound in these plant hosts, the reduced susceptibility to mutilin might mean it is feasible to use such hosts to produce this pathway intermediate.

6.2 The suitability of the heterologous host

In order to choose a plant host for heterologous expression of a desired compound, it should be taken into account whether the host is amenable to transformation and to be able to generate stable transformants in a reliable manner. Moreover, it is important that the host generates enough biomass to allow the desired production levels of the metabolite of interest. The endogenous flux of carbon through the pathway under study ought to be suitably high and flexible to provide any necessary precursors to the enzymes of the pathway. Last but not least, it is essential to eliminate the possibility of any endogenous enzymes modifying or metabolizing any intermediates or the final metabolite (Kempinski et al., 2015). While the first two criteria of amenability to transformation and generation of enough biomass can be predicted, the complexity of metabolic networks can presumably affect the stability of the precursors, the final metabolite, and/or the pathway enzymes *in planta*. Furthermore, how a multigene construct would interact with endogenous genetic circuits is unpredictable, requiring for multiple cycles of build-test-rebuild to fine-tune the flux of the new pathway and eliminate any intermediates accumulation (Gandhi, 2019). Approaches that have been proposed for optimizing expression of multigene constructs consist of using tunable genetic filters (Deans et al., 2007; Wang et al., 2014), ribosome-binding site sequences (Salis et al., 2009), protein degradation-targeting sequences (Cameron & Collins, 2014) and chemical inducers (Kelly et al., 2016).

6.3 *Agrobacterium*-infiltration of tobacco

The chlorosis seen in tobacco with the 7-gene and 5-gene constructs suggests that the vectors may have worked, although with cell-death being a possible outcome of successful gene expression, regeneration of stable tobacco transformants would be

challenging. New peaks were seen in the HPLC traces from *Agro*-infiltrated extracts with a T-DNA of the empty vector, suggesting there was considerable stress after infiltration and no additional peaks were readily apparent with the 5- or 7-gene vectors. Even searches for compounds with specific masses failed to show any production. Such searches are very sensitive suggesting either the compounds were not produced, they were modified by the host or that they were bound to targets and so not available for extraction. Presence of chlorosis would support production having occurred but with detrimental effects on the host, so they may be toxic for tobacco, with the desired precursors probably being unstable *in planta*.

6.4 *M. polymorpha* heterologous expression

The initial attempts at transformation of *Marchantia* failed to yield any transformants however this was eventually shown to be because the L1 construct had the *nptII* ORF in the anti-sense orientation so should not lead to geneticin-resistant thalli. It should be noted that this would not have impacted on the *Agrobacterium*-infiltration of tobacco discussed above, as kanamycin selection is not used during such infiltrations and the pleuromutilin transcriptional units should all still have been functional. Making the expression constructs with a corrected version of the L1 *nptII* was successful in generating geneticin-resistant transformants. Transformation of *Marchantia* is integrative and relatively low expression levels of the transgenes are reported to often be observed due to transgene silencing or positional effects, hence, it is recommended to analyze many independent lines (Kempinski et al., 2015). However time constraints due to Covid-19 limited the numbers of transformants that could be isolated and analysed. Furthermore, the repetitious use of the same promoter, as in this thesis, may lead to transcriptional gene silencing due to promoter methylation and thus inactivation. Solutions to this problem could be promoter

diversity, use of synthetic or chimeric promoters derived from conserved native ones, functional cis-elements of endogenous promoters or bidirectional promoters (Peremarti et al., 2010). Whilst this vector was designed and constructed, time constraints prevented its use in generating transformants.

6.5 *M. polymorpha* HPLC analysis

Unfortunately, in none of the Group A or C transformants were there any peaks at the desired retention time (Rt), indicating that the specific intermediates were not produced. Given that the expression levels were so low when assessed by qPCR, the desired products might only be accumulated at low concentrations, hence the more sensitive technique of GCMS, appropriate for volatile diterpenes, could be used (Hamm et al., 2005). Very few transformants had detectable transcripts for all of the transgenes, so it may need a larger population of transformants to be assessed to identify those where production was possible. Alternatively it is possible that production was limited due to enzymes going to the wrong subcellular compartments. As reported by Ban et al., 2018, after heterologous expression of the secondary metabolite aphidocolin in *A. oryzae*, fusion with GFP of the geranygeranyl diphosphate synthase and terpene cyclase showed that they were localized in the cytoplasm, while P450s derived from *Phoma betae* were localized in the ER. Thus, aphidicolin production was almost completely lost in the *Pb*P450-1 mutant lacking the transmembrane domain (Ban et al., 2018). Given the taxonomic distance between *Marchantia* and *Clitopilus*, it is possible that protein targeting sequences, if present, might not be functional, or that plant cytochrome P450 reductases might not reactivate fungal P450s in the case of the 7-gene transformants.

Two (B3, B4) out of eight lines of Group B (5-gene transformants) showed a peak at retention time (Rt) 12.24 with mass 366 in the ES- spectrum, demonstrating

the possibility of successful heterologous production of the precursor mutilin, although this was at very low levels. RNA expression levels of the genes of these samples showed that there is heterologous expression of all genes except for *p450-1* which might account for why mutilin yield was low. This is a promising result given how few transformants were analysed and that none showed strong expression of all the transgenes.

6.6 Future work

There are many directions this research could go in the future. Time constrains meant that comparatively few transformants were analysed in *Marchantia*, and that the "diverse promoters" construct was not evaluated. The analysis of more transformants, and possibility of elevated expression using the vector might support production of mutilin, even if pleuromutilin might not be possible due to toxicity. Similarly an initial aim was to duplicate this analysis in moss, and whilst plasmids were made for this, the transformation has not been tried. With a good-size population of transformants, RT-qPCR of the whole transcript of each gene would help identify those where all the genes were being efficiently expressed and help eliminate the probability of partial transcription, and thus no functional pathway. Time-permitting it would be interesting to use fluorescence fusion tags for real-time monitoring the destination of the pathway enzymes *in planta*, it might even be feasible to use the targeting sequences derived from plant diterpene biosynthesis proteins to help direct these fungal enzymes to the correct subcellular location for elevated antibiotic production.

Despite these limitations, the hint of successful production of mutilin in *Marchantia* in this work is very positive and might open up the possibility of growing antibiotics in plants in the future.

References

Adam, K. P., & Becker, H. (1993). Phenanthrenes and other phenolics from in vitro cultures of Marchantia polymorpha. *Phytochemistry*, *35*(1), 139–143. https://doi.org/https://doi.org/10.1016/S0031-9422(00)90522-3

Alberti, F., Foster, G. D., & Bailey, A. M. (2017). Natural products from filamentous fungi and production by heterologous expression. *Applied Microbiology and Biotechnology*, *101*(2), 493–500. https://doi.org/10.1007/s00253-016-8034-2

Alberti, F., Khairudin, K., Venegas, E. R., Davies, J. A., Hayes, P. M., Willis, C. L., Bailey, A. M., & Foster, G. D. (2017). Heterologous expression reveals the biosynthesis of the antibiotic pleuromutilin and generates bioactive semi-synthetic derivatives. *Nature Communications*, *8*(1), 1831. https://doi.org/10.1038/s41467-017-01659-1

An, G., Ebert, P. R., Mitra, A., & Ha, S. B. (1988). Binary vectors. *Plant Molecular Biology Manual*, *19*, 45–63. https://doi.org/10.1007/978-94-017-5294-7_3

Anchel, M. (1952). (From the New York Botanical). *J. Biol. Chem.*, *199*, *2*, 133–140.

Asakawa, Y., & Ludwiczuk, A. (2013). Bryophytes: liverworts, mosses, and hornworts: extraction and isolation procedures. *Methods in Molecular Biology (Clifton, N.J.)*, *1055*, 1–20. https://doi.org/10.1007/978-1-62703-577-4_1

Asakawa, Y., Ludwiczuk, A., & Nagashima, F. (2013). Chemical constituents of bryophytes. Bio- and chemical diversity, biological activity, and chemosystematics. *Progress in the Chemistry of Organic Natural Products*, *95*, 1–796. https://doi.org/10.1007/978-3-7091-1084-3_1

Bailey, A. M., Alberti, F., Kilaru, S., Collins, C. M., de Mattos-Shipley, K., Hartley, A. J., Hayes, P., Griffin, A., Lazarus, C. M., Cox, R. J., Willis, C. L., O'Dwyer, K., Spence, D. W., & Foster, G. D. (2016). Identification and manipulation of the pleuromutilin gene cluster from Clitopilus passeckerianus for increased rapid antibiotic production. *Scientific Reports*, *6*, 25202.

Ban, A., Tanaka, M., Fujii, R., Minami, A., Oikawa, H., Shintani, T., & Gomi, K. (2018). Subcellular localization of aphidicolin biosynthetic enzymes heterologously expressed in Aspergillus oryzae. *Bioscience, Biotechnology, and Biochemistry*, *82*(1), 139–147. https://doi.org/10.1080/09168451.2017.1399789

Baragaña, B., Forte, B., Choi, R., Nakazawa Hewitt, S., Bueren-Calabuig, J. A., Pisco, J. P.,

Peet, C., Dranow, D. M., Robinson, D. A., Jansen, C., Norcross, N. R., Vinayak, S., Anderson, M., Brooks, C. F., Cooper, C. A., Damerow, S., Delves, M., Dowers, K., Duffy, J., … Gilbert, I. H. (2019). Lysyl-tRNA synthetase as a drug target in malaria and cryptosporidiosis. *Proceedings of the National Academy of Sciences of the United States of America*, *116*(14), 7015–7020. https://doi.org/10.1073/pnas.1814685116

Birch, A. J., Holzapfel, C. W., & Rickards, R. W. (1966). The structure and some aspects of the biosynthesis of pleuromutilin. *Tetrahedron*, *22*, 359–387. https://doi.org/https://doi.org/10.1016/S0040-4020(01)90949-4

Birnboim, H. C., & Doly, J. (1979). A rapid alkaline extraction procedure for screening recombinant plasmid DNA. *Nucleic Acids Research*, *7*(6), 1513–1523. https://doi.org/10.1093/nar/7.6.1513

Blokhina, E. A., Mardanova, E. S., Stepanova, L. A., Tsybalova, L. M., & Ravin, N. V. (2020). Plant-produced recombinant influenza A virus candidate vaccine based on flagellin linked to conservative fragments of m2 protein and hemagglutintin. *Plants*, *9*(2). https://doi.org/10.3390/plants9020162

Borchardt, J. K. (2002). *Drug News Perspect*. *15*, 187–192. https://doi.org/https://doi.org/10.1358/dnp.2002.15.3.840015

Bosch, D., Castilho, A., Loos, A., & Steinkellner, A. S. and H. (2013). N-Glycosylation of Plant-produced Recombinant Proteins. In *Current Pharmaceutical Design* (Vol. 19, Issue 31, pp. 5503–5512). https://doi.org/http://dx.doi.org/10.2174/1381612811319310006

Bowman, J. L., Kohchi, T., Yamato, K. T., Jenkins, J., Shu, S., Ishizaki, K., Yamaoka, S., Nishihama, R., Nakamura, Y., Berger, F., Adam, C., Aki, S. S., Althoff, F., Araki, T., Arteaga-Vazquez, M. A., Balasubrmanian, S., Barry, K., Bauer, D., Boehm, C. R., … Schmutz, J. (2017). Insights into Land Plant Evolution Garnered from the Marchantia polymorpha Genome. *Cell*, *171*(2), 287-304.e15. https://doi.org/https://doi.org/10.1016/j.cell.2017.09.030

Brakhage, A. A. (2013). Regulation of fungal secondary metabolism. *Nature Reviews Microbiology*, *11*(1), 21–32. https://doi.org/10.1038/nrmicro2916

But, H. M. C. P. P. H. (1986). Pharmacology and Applications of Chinese Materia Medica. *World Scientific Publishing*.

Cameron, D. E., & Collins, J. J. (2014). Tunable protein degradation in bacteria. *Nature*

Biotechnology, *32*(12), 1276–1281. https://doi.org/10.1038/nbt.3053

Chiyoda, S., Linley, P. J., Yamato, K. T., Fukuzawa, H., Yokota, A., & Kohchi, T. (2007). Simple and efficient plastid transformation system for the liverwort Marchantia polymorpha L. suspension-culture cells. *Transgenic Research*, *16*(1), 41–49. https://doi.org/10.1007/s11248-006-9027-1

Chiyoda, S., Yamato, K. T., & Kohchi, T. (2014). Plastid transformation of sporelings and suspension-cultured cells from the liverwort Marchantia polymorpha L. *Methods in Molecular Biology (Clifton, N.J.)*, *1132*, 439–447. https://doi.org/10.1007/978-1-62703-995-6_30

COHEN, D. J., LOERTSCHER, R., RUBIN, M. F., TILNEY, N. L., CARPENTER, C. B., & STROM, T. B. (1984). Cyclosporine: A New Immunosuppressive Agent for Organ Transplantation. *Annals of Internal Medicine*, *101*(5), 667–682. https://doi.org/10.7326/0003-4819-101-5-667

Cox, R. J., & Al-Fahad, A. (2013). Chemical mechanisms involved during the biosynthesis of tropolones. *Current Opinion in Chemical Biology*, *17*(4), 532–536. https://doi.org/https://doi.org/10.1016/j.cbpa.2013.06.029

Da Silva, N. A., & Srikrishnan, S. (2012). Introduction and expression of genes for metabolic engineering applications in Saccharomyces cerevisiae. *FEMS Yeast Research*, *12*(2), 197–214. https://doi.org/10.1111/j.1567-1364.2011.00769.x

Davidovich, C., Bashan, A., Auerbach-Nevo, T., Yaggie, R. D., Gontarek, R. R., & Yonath, A. (2007). Induced-fit tightens pleuromutilins binding to ribosomes and remote interactions enable their selectivity. *Proceedings of the National Academy of Sciences*, *104*(11), 4291–4296. https://doi.org/10.1073/pnas.0700041104

de Mattos-Shipley, K M J, Ford, K. L., Alberti, F., Banks, A. M., Bailey, A. M., & Foster, G. D. (2016). The good, the bad and the tasty: The many roles of mushrooms. *Studies in Mycology*, *85*, 125–157. https://doi.org/https://doi.org/10.1016/j.simyco.2016.11.002

de Mattos-Shipley, Kate M J, Foster, G. D., & Bailey, A. M. (2017). Insights into the Classical Genetics of Clitopilus passeckerianus – the Pleuromutilin Producing Mushroom. *Frontiers in Microbiology*, *8*, 1056. https://doi.org/10.3389/fmicb.2017.01056

de Mattos-Shipley, Kate M J, Greco, C., Heard, D. M., Hough, G., Mulholland, N. P., Vincent, J. L., Micklefield, J., Simpson, T. J., Willis, C. L., Cox, R. J., & Bailey, A. M.

(2018). The cycloaspeptides: uncovering a new model for methylated nonribosomal peptide biosynthesis. *Chem. Sci.*, *9*(17), 4109–4117. https://doi.org/10.1039/C8SC00717A

Deans, T. L., Cantor, C. R., & Collins, J. J. (2007). A Tunable Genetic Switch Based on RNAi and Repressor Proteins for Regulating Gene Expression in Mammalian Cells. *Cell*, *130*(2), 363–372. https://doi.org/10.1016/j.cell.2007.05.045

Decker, E. L., & Reski, R. (2020). Mosses in biotechnology. *Current Opinion in Biotechnology*, *61*, 21–27. https://doi.org/https://doi.org/10.1016/j.copbio.2019.09.021

Denning, D. W. (2002). Echinocandins: a new class of antifungal. *Journal of Antimicrobial Chemotherapy*, *49*(6), 889–891. https://doi.org/10.1093/jac/dkf045

Doyle, J. (1991). DNA Protocols for Plants. In G. M. Hewitt, A. W. B. Johnston, & J. P. W. Young (Eds.), *Molecular Techniques in Taxonomy* (pp. 283–293). Springer Berlin Heidelberg. https://doi.org/10.1007/978-3-642-83962-7_18

Engler, C., Youles, M., Gruetzner, R., Ehnert, T.-M., Werner, S., Jones, J. D. G., Patron, N. J., & Marillonnet, S. (2014). A Golden Gate Modular Cloning Toolbox for Plants. *ACS Synthetic Biology*, *3*(11), 839–843. https://doi.org/10.1021/sb4001504

Farney, E. P., Feng, S. S., Schäfers, F., & Reisman, S. E. (2018). Total Synthesis of (+)-Pleuromutilin. *Journal of the American Chemical Society*, *140*(4), 1267–1270. https://doi.org/10.1021/jacs.7b13260

Fazakerley, N. J., Helm, M. D., & Procter, D. J. (2013). Total Synthesis of (+)-Pleuromutilin. *Chemistry – A European Journal*, *19*(21), 6718–6723. https://doi.org/10.1002/chem.201300968

Fazakerley, N. J., & Procter, D. J. (2014). Synthesis and synthetic chemistry of pleuromutilin. *Tetrahedron*, *70*(39), 6911–6930. https://doi.org/https://doi.org/10.1016/j.tet.2014.05.092

File Jr, T. M., Goldberg, L., Das, A., Sweeney, C., Saviski, J., Gelone, S. P., Seltzer, E., Paukner, S., Wicha, W. W., Talbot, G. H., & Gasink, L. B. (2019). Efficacy and Safety of Intravenous-to-oral Lefamulin, a Pleuromutilin Antibiotic, for the Treatment of Community-acquired Bacterial Pneumonia: The Phase III Lefamulin Evaluation Against Pneumonia (LEAP 1) Trial. *Clinical Infectious Diseases*, *69*(11), 1856–1867. https://doi.org/10.1093/cid/ciz090

Finkelstein, E., Amichai, B., & Grunwald, M. H. (1996). Griseofulvin and its uses.

International Journal of Antimicrobial Agents, *6*(4), 189–194. https://doi.org/https://doi.org/10.1016/0924-8579(95)00037-2

Fisch, K. M., Bakeer, W., Yakasai, A. A., Song, Z., Pedrick, J., Wasil, Z., Bailey, A. M., Lazarus, C. M., Simpson, T. J., & Cox, R. J. (2011). Rational Domain Swaps Decipher Programming in Fungal Highly Reducing Polyketide Synthases and Resurrect an Extinct Metabolite. *Journal of the American Chemical Society*, *133*(41), 16635–16641. https://doi.org/10.1021/ja206914q

Flores-Sandoval, E., Dierschke, T., Fisher, T. J., & Bowman, J. L. (2015). Efficient and Inducible Use of Artificial MicroRNAs in Marchantia polymorpha. *Plant and Cell Physiology*, *57*(2), 281–290. https://doi.org/10.1093/pcp/pcv068

Fraga, D., Meulia, T., & Fenster, S. (2008). Real-Time PCR. *Current Protocols Essential Laboratory Techniques*, *00*(1), 10.3.1-10.3.34. https://doi.org/10.1002/9780470089941.et1003s00

FUJII, R., MINAMI, A., TSUKAGOSHI, T., SATO, N., SAHARA, T., OHGIYA, S., GOMI, K., & OIKAWA, H. (2011). Total Biosynthesis of Diterpene Aphidicolin, a Specific Inhibitor of DNA Polymerase α: Heterologous Expression of Four Biosynthetic Genes in Aspergillus oryzae. *Bioscience, Biotechnology, and Biochemistry*, *75*(9), 1813–1817. https://doi.org/10.1271/bbb.110366

Gandhi, S. G. (2019). Synthetic Biology for Production of Commercially Important Natural Product Small Molecules. In *Current Developments in Biotechnology and Bioengineering*. Elsevier B.V. https://doi.org/10.1016/b978-0-444-64085-7.00008-3

Gao, J., Wang, G., Ma, S., Xie, X., Wu, X., Zhang, X., Wu, Y., Zhao, P., & Xia, Q. (2015). CRISPR/Cas9-mediated targeted mutagenesis in Nicotiana tabacum. *Plant Molecular Biology*, *87*(1), 99–110. https://doi.org/10.1007/s11103-014-0263-0

Garabagi, F., McLean, M. D., & Hall, J. C. (2012). Transient and stable expression of antibodies in Nicotiana species. *Methods in Molecular Biology (Clifton, N.J.)*, *907*, 389–408. https://doi.org/10.1007/978-1-61779-974-7_23

Gaweł-Bęben, K., Osika, P., Asakawa, Y., Antosiewicz, B., Głowniak, K., & Ludwiczuk, A. (2019). Evaluation of anti-melanoma and tyrosinase inhibitory properties of marchantin A, a natural macrocyclic bisbibenzyl isolated from Marchantia species. *Phytochemistry Letters*, *31*, 192–195. https://doi.org/https://doi.org/10.1016/j.phytol.2019.04.008

Gibbons, E. G. (1982). Total synthesis of (.+-.)-pleuromutilin. *Journal of the American*

Chemical Society, *104*(6), 1767–1769. https://doi.org/10.1021/ja00370a067

Gibson, D. G. (2009). Synthesis of DNA fragments in yeast by one-step assembly of overlapping oligonucleotides. *Nucleic Acids Research*, *37*(20), 6984–6990. https://doi.org/10.1093/nar/gkp687

Gidijala, L., Kiel, J. A. K. W., Bovenberg, R. A. L., Van Der Klei, I. J., & Berg, M. A. Van Den. (2010). Biosynthesis of active pharmaceuticals: β-lactam biosynthesis in filamentous fungi. *Biotechnology and Genetic Engineering Reviews*, *27*(1), 1–32. https://doi.org/10.1080/02648725.2010.10648143

Gitzinger, M., Parsons, J., Reski, R., & Fussenegger, M. (2009). Functional cross-kingdom conservation of mammalian and moss (Physcomitrella patens) transcription, translation and secretion machineries. *Plant Biotechnology Journal*, *7*(1), 73–86. https://doi.org/10.1111/j.1467-7652.2008.00376.x

Goethe, O., Heuer, A., Ma, X., Wang, Z., & Herzon, S. B. (2018). Antibacterial properties and clinical potential of pleuromutilins. *Nat. Prod. Rep.* https://doi.org/10.1039/C8NP00042E

Hamm, S., Bleton, J., Connan, J., & Tchapla, A. (2005). A chemical investigation by headspace SPME and GC–MS of volatile and semi-volatile terpenes in various olibanum samples. *Phytochemistry*, *66*(12), 1499–1514. https://doi.org/https://doi.org/10.1016/j.phytochem.2005.04.025

Hargreaves, J., Park, J., Ghisalberti, E. L., Sivasithamparam, K., Skelton, B. W., & White, A. H. (2002). New Chlorinated Diphenyl Ethers from an Aspergillus Species. *Journal of Natural Products*, *65*(1), 7–10. https://doi.org/10.1021/np0102758

Harrison, C. J., Roeder, A. H. K., Meyerowitz, E. M., & Langdale, J. A. (2009). Local cues and asymmetric cell divisions underpin body plan transitions in the moss Physcomitrella patens. *Current Biology : CB*, *19*(6), 461–471. https://doi.org/10.1016/j.cub.2009.02.050

Hellwig, S., Drossard, J., Twyman, R. M., & Fischer, R. (2004). Plant cell cultures for the production of recombinant proteins. *Nature Biotechnology*, *22*(11), 1415–1422. https://doi.org/10.1038/nbt1027

Heneghan, M. N., Yakasai, A. A., Halo, L. M., Song, Z., Bailey, A. M., Simpson, T. J., Cox, R. J., & Lazarus, C. M. (2010). First Heterologous Reconstruction of a Complete Functional Fungal Biosynthetic Multigene Cluster. *ChemBioChem*, *11*(11), 1508–1512.

https://doi.org/10.1002/cbic.201000259

Hoepfner, D., McNamara, C. W., Lim, C. S., Studer, C., Riedl, R., Aust, T., McCormack, S. L., Plouffe, D. M., Meister, S., Schuierer, S., Plikat, U., Hartmann, N., Staedtler, F., Cotesta, S., Schmitt, E. K., Petersen, F., Supek, F., Glynne, R. J., Tallarico, J. A., … Winzeler, E. A. (2012). Selective and specific inhibition of the plasmodium falciparum lysyl-tRNA synthetase by the fungal secondary metabolite cladosporin. *Cell Host & Microbe*, *11*(6), 654–663. https://doi.org/10.1016/j.chom.2012.04.015

Hogune Im1*, J. S. and D. W. R. (2011). The Inoue Method for Preparation and Transformation of Competent. *Bio-Protocol*, *1*(20), 1–7.

Hohe, A., Egener, T., Lucht, J. M., Holtorf, H., Reinhard, C., Schween, G., & Reski, R. (2004). An improved and highly standardised transformation procedure allows efficient production of single and multiple targeted gene-knockouts in a moss, Physcomitrella patens. *Current Genetics*, *44*(6), 339–347. https://doi.org/10.1007/s00294-003-0458-4

Hohe, A., & Reski, R. (2002). Optimisation of a bioreactor culture of the moss Physcomitrella patens for mass production of protoplasts. *Plant Science*, *163*(1), 69–74. https://doi.org/https://doi.org/10.1016/S0168-9452(02)00059-6

Hojjati, M. R., Li, Z., Zhou, H., Tang, S., Huan, C., Ooi, E., Lu, S., & Jiang, X.-C. (2005). Effect of Myriocin on Plasma Sphingolipid Metabolism and Atherosclerosis in apoE-deficient Mice. *Journal of Biological Chemistry* , *280*(11), 10284–10289. https://doi.org/10.1074/jbc.M412348200

Holtorf, H., Hohe, A., Wang, H.-L., Jugold, M., Rausch, T., Duwenig, E., & Reski, R. (2002). Promoter subfragments of the sugar beet V-type H+-ATPase subunit c isoform drive the expression of transgenes in the moss Physcomitrella patens. *Plant Cell Reports*, *21*(4), 341–346. https://doi.org/10.1007/s00299-002-0521-5

Horstmann, V., Huether, C. M., Jost, W., Reski, R., & Decker, E. L. (2004). Quantitative promoter analysis in Physcomitrella patens: a set of plant vectors activating gene expression within three orders of magnitude. *BMC Biotechnology*, *4*(1), 13. https://doi.org/10.1186/1472-6750-4-13

Huether, C. M., Lienhart, O., Baur, A., Stemmer, C., Gorr, G., Reski, R., & Decker, E. L. (2005). *Glyco-Engineering of Moss Lacking Plant-Specific Sugar Residues*. *7*, 292–299. https://doi.org/10.1055/s-2005-837653

Hurst, L. D., Pál, C., & Lercher, M. J. (2004). The evolutionary dynamics of eukaryotic gene

order. *Nature Reviews Genetics*, *5*(4), 299–310. https://doi.org/10.1038/nrg1319

Inoue, H., Nojima, H., & Okayama, H. (1990). High efficiency transformation of Escherichia coli with plasmids. *Gene*, *96*(1), 23–28. https://doi.org/10.1016/0378-1119(90)90336-p

Ishizaki, K. (2017). Evolution of land plants: insights from molecular studies on basal lineages. *Bioscience, Biotechnology, and Biochemistry*, *81*(1), 73–80. https://doi.org/10.1080/09168451.2016.1224641

Ishizaki, K., Nishihama, R., Yamato, K. T., & Kohchi, T. (2016). Molecular Genetic Tools and Techniques for Marchantia polymorpha Research. *Plant & Cell Physiology*, *57*(2), 262–270. https://doi.org/10.1093/pcp/pcv097

Jantwal, A., Rana, M., Joshi Rana, A., Upadhyay, J., Durgapal, S., & Arvind Jantwal, C. (2019). Pharmacological potential of genus Marchantia: A Review. *~ 641 ~ Journal of Pharmacognosy and Phytochemistry*, *8*(2), 641–645.

Jones, R. N., Fritsche, T. R., Sader, H. S., & Ross, J. E. (2006). Activity of Retapamulin (SB-275833), a Novel Pleuromutilin, against Selected Resistant Gram-Positive Cocci. *Antimicrobial Agents and Chemotherapy*, *50*(7), 2583–2586. https://doi.org/10.1128/AAC.01432-05

Jost, W., Link, S., Horstmann, V., Decker, E. L., Reski, R., & Gorr, G. (2005). Isolation and characterisation of three moss-derived beta-tubulin promoters suitable for recombinant expression. *Current Genetics*, *47*(2), 111–120. https://doi.org/10.1007/s00294-004-0555-z

Kahan, B. D. (1985). Cyclosporine: the agent and its actions. *Transplantation Proceedings*, *17*(4 Suppl 1), 5—18.

Kahn, M. (1980). Anionic oxy-cope reaction of a divinyl cyclobutanol, pleuromutilin model study. *Tetrahedron Letters*, *21*(47), 4547–4548. https://doi.org/https://doi.org/10.1016/S0040-4039(00)74547-3

Kapoor, L. (2001). *Handbook of Ayurvedic Medicinal Plants*. *1st Editio*(New York: Routledge).

Kasten, B., & Reski, R. (1997). Antibiotics Inhibit Chloroplast Division b. *Journal of Plant Physiology*, *150*(1–2), 137–140. https://doi.org/10.1016/S0176-1617(97)80193-9

Katayama, N., Takano, H., Sugiyama, M., Takio, S., Sakai, A., Tanaka, K., Kuroiwa, H., & Ono, K. (2003). Effects of Antibiotics that Inhibit the Bacterial Peptidoglycan Synthesis

Pathway on Moss Chloroplast Division. *Plant & Cell Physiology*, *44*, 776–781. https://doi.org/10.1093/pcp/pcg096

Kavanagh, F, Hervey, A., & Robbins, W. J. (1951). Antibiotic Substances From Basidiomycetes: VIII. Pleurotus Multilus (Fr.) Sacc. and Pleurotus Passeckerianus Pilat. *Proceedings of the National Academy of Sciences of the United States of America*, *37*(9), 570–574.

Kavanagh, Frederick, Hervey, A., & Robbins, W. J. (1952). Antibiotic Substances from Basidiomycetes. *Proceedings of the National Academy of Sciences*, *38*(7), 555–560. https://doi.org/10.1073/pnas.38.7.555

Kelly, C. L., Liu, Z., Yoshihara, A., Jenkinson, S. F., Wormald, M. R., Otero, J., Estévez, A., Kato, A., Marqvorsen, M. H. S., Fleet, G. W. J., Estévez, R. J., Izumori, K., & Heap, J. T. (2016). Synthetic Chemical Inducers and Genetic Decoupling Enable Orthogonal Control of the rhaBAD Promoter. *ACS Synthetic Biology*, *5*(10), 1136–1145. https://doi.org/10.1021/acssynbio.6b00030

Kempinski, C., Jiang, Z., Bell, S., & Chappell, J. (2015). Metabolic engineering of higher plants and algae for isoprenoid production. *Advances in Biochemical Engineering/Biotechnology*, *148*, 161–199. https://doi.org/10.1007/10_2014_290

Khairul Ikram, N. K. B., Beyraghdar Kashkooli, A., Peramuna, A. V., van der Krol, A. R., Bouwmeester, H., & Simonsen, H. T. (2017). Stable Production of the Antimalarial Drug Artemisinin in the Moss Physcomitrella patens. *Frontiers in Bioengineering and Biotechnology*, *5*, 47. https://doi.org/10.3389/fbioe.2017.00047

Khraiwesh, B., Ossowski, S., Weigel, D., Reski, R., & Frank, W. (2008). Specific Gene Silencing by Artificial MicroRNAs in Physcomitrella patens: An Alternative to Targeted Gene Knockouts. *Plant Physiology*, *148*(2), 684–693. https://doi.org/10.1104/pp.108.128025

King, B. C., Vavitsas, K., Ikram, N. K. B. K., Schrøder, J., Scharff, L. B., Bassard, J.-É., Hamberger, B., Jensen, P. E., & Simonsen, H. T. (2016). In vivo assembly of DNA-fragments in the moss, Physcomitrella patens. *Scientific Reports*, *6*, 25030.

Kjærbølling, I., Mortensen, U. H., Vesth, T., & Andersen, M. R. (2019). Strategies to establish the link between biosynthetic gene clusters and secondary metabolites. *Fungal Genetics and Biology*, *130*(May), 107–121. https://doi.org/10.1016/j.fgb.2019.06.001

Kopischke, S., Schüßler, E., Althoff, F., & Zachgo, S. (2017). TALEN-mediated genome-

editing approaches in the liverwort Marchantia polymorpha yield high efficiencies for targeted mutagenesis. *Plant Methods*, *13*(1), 20. https://doi.org/10.1186/s13007-017-0167-5

Koprivova, A., Stemmer, C., Altmann, F., Hoffmann, A., Kopriva, S., Gorr, G., Reski, R., & Decker, E. L. (2004). Targeted knockouts of Physcomitrella lacking plant-specific immunogenic N-glycans. *Plant Biotechnology Journal*, *2*(6), 517–523. https://doi.org/10.1111/j.1467-7652.2004.00100.x

Kubo, M., Imai, A., Nishiyama, T., Ishikawa, M., Sato, Y., Kurata, T., Hiwatashi, Y., Reski, R., & Hasebe, M. (2013). System for Stable β-Estradiol-Inducible Gene Expression in the Moss Physcomitrella patens. *PLOS ONE*, *8*(9), e77356.

KUBOTA, A., ISHIZAKI, K., HOSAKA, M., & KOHCHI, T. (2013). Efficient Agrobacterium-Mediated Transformation of the Liverwort Marchantia polymorpha Using Regenerating Thalli. *Bioscience, Biotechnology, and Biochemistry*, *77*(1), 167–172. https://doi.org/10.1271/bbb.120700

Kumar, P., Mahato, D. K., Kamle, M., Mohanta, T. K., & Kang, S. G. (2017). Aflatoxins: A Global Concern for Food Safety, Human Health and Their Management. *Frontiers in Microbiology*, *7*, 2170. https://doi.org/10.3389/fmicb.2016.02170

Kupfer, D. M., Drabenstot, S. D., Buchanan, K. L., Lai, H., Zhu, H., Dyer, D. W., Roe, B. A., & Murphy, J. W. (2004). Introns and splicing elements of five diverse fungi. *Eukaryotic Cell*, *3*(5), 1088–1100. https://doi.org/10.1128/EC.3.5.1088-1100.2004

Kytidou, K., Beenakker, T. J. M., Westerhof, L. B., Hokke, C. H., Moolenaar, G. F., Goosen, N., Mirzaian, M., Ferraz, M. J., de Geus, M., Kallemeijn, W. W., Overkleeft, H. S., Boot, R. G., Schots, A., Bosch, D., & Aerts, J. M. F. G. (2017). Human Alpha Galactosidases Transiently Produced in Nicotiana benthamiana Leaves: New Insights in Substrate Specificities with Relevance for Fabry Disease. *Frontiers in Plant Science*, *8*, 1026. https://doi.org/10.3389/fpls.2017.01026

Lazarus, C. M., Williams, K., & Bailey, A. M. (2014). Reconstructing fungal natural product biosynthetic pathways. *Nat. Prod. Rep.*, *31*(10), 1339–1347. https://doi.org/10.1039/C4NP00084F

Li, X. (2011). Infiltration of Nicotiana benthamiana Protocol for Transient Expression via Agrobacterium. *Bio-Protocol*, *1*(14), e95. https://doi.org/10.21769/BioProtoc.95

Liew, W.-P.-P., & Mohd-Redzwan, S. (2018). Mycotoxin: Its Impact on Gut Health and

Microbiota. *Frontiers in Cellular and Infection Microbiology*, *8*, 60. https://doi.org/10.3389/fcimb.2018.00060

Liu, C., Minami, A., Ozaki, T., Wu, J., Kawagishi, H., Maruyama, J., & Oikawa, H. (2019). Efficient Reconstitution of Basidiomycota Diterpene Erinacine Gene Cluster in Ascomycota Host Aspergillus oryzae Based on Genomic DNA Sequences. *Journal of the American Chemical Society*, *141*(39), 15519–15523. https://doi.org/10.1021/jacs.9b08935

Liu, J., Lotesta, S. D., & Sorensen, E. J. (2011). A concise synthesis of the molecular framework of pleuromutilin. *Chemical Communications*, *47*(5), 1500–1502. https://doi.org/10.1039/C0CC04077K

Manzoni, M., & Rollini, M. (2002). Biosynthesis and biotechnological production of statins by filamentous fungi and application of these cholesterol-lowering drugs. *Applied Microbiology and Biotechnology*, *58*(5), 555–564. https://doi.org/10.1007/s00253-002-0932-9

Marillonnet, S., & Werner, S. (2015). *Assembly of Multigene Constructs Using Golden Gate Cloning BT - Glyco-Engineering: Methods and Protocols* (A. Castilho (Ed.); pp. 269–284). Springer New York. https://doi.org/10.1007/978-1-4939-2760-9_19

McCormick, S. P., Stanley, A. M., Stover, N. A., & Alexander, N. J. (2011). Trichothecenes: from simple to complex mycotoxins. *Toxins*, *3*(7), 802–814. https://doi.org/10.3390/toxins3070802

McLean, K. J., Hans, M., Meijrink, B., van Scheppingen, W. B., Vollebregt, A., Tee, K. L., van der Laan, J.-M., Leys, D., Munro, A. W., & van den Berg, M. A. (2015). Single-step fermentative production of the cholesterol-lowering drug pravastatin via reprogramming of Penicillium chrysogenum. *Proceedings of the National Academy of Sciences*, *112*(9), 2847–2852. https://doi.org/10.1073/pnas.1419028112

Medema, M. H., & Fischbach, M. A. (2015). Computational approaches to natural product discovery. *Nature Chemical Biology*, *11*(9), 639–648. https://doi.org/10.1038/nchembio.1884

Miyagishima, S. ya, Kabeya, Y., Sugita, C., Sugita, M., & Fujiwara, T. (2014). DipM is required for peptidoglycan hydrolysis during chloroplast division. *BMC Plant Biology*, *14*(1), 1–15. https://doi.org/10.1186/1471-2229-14-57

Morath, V., Truong, D.-J. J., Albrecht, F., Polte, I., Ciccone, R. A., Funke, L. F., Reichart, L.,

Wolf, C. G., Brunner, A.-D., Fischer, K., Schneider, P. C., Brüggenthies, J. B., Fröhlich, F., Wiedemann, G., Reski, R., & Skerra, A. (2014). Design and Characterization of a Modular Membrane Protein Anchor to Functionalize the Moss Physcomitrella patens with Extracellular Catalytic and/or Binding Activities. *ACS Synthetic Biology*, *3*(12), 990–994. https://doi.org/10.1021/sb5000302

Mosquna, A., Katz, A., Decker, E. L., Rensing, S. A., Reski, R., & Ohad, N. (2009). Regulation of stem cell maintenance by the Polycomb protein FIE has been conserved during land plant evolution. *Development*, *136*(14), 2433–2444. https://doi.org/10.1242/dev.035048

Mueller, S. J., Lang, D., Hoernstein, S. N. W., Lang, E. G. E., Schuessele, C., Schmidt, A., Fluck, M., Leisibach, D., Niegl, C., Zimmer, A. D., Schlosser, A., & Reski, R. (2014). Quantitative Analysis of the Mitochondrial and Plastid Proteomes of the Moss Physcomitrella patens Reveals Protein Macrocompartmentation and Microcompartmentation. *Plant Physiology*, *164*(4), 2081–2095. https://doi.org/10.1104/pp.114.235754

Müller, K., Siegel, D., Rodriguez Jahnke, F., Gerrer, K., Wend, S., Decker, E. L., Reski, R., Weber, W., & Zurbriggen, M. D. (2014). A red light-controlled synthetic gene expression switch for plant systems. *Mol. BioSyst.*, *10*(7), 1679–1688. https://doi.org/10.1039/C3MB70579J

Müller, S. J., Gütle, D. D., Jacquot, J.-P., & Reski, R. (2016). Can mosses serve as model organisms for forest research? *Annals of Forest Science*, *73*(1), 135–146. https://doi.org/10.1007/s13595-015-0468-7

Munawar, A., Marshall, J. W., Cox, R. J., Bailey, A. M., & Lazarus, C. M. (2013). Isolation and Characterisation of a Ferrirhodin Synthetase Gene from the Sugarcane Pathogen Fusarium sacchari. *ChemBioChem*, *14*(3), 388–394. https://doi.org/10.1002/cbic.201200587

Murén, E., Nilsson, A., Ulfstedt, M., Johansson, M., & Ronne, H. (2009). Rescue and characterization of episomally replicating DNA from the moss Physcomitrella. *Proceedings of the National Academy of Sciences of the United States of America*, *106*(46), 19444–19449. https://doi.org/10.1073/pnas.0908037106

Murphy, S. K., Zeng, M., & Herzon, S. B. (2017). A modular and enantioselective synthesis of the pleuromutilin antibiotics. *Science*, *356*(6341), 956 LP – 959. https://doi.org/10.1126/science.aan0003

Nei, M. (1967). Modification of linkage intensity by natural selection. *Genetics*, *57*(3), 625–641.

Nevalainen, K. M. H., Te'o, V. S. J., & Bergquist, P. L. (2005). Heterologous protein expression in filamentous fungi. *Trends in Biotechnology*, *23*(9), 468–474. https://doi.org/https://doi.org/10.1016/j.tibtech.2005.06.002

Newman, D. J., & Cragg, G. M. (2010). Natural products of therapeutic importance. *Comprehensive Natural Products II: Chemistry and Biology*, *2*, 623–650. https://doi.org/10.1016/b978-008045382-8.00055-1

Nielsen, M. T., Nielsen, J. B., Anyaogu, D. C., Holm, D. K., Nielsen, K. F., Larsen, T. O., & Mortensen, U. H. (2013). Heterologous Reconstitution of the Intact Geodin Gene Cluster in Aspergillus nidulans through a Simple and Versatile PCR Based Approach. *PLOS ONE*, *8*(8), e72871.

Nishihama, R., Ishida, S., Urawa, H., Kamei, Y., & Kohchi, T. (2015). Conditional Gene Expression/Deletion Systems for Marchantia polymorpha Using its Own Heat-Shock Promoter and Cre/ lox P-Mediated Site-Specific Recombination . *Plant and Cell Physiology*, *57*(2), 271–280. https://doi.org/10.1093/pcp/pcv102

Nofiani, R., de Mattos-Shipley, K., Lebe, K. E., Han, L.-C., Iqbal, Z., Bailey, A. M., Willis, C. L., Simpson, T. J., & Cox, R. J. (2018). Strobilurin biosynthesis in Basidiomycete fungi. *Nature Communications*, *9*(1), 3940. https://doi.org/10.1038/s41467-018-06202-4

Osbourn, A. (2010). *Gene Clusters for Secondary Metabolic Pathways : An Emerging Theme in Plant Biology 1*. *154*(October), 531–535. https://doi.org/10.1104/pp.110.161315

Pang, E. L., Peyret, H., Ramirez, A., Loh, H.-S., Lai, K.-S., Fang, C.-M., Rosenberg, W. M., & Lomonossoff, G. P. (2019). Epitope Presentation of Dengue Viral Envelope Glycoprotein Domain III on Hepatitis B Core Protein Virus-Like Particles Produced in Nicotiana benthamiana. *Frontiers in Plant Science*, *10*, 455. https://doi.org/10.3389/fpls.2019.00455

Parsons, J., Altmann, F., Arrenberg, C. K., Koprivova, A., Beike, A. K., Stemmer, C., Gorr, G., Reski, R., & Decker, E. L. (2012). Moss-based production of asialo-erythropoietin devoid of Lewis A and other plant-typical carbohydrate determinants. *Plant Biotechnology Journal*, *10*(7), 851–861. https://doi.org/10.1111/j.1467-7652.2012.00704.x

Paukner, S., & Riedl, R. (2017). Pleuromutilins: Potent Drugs for Resistant Bugs—Mode of

Action and Resistance. *Cold Spring Harbor Perspectives in Medicine , 7*(1).

Peramuna, A., Bae, H., Rasmussen, E. K., Dueholm, B., Waibel, T., Critchley, J. H., Brzezek, K., Roberts, M., & Simonsen, H. T. (2018). Evaluation of synthetic promoters in Physcomitrella patens. *Biochemical and Biophysical Research Communications*, *500*(2), 418–422. https://doi.org/https://doi.org/10.1016/j.bbrc.2018.04.092

Peremarti, A., Twyman, R. M., Gómez-Galera, S., Naqvi, S., Farré, G., Sabalza, M., Miralpeix, B., Dashevskaya, S., Yuan, D., Ramessar, K., Christou, P., Zhu, C., Bassie, L., & Capell, T. (2010). Promoter diversity in multigene transformation. *Plant Molecular Biology*, *73*(4–5), 363–378. https://doi.org/10.1007/s11103-010-9628-1

Poulsen, S. M., Karlsson, M., Johansson, L. B., & Vester, B. (2001). The pleuromutilin drugs tiamulin and valnemulin bind to the RNA at the peptidyl transferase centre on the ribosome. *Molecular Microbiology*, *41*(5), 1091–1099. https://doi.org/10.1046/j.1365-2958.2001.02595.x

Reddy, L., & Bhoola, K. (2010). Ochratoxins-food contaminants: impact on human health. *Toxins*, *2*(4), 771–779. https://doi.org/10.3390/toxins2040771

Reed, J., & Osbourn, A. (2018). Engineering terpenoid production through transient expression in Nicotiana benthamiana. *Plant Cell Reports*, *37*(10), 1431–1441. https://doi.org/10.1007/s00299-018-2296-3

Reski, R., Bae, H., & Simonsen, H. T. (2018). Physcomitrella patens, a versatile synthetic biology chassis. *Plant Cell Reports*, *37*(10), 1409–1417. https://doi.org/10.1007/s00299-018-2293-6

Reski, R., Parsons, J., & Decker, E. L. (2015). Moss-made pharmaceuticals: from bench to bedside. *Plant Biotechnology Journal*, *13*(8), 1191–1198. https://doi.org/10.1111/pbi.12401

Reutter, K., Atzorn, R., Hadeler, B., Schmülling, T., & Reski, R. (1998). Expression of the bacterial ipt gene in Physcomitrella rescues mutations in budding and in plastid division. *Planta*, *206*(2), 196–203. https://doi.org/10.1007/s004250050391

Saidi, Y., Finka, A., Chakhporanian, M., Zrÿd, J.-P., Schaefer, D. G., & Goloubinoff, P. (2005). Controlled Expression of Recombinant Proteins in Physcomitrella patens by a Conditional Heat-shock Promoter: a Tool for Plant Researchand Biotechnology. *Plant Molecular Biology*, *59*(5), 697–711. https://doi.org/10.1007/s11103-005-0889-z

Saint-Marcoux, D., Proust, H., Dolan, L., & Langdale, J. A. (2015). Identification of

Reference Genes for Real-Time Quantitative PCR Experiments in the Liverwort Marchantia polymorpha. *PLOS ONE*, *10*(3), e0118678.

Salis, H. M., Mirsky, E. A., & Voigt, C. A. (2009). Automated design of synthetic ribosome binding sites to control protein expression. *Nature Biotechnology*, *27*(10), 946–950. https://doi.org/10.1038/nbt.1568

Sam Mugford, S. H. (2018). *Bounce PCR*. Protocols.Io Dx.Doi.Org/10.17504/Protocols.Io.Vhge.

San Andrés Larrea, M. I., San Andrés Larrea, M. D., & Rodriguez Fernández, C. (2014). *Plants, Poisonous (Animals)* (P. B. T.-E. of T. (Third E. Wexler (Ed.); pp. 960–969). Academic Press. https://doi.org/https://doi.org/10.1016/B978-0-12-386454-3.00462-0

Sato, S., Okusa, N., Ogawa, A., Ikenoue, T., Seki, T., & Tsuji, T. (2005). Identification and Preliminary SAR Studies of (+)-Geodin as a Glucose Uptake Stimulator for Rat Adipocytes. *The Journal of Antibiotics*, *58*(9), 583–589. https://doi.org/10.1038/ja.2005.79

Sauret-Güeto, S., Frangedakis, E., Silvestri, L., Rebmann, M., Tomaselli, M., Markel, K., Delmans, M., West, A., Patron, N. J., & Haseloff, J. (2020). Systematic Tools for Reprogramming Plant Gene Expression in a Simple Model, Marchantia polymorpha. *ACS Synthetic Biology*, *9*(4), 864–882. https://doi.org/10.1021/acssynbio.9b00511

Schaaf, A., Tintelnot, S., Baur, A., Reski, R., Gorr, G., & Decker, E. L. (2005). Use of endogenous signal sequences for transient production and efficient secretion by moss (Physcomitrella patens) cells. *BMC Biotechnology*, *5*(1), 30. https://doi.org/10.1186/1472-6750-5-30

Schaefer, D., Zryd, J.-P., Knight, C. D., & Cove, D. J. (1991). Stable transformation of the moss Physcomitrella patens. *Molecular and General Genetics MGG*, *226*(3), 418–424. https://doi.org/10.1007/BF00260654

Schlünzen, F., Pyetan, E., Fucini, P., Yonath, A., & Harms, J. M. (2004). Inhibition of peptide bond formation by pleuromutilins: the structure of the 50S ribosomal subunit from Deinococcus radiodurans in complex with tiamulin. *Molecular Microbiology*, *54*(5), 1287–1294. https://doi.org/10.1111/j.1365-2958.2004.04346.x

Schmid, M. W., Giraldo-Fonseca, A., Rövekamp, M., Smetanin, D., Bowman, J. L., & Grossniklaus, U. (2018). Extensive epigenetic reprogramming during the life cycle of Marchantia polymorpha. *Genome Biology*, *19*(1), 9. https://doi.org/10.1186/s13059-017-

1383-z

Schmidt-Dannert, C. (2015). NextGen microbial natural products discovery. *Microbial Biotechnology*, *8*(1), 26–28. https://doi.org/10.1111/1751-7915.12184

Smanski, Michael J.; Mead, David; Gustafsson, Claes; Thomas, M. G. (2017). Meeting Report for Synthetic Biology for Natural Products 2017: The Interface of (Meta)Genomics, Machine Learning, and Natural Product Discovery. *ACS Synthetic Biology*, *6*(5), 737–743. https://doi.org/10.1021/acssynbio.7b00132

Some studies in the biosynthesis of terpenes and related compounds . (1968). In *Pure and Applied Chemistry* (Vol. 17, p. 331). https://doi.org/10.1351/pac196817030331

Sørensen, H. P., & Mortensen, K. K. (2005). Advanced genetic strategies for recombinant protein expression in Escherichia coli. *Journal of Biotechnology*, *115*(2), 113–128. https://doi.org/https://doi.org/10.1016/j.jbiotec.2004.08.004

Sproul, D., Gilbert, N., & Bickmore, W. A. (2005). The role of chromatin structure in regulating the expression of clustered genes. *Nature Reviews Genetics*, *6*(10), 775–781. https://doi.org/10.1038/nrg1688

Strader, C. R., Pearce, C. J., & Oberlies, N. H. (2011). Fingolimod (FTY720): A Recently Approved Multiple Sclerosis Drug Based on a Fungal Secondary Metabolite. *Journal of Natural Products*, *74*(4), 900–907. https://doi.org/10.1021/np2000528

Sugano, S. S., Nishihama, R., Shirakawa, M., Takagi, J., Matsuda, Y., Ishida, S., Shimada, T., Hara-Nishimura, I., Osakabe, K., & Kohchi, T. (2018). Efficient CRISPR/Cas9-based genome editing and its application to conditional genetic analysis in Marchantia polymorpha. *PLOS ONE*, *13*(10), e0205117.

Tagami, K., Liu, C., Minami, A., Noike, M., Isaka, T., Fueki, S., Shichijo, Y., Toshima, H., Gomi, K., Dairi, T., & Oikawa, H. (2013). Reconstitution of Biosynthetic Machinery for Indole-Diterpene Paxilline in Aspergillus oryzae. *Journal of the American Chemical Society*, *135*(4), 1260–1263. https://doi.org/10.1021/ja3116636

Tagami, K., Minami, A., Fujii, R., Liu, C., Tanaka, M., Gomi, K., Dairi, T., & Oikawa, H. (2014). Rapid Reconstitution of Biosynthetic Machinery for Fungal Metabolites in Aspergillus oryzae: Total Biosynthesis of Aflatrem. *ChemBioChem*, *15*(14), 2076–2080. https://doi.org/10.1002/cbic.201402195

Takahashi, H., & Asakawa, Y. (2017). Transcriptome Analysis of Marchantin Biosynthesis from the Liverwort Marchantia polymorpha. *Natural Product Communications*, *12*(8),

1934578X1701200831. https://doi.org/10.1177/1934578X1701200831

Takemura, M., Kanamoto, H., Nagaya, S., & Ohyama, K. (2013). Bioproduction of prostaglandins in a transgenic liverwort, Marchantia polymorpha. *Transgenic Research*, *22*(5), 905–911. https://doi.org/10.1007/s11248-013-9699-2

Takenaka, M., Yamaoka, S., Hanajiri, T., Shimizu-Ueda, Y., Yamato, K. T., Fukuzawa, H., & Ohyama, K. (2000). Direct transformation and plant regeneration of the haploid liverwort Marchantia polymorpha L. *Transgenic Research*, *9*(3), 179–185. https://doi.org/10.1023/A:1008963410465

Tounou, E., Takio, S., Sakai, A., Ono, K., & Takano, H. (2002). Ampicillin Inhibits Chloroplast Division in Cultured Cells of the Liverwort Marchantia polymorpha. *CYTOLOGIA*, *67*(4), 429–434. https://doi.org/10.1508/cytologia.67.429

Tran, P. N., Yen, M.-R., Chiang, C.-Y., Lin, H.-C., & Chen, P.-Y. (2019). Detecting and prioritizing biosynthetic gene clusters for bioactive compounds in bacteria and fungi. *Applied Microbiology and Biotechnology*, *103*(8), 3277–3287. https://doi.org/10.1007/s00253-019-09708-z

Tsuboyama, S., & Kodama, Y. (2018). AgarTrap Protocols on your Benchtop: Simple Methods for Agrobacterium-mediated Genetic Transformation of the Liverwort Marchantia polymorpha. *Plant Biotechnology (Tokyo, Japan)*, *35*(2), 93–99. https://doi.org/10.5511/plantbiotechnology.18.0312b

Ulfstedt, M., Hu, G.-Z., Johansson, M., & Ronne, H. (2017). Testing of Auxotrophic Selection Markers for Use in the Moss Physcomitrella Provides New Insights into the Mechanisms of Targeted Recombination. *Frontiers in Plant Science*, *8*, 1850. https://doi.org/10.3389/fpls.2017.01850

Vardakou, M., Sainsbury, F., Rigby, N., Mulholland, F., & Lomonossoff, G. P. (2012). Expression of active recombinant human gastric lipase in Nicotiana benthamiana using the CPMV-HT transient expression system. *Protein Expression and Purification*, *81*(1), 69–74. https://doi.org/https://doi.org/10.1016/j.pep.2011.09.005

Veve, M. P. (2018). *R EVIEWS OF T HERAPEUTICS Lefamulin : Review of a Promising Novel Pleuromutilin Antibiotic*. https://doi.org/10.1002/phar.2166

Wang, Baojun, Barahona, M., & Buck, M. (2014). Engineering modular and tunable genetic amplifiers for scaling transcriptional signals in cascaded gene networks. *Nucleic Acids Research*, *42*(14), 9484–9492. https://doi.org/10.1093/nar/gku593

Wang, Bo, Kashkooli, A. B., Sallets, A., Ting, H.-M., de Ruijter, N. C. A., Olofsson, L., Brodelius, P., Pottier, M., Boutry, M., Bouwmeester, H., & van der Krol, A. R. (2016). Transient production of artemisinin in Nicotiana benthamiana is boosted by a specific lipid transfer protein from A. annua. *Metabolic Engineering*, *38*, 159–169. https://doi.org/https://doi.org/10.1016/j.ymben.2016.07.004

Weber, E., Engler, C., Gruetzner, R., Werner, S., & Marillonnet, S. (2011). A Modular Cloning System for Standardized Assembly of Multigene Constructs. *PLOS ONE*, *6*(2), 1–11. https://doi.org/10.1371/journal.pone.0016765

Werner, S., Engler, C., Weber, E., Gruetzner, R., & Marillonnet, S. (2012). Fast track assembly of multigene constructs using Golden Gate cloning and the MoClo system. *Bioengineered*, *3*(1), 38–43. https://doi.org/10.4161/bbug.3.1.18223

Wuest, D. M., Hou, S., & Lee, K. H. (2011). *3.52 - Metabolic Engineering* (M. B. T.-C. B. (Second E. Moo-Young (Ed.); pp. 617–628). Academic Press. https://doi.org/https://doi.org/10.1016/B978-0-08-088504-9.00229-4

Yamane, M., Minami, A., Liu, C., Ozaki, T., Takeuchi, I., Tsukagoshi, T., Tokiwano, T., Gomi, K., & Oikawa, H. (2017). Biosynthetic Machinery of Diterpene Pleuromutilin Isolated from Basidiomycete Fungi. *ChemBioChem*, *18*(23), 2317–2322. https://doi.org/10.1002/cbic.201700434

Zhang, J. D., Ruschhaupt, M., & Biczok, R. (2015). ddCt method for qRT – PCR data analysis. *Bioconductor*, 1–8.

Zhang, Y., Zhang, F., Li, X., Baller, J. A., Qi, Y., Starker, C. G., Bogdanove, A. J., & Voytas, D. F. (2013). Transcription activator-like effector nucleases enable efficient plant genome engineering. *Plant Physiology*, *161*(1), 20–27. https://doi.org/10.1104/pp.112.205179

Appendices

Appendix A: Coding sequences of the genes after domestication and plasmid maps of Level 0, Level 1, Level 2

A1. *Geranylgeranyl synthase* coding sequence

ATGAGAATACCTAACGTCTTTCTCTCTTACCTGCGACAAGTCGCCGTCGACGCCACTCTGT
CATCTTGCTCTGGAGTGAAGTCACGAAAGCCGGTCATTGCCTATGGCTTTGACGACTCGCA
AGACTCTCGCGTCGATGAGAATGACGAAAAAATATTGGAGCCCTTTGGCTACTATCGTCA
TCTTCTGAAAGGCAAGAGCGCCAGGACGGTGTTGATGCACTGCTTCAACGCGTTCCTTGG
ACTGCCCGAAGATTGGGTCATTGGCGTAACAAAGGCCATTGAGGACCTTCATAATGCATC
CCTACTAATTGATGACATCGAAGATGAGTCTGCCCTCCGTCGTGGTTCACCAGCTGCCCAC
ATGAAGTACGGGATTGCGCTCACCATGAACGCGGGGAATCTTGTCTACTTCACGGTCCTTC
AAGACGTCTATGACCTTGGCATGAAAACAGGTGGCACACAGGTTGCCAACGCAATGGCTC
GCATCTACACTGAAGAGATGATTGAGCTCCATCGCGGTCAGGGCATCGAAATCTGGTGGC
GTGACCAGCGGTCCCCTCCCTCCGTCGATCAATACATTCACATGCTCGAGCAGAAAACCG
GCGGCCTGCTCAGGCTTGGCGTACGGCTCTTGCAATGCCATCCCGGTGTCAATAGCAGGG
CCGACCTCTCCGACATTGCGCTCCGTATTGGTGTCTACTACCAACTTCGCGACGACTACAT
CAACCTCATGTCCACAAGCTACCACGACGAGCGTGGATTTGCTGAGGACATTACCGAAGG
AAAGTATACCTTCCCGATGTTGCACTCTCTCAAGAGGTCACCCGACTCTGGACTGCGTGAA
ATCTTGGACCTTAAGCCGGCCGACATCGCCCTGAAAAAGAAAGCTATCGCTATCATGCAA
GAGACAGGATCGCTTGTTGCAACCCGGAACCTTCTCGGTGCAGTCAGGAATGATCTCAGT
GGATTGGTTGCTGAACAGCGTGGAGACGACTACGCTATGAGCGCGGGTCTTGAACGATTC
TTGGAAAAGTTGTACATCGCAGAGTAG

A2. *Cyclase* coding sequence

ATGGGTCTATCTGAAGATCTTCATGCACGCGCCCGAACCCTCATGCAGACTCTCGAGTCTG
CGCTCAATACGCCAGGTTCTAGGGGTATTGGCACCGCGAATCCGACTATCTACGACACTG
CTTGGGTAGCCATGGTATCCCGTGAGATCGACGGCAAACAAGTCTTTGTCTTTCCAGAGAC
ATTCACCTACATCTACGAGCACCAGGAGGCTGACGGCAGTTGGTCAGGGGATGGATCCCT
CATTGACTCCATCGTCAATACTCTGGCCTGCCTTGTCGCTCTCAAGATGCACGAGAGCAAC
GCCTCAAAACCCGACATACCTGCCCGTGCCAGAGCCGCTCAAAATTATCTCGACGATGCC
CTAAAGCGCTGGGACATCATGGAGACTGAGCGTGTCGCGTACGAGATGATCGTACCCTGC
CTCCTCAAACAACTCGATGCCTTTGGCGTATCCTTCAGCTTCCCCCATCATGACCTTCTGTA
CAACATGTACGCCGGAAAACTGGCGAAGCTTAACTGGGAGGCTATCTACGCCAAGAACAG
CTCCTTGCTTCACTGCATGGAGGCATTCGTTGGTGTCTGCGACTTCGATCGCATGCCTCATC
TCCTACGTGATGGTAACTTCATGGCTACGCCATCTACCACCGCTGCATACCTCATGAAGGC
CACCAAGTGGGATGACCGAGCGGAGGATTACCTTCGCCACGTTATCGAGGTCTACGCACC
CCATGGCCGAGATGTTGTTCCTAACCTCTGGCCGATGACCTTCTTCGAGATCGTATGGTCG
CTCAGCTCCCTTTATGACAACAACCTGGAGTTTGCACAAATGGATCCGGAATGCTTGGATC
GCATTGCCCTCAAACTACGTGAATTCCTTGTGGCAGGAAAAGGTGTCTTAGGCTTCGTTCC
CGGCACCACTCACGACGCTGACATGAGCTCGAAAACCCTGATGCTCTTGCAAGTTCTCAA
CCACCCATATGCCCATGACGAATTCGTCACAGAGTTTGAGGCACCTACCTACTTCCGTTGC
TACTCTTTCGAAAGGAACGCAAGCGTGACCGTCAACTCCAACTGCCTTATGTCGCTCCTCC

ACGCCCCTGATGTCAACATGTACGAATCCCAAATCGTCAAGATCGCCACCTACGTCGCCG
ATGTCTGGTGGACATCAGCAGGTGTCGTCAAAGACAAATGGAATGTATCAGAATGGTACT
CCTCTATGCTGTCCTCACAGGCGCTTGTCCGTCTCCTTTTCGAGCACGGAAAGGGCAACCT
TAAATCCATATCTGAGGAGCTTCTGTCCAGGGTGTCCATCGCCTGCTTCACAATGATCAGT
CGTATTCTCCAGAGCCAGAAGCCCGATGGCTCTTGGGGATGCGCTGAAGAAACCTCATAC
GCTCTCATTACACTCGCCAACGTCGCTTCTCTTCCCACTTGCGACCTCATCCGCGACCACCT
GTACAAAGTCATTGAATCCGCGAAGGCATACCTCACCTCCATCTTCTACGCCCGCCCTGCT
GCCAAACCGGAGGACCGTGTCTGGATTGACAAGGTTACATATAGCGTCGAGTCATTCCGC
GATGCCTACCTCGTTTCTGCTCTCAACGTACCCATCCCCCGCTTCGATCCATCTTCCATCAG
CACTCTTCCTACTATCTCGCAAACCTTGCCAAAGGAACTCTCTAAGTTCTTCGGGCGTCTT
GACATGTTCAAGCCTGCTCCCGAATGGCGCAAGCTTACGTGGGGCATTGAGGCCACTCTC
ATGGGCCCCGAGCTCAACCGTGTCCCATCGTCCACGTTCGCCAAGGTAGAGAAGGGAGCG
GCGGGCAAATGGTTCGAGTTCTTGCCATACATGACCATCGCTCCGAGCAGCTTGGAAGGC
ACTCCTATCAGTTCACAAGGGATGCTGGACGTGCTCGTTCTCATCCGCGGTCTTTACAACA
CCGACGACTACCTCGATATGACCCTCATCAAGGCCACCAATGACGACTTGAACGACCTCA
AGAAGAAGATCCGCGACCTGTTCGCGGATCCGAAGTCGTTCTCGACCCTCAGCGAGGTCC
CGGATGACCGGATGCCTACGCACATCGAGGTCATTGAGCGCTTTGCCTATTCCCTGTTGAA
CCATCCCCGTGCACAGCTCGCCAGCGATAACGATAAGGCTCTCCTCCGCTCCGAAATCGA
GCACTATTTCCTGGCAGGTATTGGTCAGTGCGAAGAAAACATTCTCCTTCGTGAACGTGGA
CTCGACAAGGAGCGCATCGGAACCTCTCACTATCGCTGGACACATGTCGTTGGCGCTGAC
AACGTCGCCGGGACCATCGCCCTCGTCTTTGCCCTTTGTCTCCTTGGTCATCAGATCAATG
AAGAACGAGGCTCTCGCGATTTGGTGGACGTTTTCCCCTCCCCAGTCCTGAAGTACTTGTT
CAACGACTGCGTCATGCACTTCGGTACATTCTCAAGGCTCGCCAACGATCTTCACAGTATC
TCCCGCGACTTCAACGAAGTCAATCTCAACTCCATCATGTTCTCCGAATTCACAGGACCAA
AGTCTGGTACAGATACAGAGAAGGCTCGTGAAGCTGCTCTGCTTGAATTGACCAAATTCG
AACGCAAGGCCACCGACGATGGGTTCGAGTACTTGGTCAAGCAACTCACTCCACATGTCG
GTGCCAAACGTGCACGGGATTATATCAATATCATCCGGGTCACCTACCTGCACACGGCAC
TCTACGATGACCTTGGTCGTCTCACTCGCGCTGATATCAGCAACGCCAACCAGGAGGTTTC
CAAAGGTACCAATGGGGTTAAGAAAGCTAATGGGTCGGCGACAAATGGGATCAAGGTCA
CAGCAAACGGGAGCAATGGAATCCACCATTGA

A3. *Cytochrome p450-1* coding sequence

ATGCTGTCCGTCGACCTCCCGTCTGTTGCGAACTTGGATCCCGTGATCGTGGCTGCTGCTG
CAGGTTCCGCTGTTGCCGTCTATAAGCTCCTTCAGCTAGGCTCCAGGGAGAACTTCTTGCC
ACCCGGGCCACCTACCAAGCCTGTTCTCGGAAATGCTCATCTCATGACGAAGATGTGGCTT
CCAATGCAATTGACAGAGTGGGCCAGGGAGTATGGCGAAGTGTACTCTCTCAAATTGATG
AATCGCACTGTGATTGTTCTGAACAGTCCAAAGGCTGTTCGGACTATTCTTGACAAGCAGG
GTAATATCACAGGAGATCGGCCATTTTCGCCCATGATTGCCCGGTATACAGAAGGCCTGA
ATCTCACGGTGGAAAGCATGGACACTTCCGTATGGAAAACTGGTCGCAAAGGTATCCACA
ATTACCTAACGCCAAGTGCCTTGAGTGGCTACATACCGCGACAAGAAGAGGAATCTGTGA
ACCTCATGCACGATCTATTGATGGACGCTCCTAATCGGCCGATCCATATTAGGCGTGCTAT
GATGTCGCTACTCCTGCACATTGTGTATGGCCAGCCACGTTGCGAAAGTTACTATGGCACG
ATTATCGAGAATGCATACGAAGCTGCCACCAGAATTGGTCAAATCGCTCACAACGGTGCA
GCGGTCGACGCTTTCCCCTTCTTAGACTACATCCCTCGCGGTTTCCCCGGGGCCGGCTGGA
AAACCATTGTGGATGAATTCAAGGATTTCCGTAATGGTGTCTACAATTCTCTCTTGGAAGG
TGCCAAGAAGGCGATGGATTCCGGGGTCAGGACCGGATCTTTTGCAGAGTCCGTGATTGA
CCATCCGGATGGTCGTAGCTGGCTTGAGTTATCAAACCTTAGCGGTGGTTTCTTGGACGCC
GGCGCGAAAACCACGATATCGTACATCGAATCGTGTATTCTTGCTCTTATCGCCCACCCGA
ACTGCCAGCGCAAGATACAGGACGAGCTGGACAATGTTTTGGGGACCGAAACCATGCCAT
GCTTCAATGATTTGGAACGGTTGCCTTATCTCAAGGCGTTCCTACAGGAGGTCCTTCGGCT
TCGGCCAGTCGGCCCTGTAGCCCTTCCCCACGTCTCGCGGGAGAGCTTGTCTTATGGCGGT

TACGTACTGCCAGAGGGAAGTATGATCTTCATGAACATCTGGGGAATGGGCCATGACCCC
GAGCTCTTCGACGAACCTGAGGCCTTCAAGCCTGAACGCTATTTCTTGTCGCCAAACGGCA
CGAAGCCAGGCTTATCTGAAGATGTCAATCCCGATTTCCTGTTCGGTGCTGGACGTAGAGT
CTGCCCAGGCGATAAGCTGGCAAAACGATCAACTGGTCTATTCATCATGAGGCTCTGTTG
GGCATTCAATTTTTACCCAGATTCTTCAAACAAGGACACTGTGAAGAATATGAACATGGA
GGACTGTTACGACAAGTCGGTTTCTCTTGAGACTCTTCCACTTCCGTTCGCATGCAAAATT
GAACCTCGAGATAAGATGAAGGAAGATCTGATTAAGGAAGCGTTCGCTGCGTTGTAG

A4. *Cytochrome p450-2* coding sequence

ATGAATCTTTCTGCTCTGAAGGCTGCTCTGCTTGACAGCAACATGATCGCACCTGTGGCCA
TCCCTTTGGCATGCTACTTGGTCTACAAGCTGCTTCGTATGGGGTCGAGGGAGAAAACGTT
ACCTCCTGGGCCACCTACGAAGCCGGTGTTGGGTAATCTCCACCAGATGCCAGCAATGGA
CGACATGCACCTTCAGCTTAGCCGATGGGCACAAGAATATGGAGGAATATACAGCTTGAA
GATCTTCTTCAAGAACGTTATCGTCCTAACAGACTCAGCCTCCGTTACTGGCATTCTTGAC
AAGCTGAATGCCAAGACTGCTGAAAGACCCACTGGTTTCCTCCCTGCTCCTATCAAAGAC
GACCGTTTCCTTCCTATCGCCTCCTACAAATCCGACGAATTCCGAATCAACCACAAGGCCT
TTAAGTTGCTCATTAGCAACGACAGTATTGATCGATATGCAGAGAACATTGAGACGGAGA
CAATCGTGCTGATGAAGGAGCTGTTGGCTGAGCCCAAGGAATTCTTTAGGCATCTCGTCCG
CACCAGCATGTCCAGTATTGTTGCTATCGCTTATGGTGAACGCGTCCTCACCTCCTCAGAC
CCATTCATTCCCTACCACGAAGAATATCTTCACGACTTCGAAAACATGATGGGTCTACGAG
GTGTTCACTTCACCGCTCTAATTCCTTGGCTCGCCAAGTGGCTTCCTGATAGTCTGGCCGG
CTGGAGGGTCATGGCTCAAGGTATCAAGGACAAGCAACTTGGTATCTTTAATGATTTCCTC
GGAAGGGTTGAGAAGAGAATGGAAGCTGGCGTATTCGACGGGTCACACATGCAGACCAT
TCTTCAGAGGAAGGATGAGTTTGGATTCAAGGATAGGGATCTTATTGCCTATCACGGAGG
CGTCATGATTGACGGAGGAACTGATACCCTCGCTATGTTCACTCGTGTCTTTGTGCTCATG
ATGACGATGCACCCCGAATGCCAGCAGAAGATTCGTGATGAGCTGAAGGAGGTCATGGGC
GATGAATACGACTCGCGTTTGCCAACTTATCAAGATGCATTGAAGATGAAATACTTCAATT
GCGTCGTCAGAGAGGTAACTCGCATCTGGCCTCCGAGTCCCATCGTACCGCCTCATTACTC
GACAGAGGATTTCGAATACAATGGCTACTTCATCCCGAAGGGTACCGTCATCGTGATGAA
CCTTTATGGCATCCAACGAGATCCAAATGTTTTCGAGGCCCCAGACGATTTCCGCCCCGAA
CGGTACATGGAGTCTGAATTTGGCACAAAACCAAGCGTTGACCTGACTGGCTACCGTCAT
ACCTTCACTTTCGGCGCTGGGCGCAGGCTCTGTCCTGGACTCAAGATGGCTGAAATTTTCA
AGCGCACTGTATCTTTGAACATCATCTGGGGATTCGACATCAAGCCCCTGCCTAACAGCCC
CAAGTCAATGAAGGACGATGTCGTTGTACCCGGTCCGGTTTCGATGCCAAAACCGTTTGA
ATGCGAGATGGTACCACGTAGTCAGTCAGTTGTGCAGGTGATCCACGATGTTGCAGACTA
TTAG

A5. *Short-chain reductase* coding sequence

ATGGAAGGCAAGGTCGCAATCGTCACAGGCGCATCCAATGGCATTGGACTCGCCACCGTC
AATCTCCTCCTCGCAGCAGGAGCGTCTGTCTTTGGCGTAGACCTCGCTCTAGCACCGCCCT
CGGTGACCTCCGGAAAATTCAAATTCCTACAACTCAACATCTGCGACAAGGATGCACCCG
CCAGGATTGTGTCCGGCTCCAAGGACGCCTTTGGAAGCGAGAGAATCGACGCCCTCTTGA
ACGTCGCTGGTATCTCGGACTACTTCCAGACCGCGTTGACCTTCGAGGACGATGTATGGGA
CAGAGTCATCGATGTCAACCTGGCTGCACAAGTGAGGTTGATGAGAGAGGTATTGAAGGT
TATGAAGGTCCAGAAGTCAGGTAGTATCGTGAACGTAGTCAGCAAGCTGGCCCTCAGCGG
TGCTTGTGGAGGTGTCGCATACGTTGCGAGTAAACATGCCTTGCTTGGTGTGACAAAGAA
CACCGCGTGGATGTTCAAGGACGATGGTATTCGATGCAATGCCGTGGCGCCTGGCTCGAC
CGACACCAACATTCGAAACACGACAGACCCGACCAAAATAGATTATGATGCATTCTCTCG

AGCCATGCCTGTTATCGGCGTACACTGCAACTTGCAGACCGGCGAGGGTATGATGAGCCC
TGAACCTGCAGCCCAAGCGATCTTCTTCTTAGCTTCAGACTTGAGTAACGGGACAAATGGC
GTCGTTATTCCGGTCGATAACGGGTGGAGTGTCATTTAG

A6. *Acetyltransferase* coding sequence

ATGAAGCCCTTCTCACCAGAACTTCTGGTTCTATCTTTCATTCTATTGGTACTATCTTGTGC
CATCCGGCCTGCTAGAGGACGATGGGTTCTCTGGGTCATTATTGTTGGGCTCAACACCTAC
CTCACCCTGACTCCGACCGGCGATTCGACCTTGGATTATGACATTGCCAATAACCTCTTCG
TTATTACCCTCACGGCCACAGATTATATTCTCTTGACGGACGTCCAGAGAGAGTTACAATT
CCGCAACCAGAAAGGTGTCGAGCAAGCCTCGTTGCTTGAACGCATCAAGTGGGCGACCTG
GCTGGTGCAAAGTCGGCGTGGTGTGGGCTGGAATTGGGAGCCGAAGATTTTCGTCCACAA
GTTTGACCCAAAGACTTCACGCCTTTCATTCCTCCTCCAGCAACTCGTCACAGGTTTTCGG
CATTACCTTATTTGCGATCTAGTCTCGCTATATAGCCGCAGTCCAGTCGCCTTCATCGAAC
CTCTTGCTTCTCGCCCTCTGATCTGGCGGTGTGCAGATATTACCGCATGGCTCCTGTTCACG
ACGAACCAAGTATCAATTCTTCTTACGGCATTGAGTGTCATGCAAGTTCTCTCAGGTTACT
CAGAACCACAGGACTGGGTCCCCGTGTTTGGCCGCTGGAGAGATGCTTATACCGTTAGGC
GGTTCTGGGGTCGATCGTGGCATCAATTGGTTCGCAGATGCCTATCAGCCCCAGGAAAAC
ATCTTTCCACGAAGATTCTAGGCTTGAAGTCTGGCTCTAACCCGGCGCTTTACGTACAACT
GTACACCGCATTCTTCCTCTCGGGAGTTTTGCATGCGATTGGGGACTTCAAGGTTCACGCA
GATTGGTACAAAGCCGGGACTATGGAGTTCTTCTGTGTTCAAGCGGCGATCATACAGATG
GAGGATGGGGTTCTCTGGGTCGGAAGGAAGCTTGGTATCAAGCCGACTTCGTACTGGAAG
GCCCTTGGACATCTTTGGACTGTGGCATGGTTCGTCTACAGCTGCCCGAATTGGCTGGGGG
CAACTGTCTCGGGAAGGGGAAAGGCCTCAATGTCGTTGGAGAGTAGTCTCATTCTTGGTCT
GTACCGGGGGGAATGGAATCCCCCTCGTGTAGCACAGTAG

A7. *Cytochrome p450-3* coding sequence

ATGGCTCCGTCAACGGAACGTGCTCTACCAGTCCTTGTAATATGGACTGCTATAGGCTTGG
CCTACTGGATAGATTCTCAGAAGAAGAAAAAGCAGCACCTGCCGCCTGGGCCAAAGAAA
CTTCCAATTATTGGCAACGTCATGGACCTACCAGCGAAGGTCGAATGGGAAACCTATGCT
CGCTGGGGTAAAGAGTACAACTCTGATATCATACATGTTAGCGCCATGGGAACCTCGATC
GTAATACTGAATTCTGCCAACGCCGCCAATGACTTGTTGCTGAAGAGGTCGGCGATCTACT
CGAGCAGACCACACAGCACGATGCACCACGAGCTGTCAGGATGGGGCTTTACGTGGGCCT
TAATGCCATACGGCGAGTCATGGCGGGCTGGTCGAAGAAGCTTCACCAAGCACTTCAACT
CTTCAAACCCCGGTATAAACCAACCTCGTGAGTTGCGATATGTGAAACGGTTCCTCAAGC
AGCTTTACGAGAAGCCCGACGACGTTCTCGATCATGTACGGAACTTGGTCGGCTCTACGA
CGCTTTCAATGACCTATGGCCTTGAGACTGAACCTTATAACGACCCCTATGTTGACCTGGT
CGAGAAAGCTGTCCTTGCAGCGTCTGAGATTATGACGTCTGGCGCCTTTCTTGTTGACATC
ATCCCTGCGATGAAACACATTCCTCCATGGGTCCCAGGGACTATCTTCCATCAAAAGGCTG
CCTTAATGCGAGGTCATGCGTACTATGTTCGTGAACAGCCATTCAAAGTTGCCCAGGAGAT
GATTAAAACTGGCGATTATGAGCCCTCCTTTGTATCTGACGCTCTCCGAGATCTTCAGAAC
TCGGAAAACCAGGAGGCAGATTTGGAGCACCTCAAGGATGTTGCTGGTCAAGTCTACATT
GCTGGTGCTGATACGACTGCATCCGCCTTGGGGACTTTCTTCCTCGCCATGGTCTGTTTCCC
CGAAGTACAGAAGAAAGCACAACGAGAATTAGATAGTGTTCTCAATGGAAGGATGCCCG
AGCACGCCGACTTCCCCTCTTTCCCATACCTCAACGCTGTGATCAAGGAGGTTTACCGCTG
GAGGCCTGTGACTCCTATGGGCGTACCTCATCAAACCATCTCAGATGACGTTTACAGGGA
ATACCACATCCCTAAGGGATCCATCGTGTTTGCCAACCAATGGGCGATGTCCAACGACGA
AACCGATTACCCCCAGCCAGACGAATTCCGGCCTGAGCGATACTTGACCGAGGACGGTAA
GCCTAACAAGGCTGTCAGAGATCCCTTTGATATCGCATTCGGCTTCGGTAGAAGAATTTGC

GCTGGTCGTTACCTCGCTCATTCCACCATCACCTTGGCTGCGGCCTCTGTTCTGTCGCTGTT
TGATCTCTTAAAAGCAGTTGACGAAAATGGCAAAGAAATTGAGCCTACTAGAGAGTATCA
CCAGGCTATGATCTCACGTCCACTAGATTTCCCTTGCCGCATCAAGCCAAGAAGTAAGGA
AGCTGAGGAGGTCATCCGTGCTTGCCCGTTGACGTTCACGAAGCCTGCTAGTGGCTAG

A8. *Neomycin phosphotransferase* coding sequence

ATGGTTGAACAAGATGGATTGCACGCAGGTTCTCCGGCCGCTTGGGTGGAGAGGCTATTC
GGCTATGACTGGGCACAACAGACAATCGGCTGCTCTGATGCCGCCGTGTTCCGGCTGTCA
GCGCAGGGGCGCCCGGTTCTTTTTGTCAAGACCGACCTGTCCGGTGCCCTGAATGAACTGC
AGGACGAGGCAGCGCGGCTATCGTGGCTGGCCACGACGGGCGTTCCTTGCGCAGCTGTGC
TCGACGTTGTCACTGAAGCGGGAAGGGACTGGCTGCTATTGGGCGAAGTGCCGGGGCAGG
ATCTCCTGTCATCTCACCTTGCTCCTGCCGAGAAAGTATCCATCATGGCTGATGCAATGCG
GCGGCTGCATACGCTTGATCCGGCTACCTGCCCATTCGACCACCAAGCGAAACATCGCAT
CGAGCGAGCACGTACTCGGATGGAAGCCGGTCTTGTCGATCAGGATGATCTGGACGAAGA
GCATCAGGGGCTCGCGCCAGCCGAACTGTTCGCCAGGCTCAAGGCGCGCATGCCCGACGG
CGAGGATCTCGTCGTGACTCATGGCGATGCCTGCTTGCCGAATATCATGGTGGAAAATGG
CCGCTTTTCTGGATTCATCGACTGTGGCCGGCTGGGTGTGGCGGACCGCTATCAGGACATA
GCGTTGGCTACCCGTGATATTGCTGAAGAGCTTGGCGGCGAATGGGCTGACCGCTTCCTCG
TGCTTTACGGTATCGCCGCTCCCGATTCGCAGCGCATCGCCTTCTATCGCCTTCTTGACGA
GTTCTTCTGA

A9. Level 0 and Level 1 (35S and Diverse promoter) plasmids

Level 0 (left), **Level 1** – 35S (middle) and **Level 1** – Diverse (right) plasmids of ***ggs*** gene

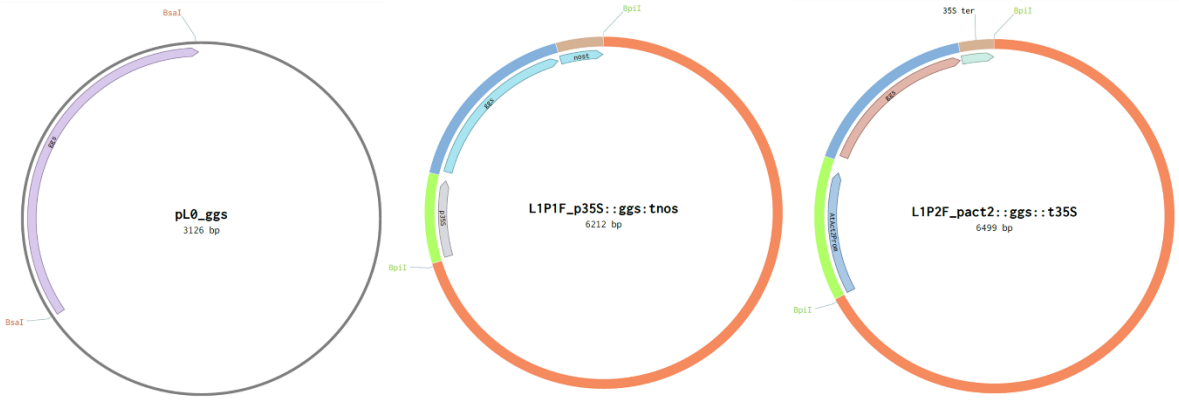

Level 0 (left), **Level 1** – 35S (middle) and **Level 1** – Diverse (right) plasmids of ***cyc*** gene

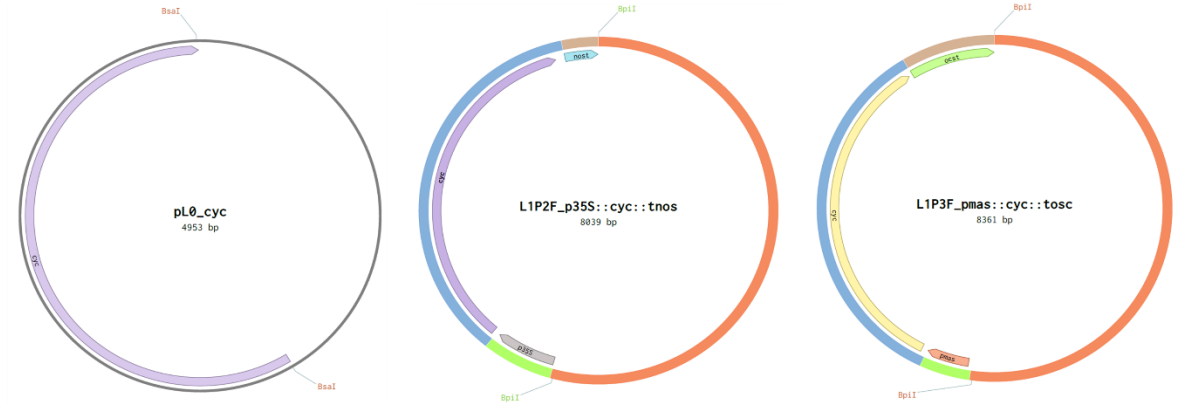

Level 0 (left), **Level 1** – 35S (middle) and **Level 1** – Diverse (right) plasmids of ***nptII*** gene

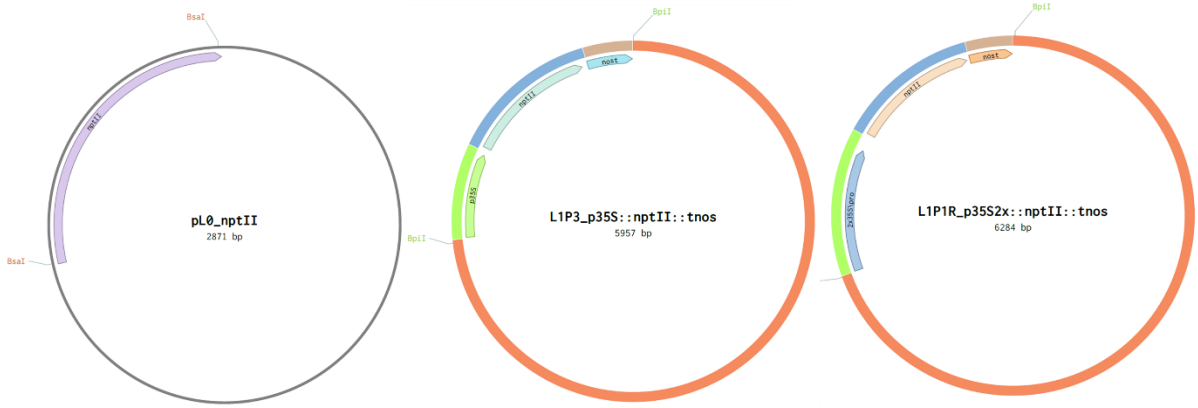

Level 0 (left), **Level 1** – 35S (middle) and **Level 1** – Diverse (right) plasmids of ***p450-1*** gene

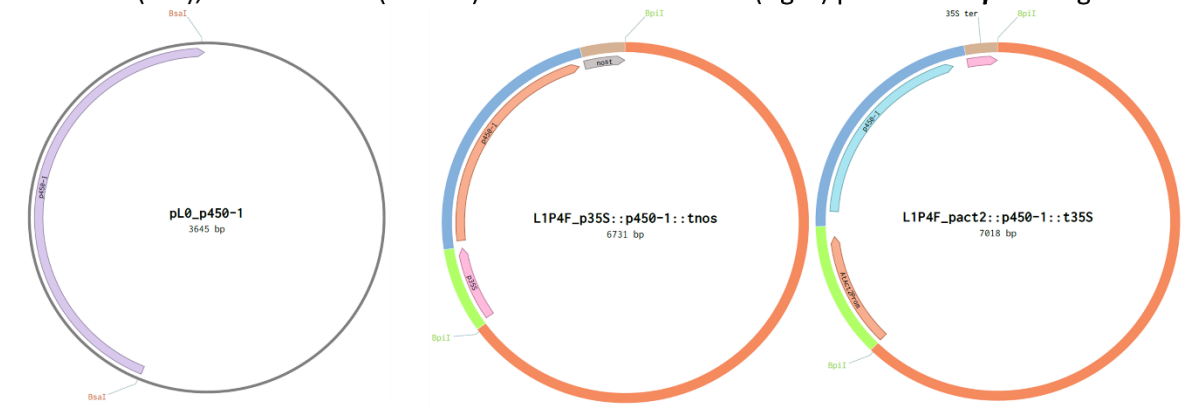

Level 0 (left), **Level 1** – 35S (middle) and **Level 1** – Diverse (right) plasmids of ***p450-2*** gene

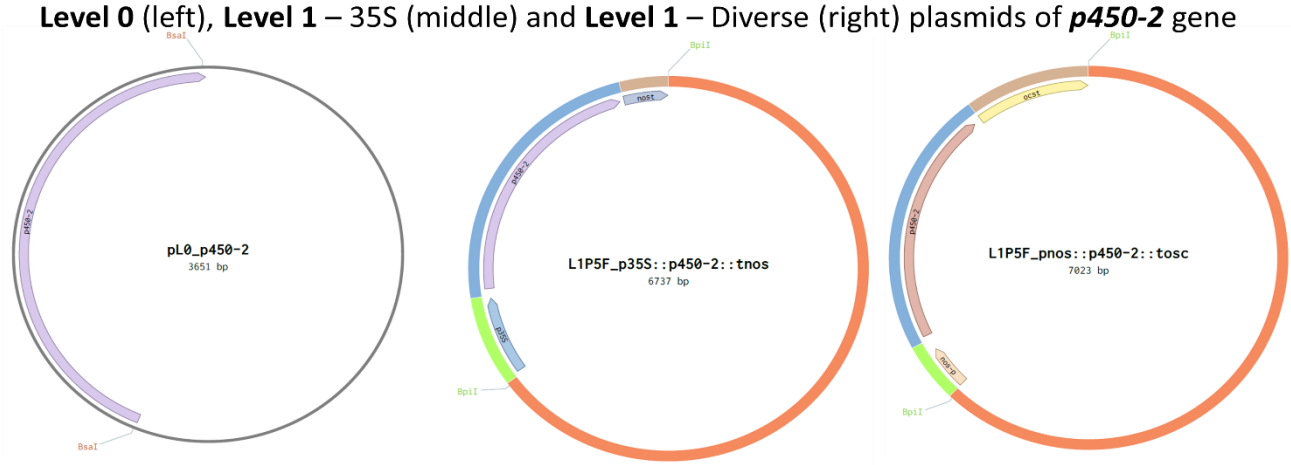

Level 0 (left), **Level 1** – 35S (middle) and **Level 1** – Diverse (right) plasmids of ***sdr*** gene

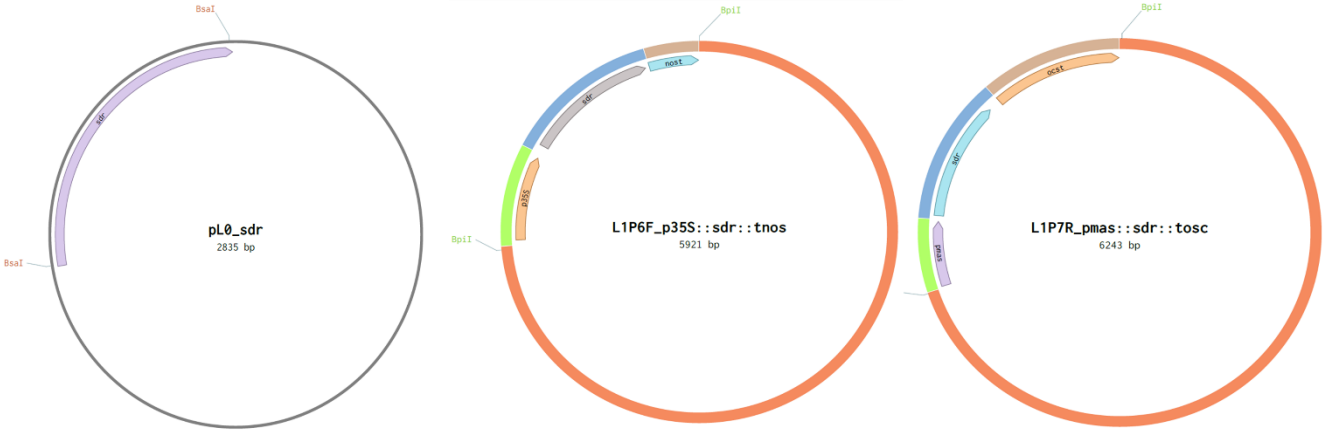

Level 0 (left), **Level 1** – 35S (middle) and **Level 1** – Diverse (right) plasmids of ***atf*** gene

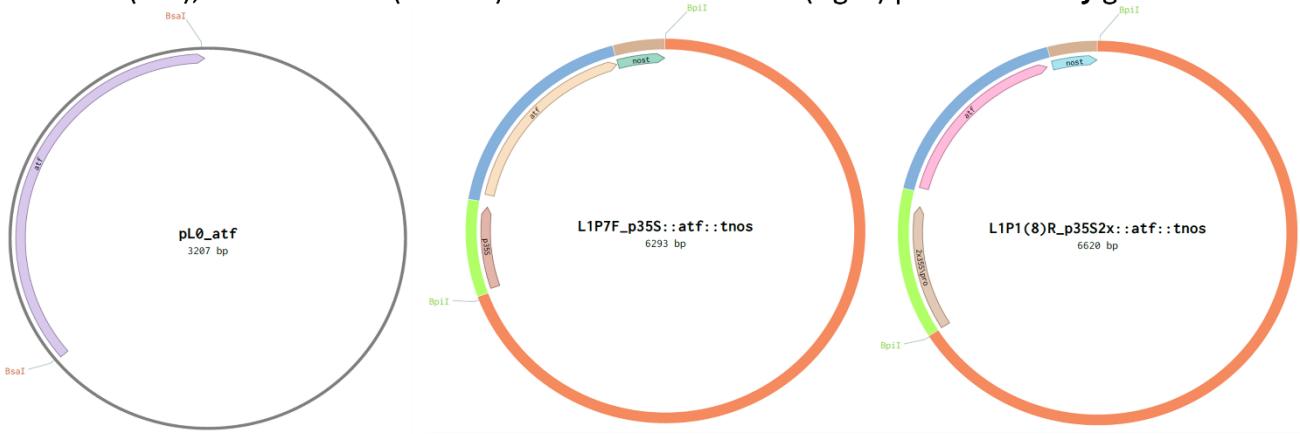

Level 0 (left), **Level 1** – 35S (middle) and **Level 1** – Diverse (right) plasmids of ***p450-3*** gene

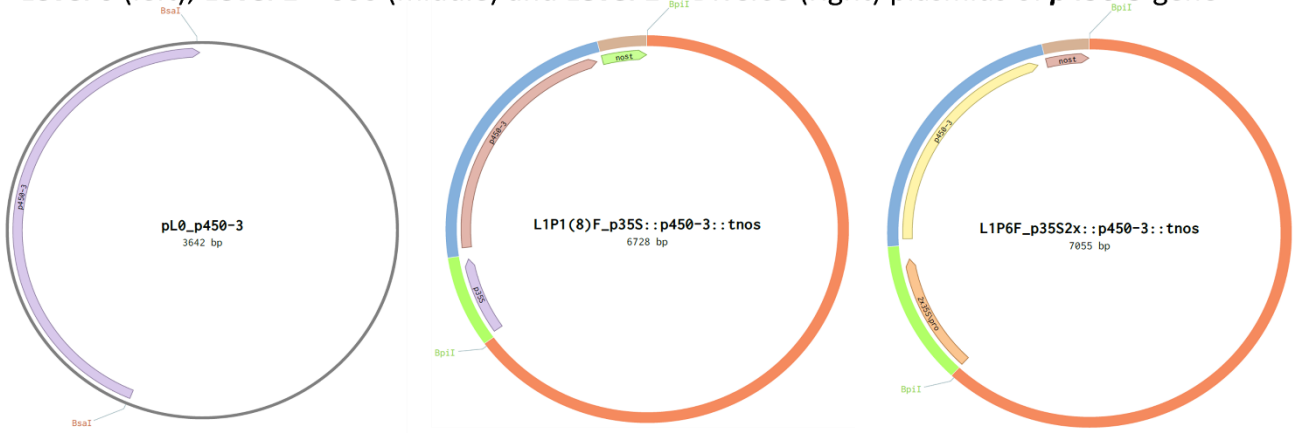

A10. Level 2.3 (left), 2.4 (middle) and 2.6 (right) of 35S promoter plasmids

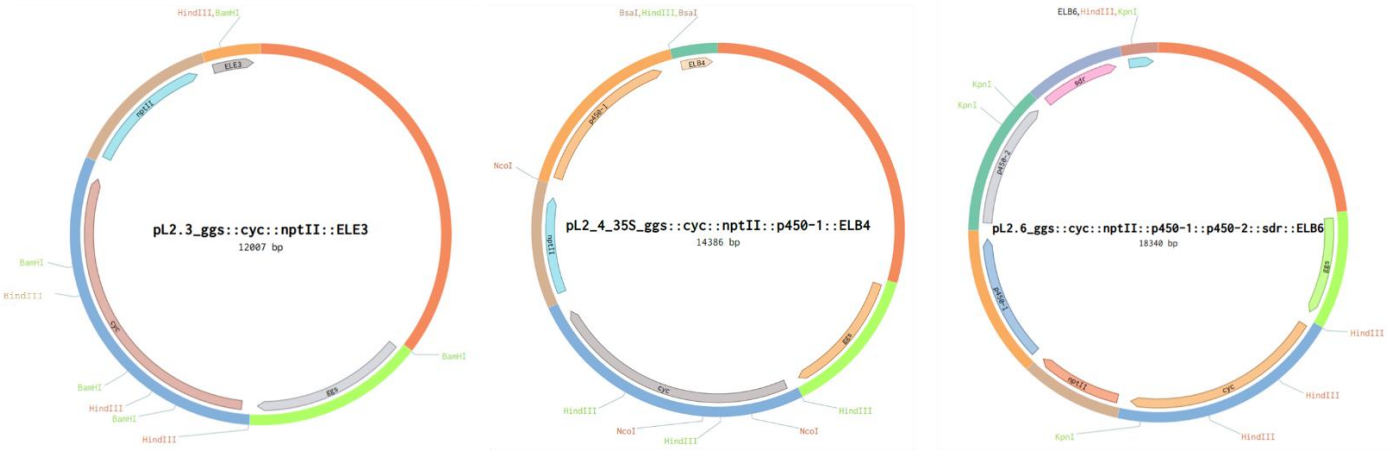

Appendix B: Antibiotic treatments

Antibiotic treatments for *P. patens* and *M. polymorpha*, at concentrations ranging from 1 to 500µg/ml. Mock assays were treated using solvent (untreated). Each assay consisted of 2 or 3 technical replicates. Scale bar is at 25mm.

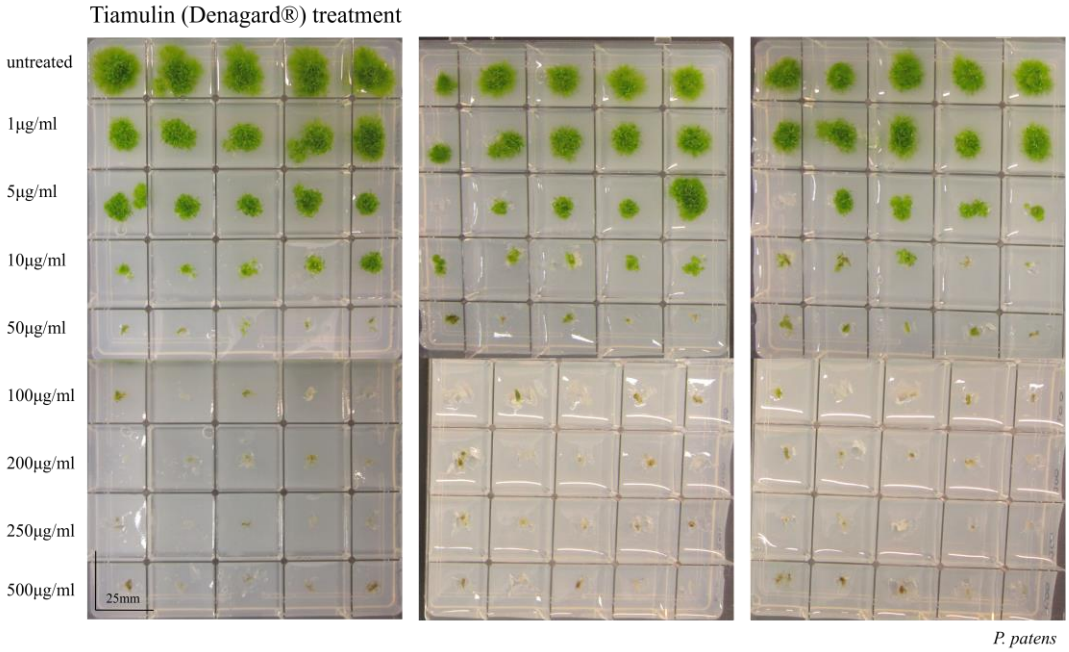

P. patens

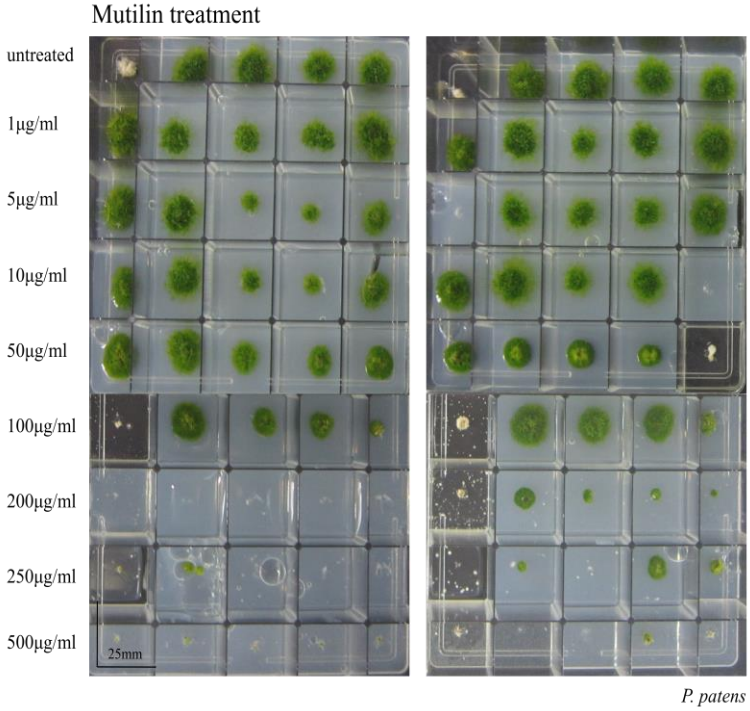

P. patens

Chloramphenicol treatment

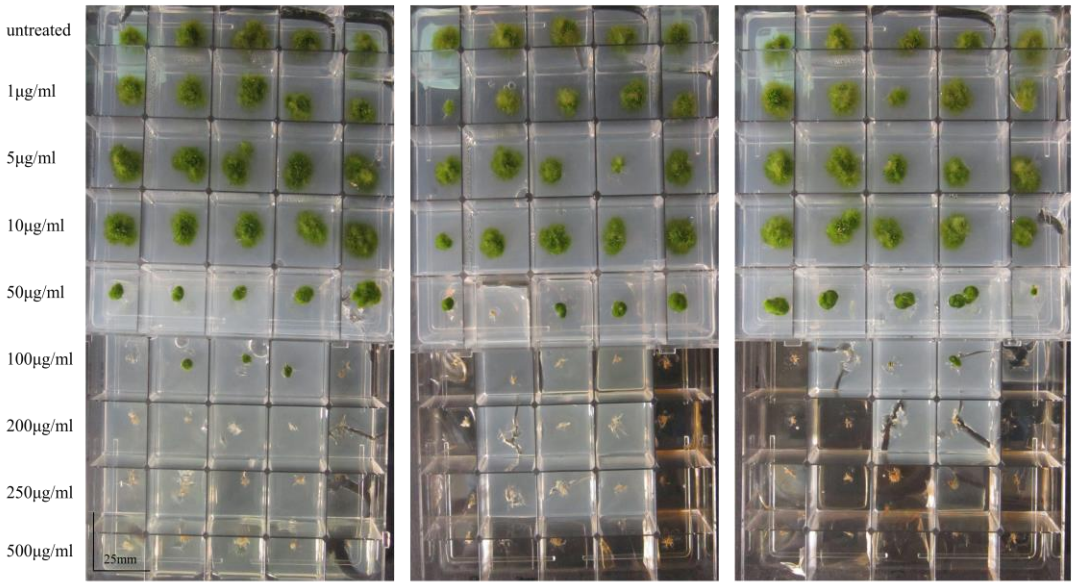

P. patens

Kanamycin treatment

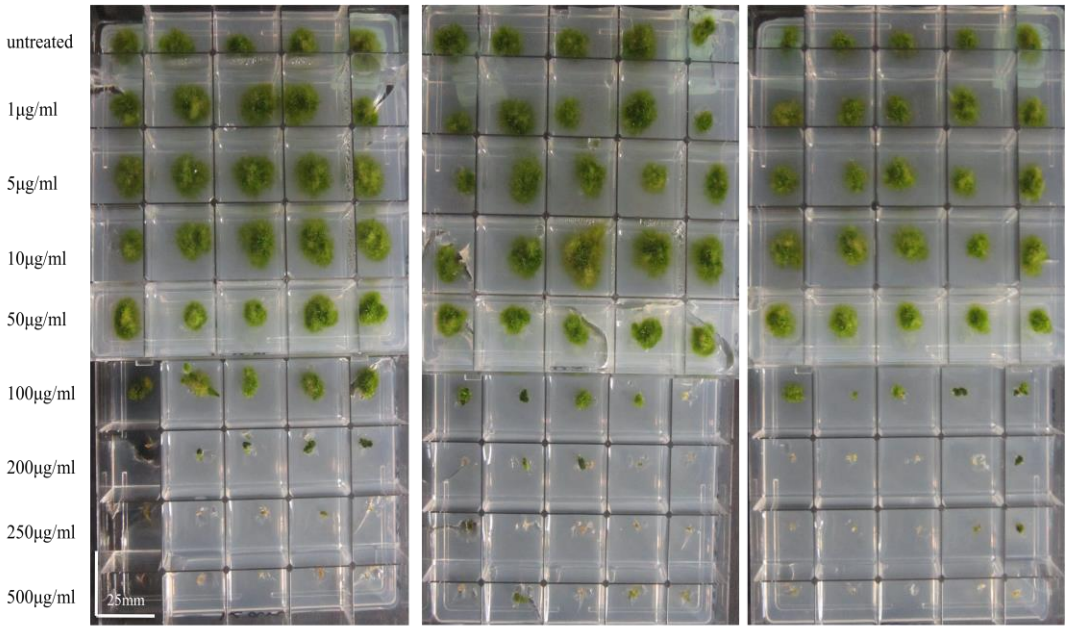

P. patens

Nalidixic acid treatment

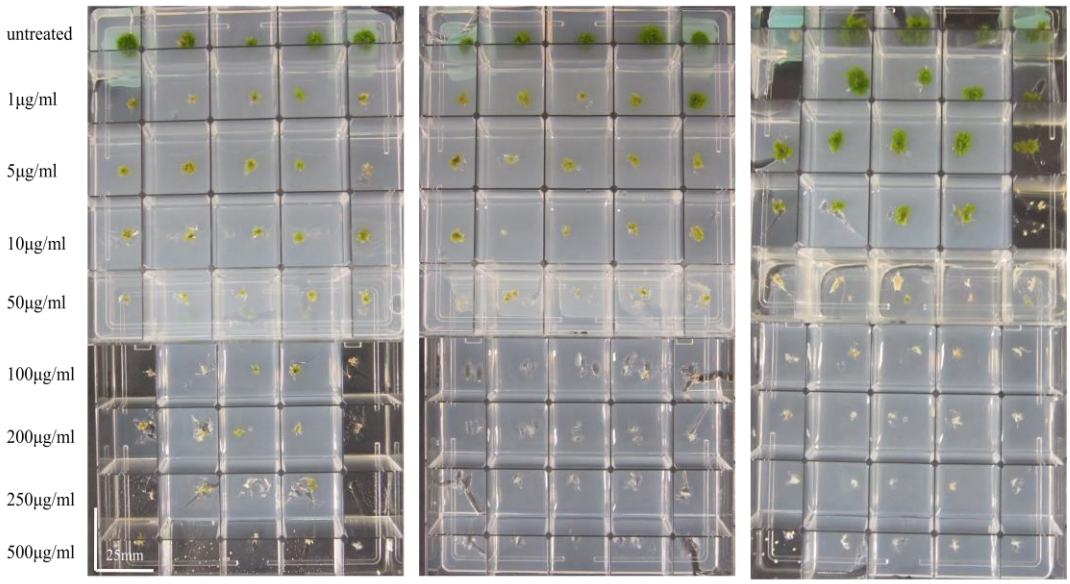

P. patens

Tiamulin (Denagard®) treatment

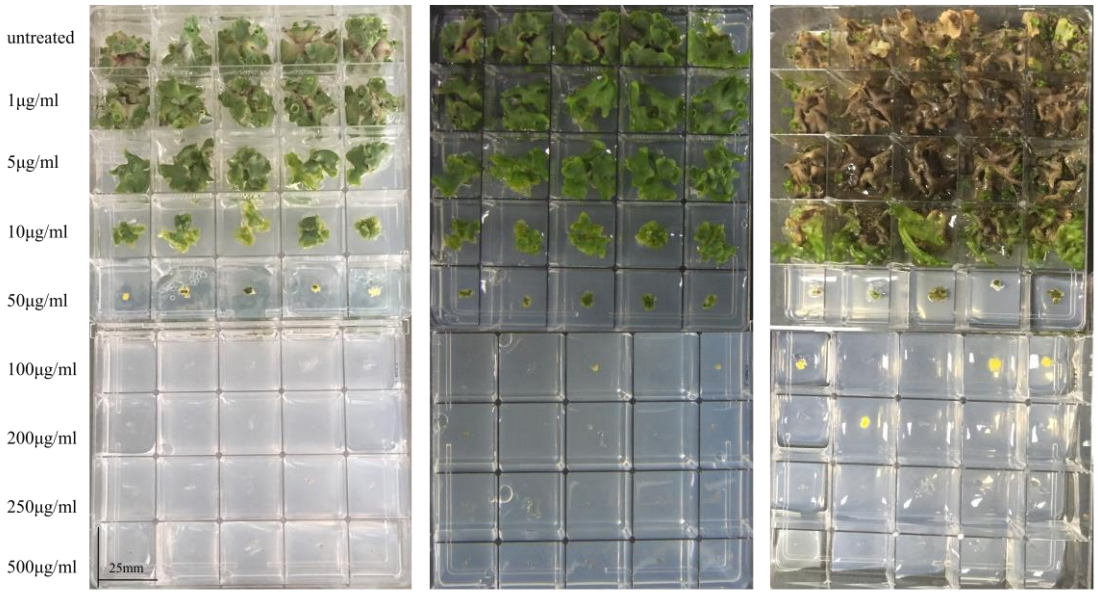

M. polymorpha

Mutilin treatment

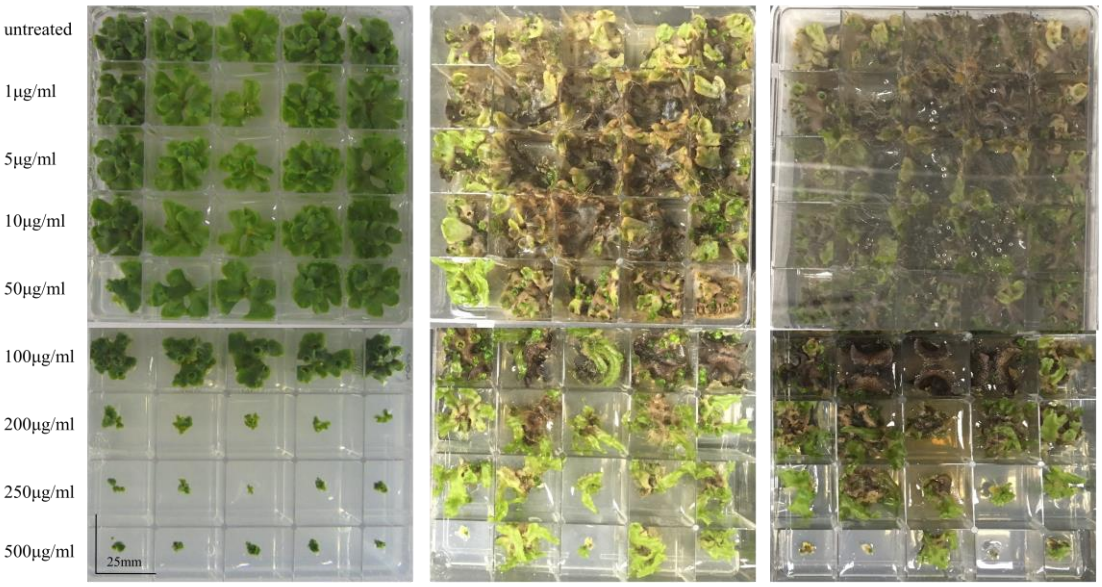

M. polymorpha

Ampicillin treatment

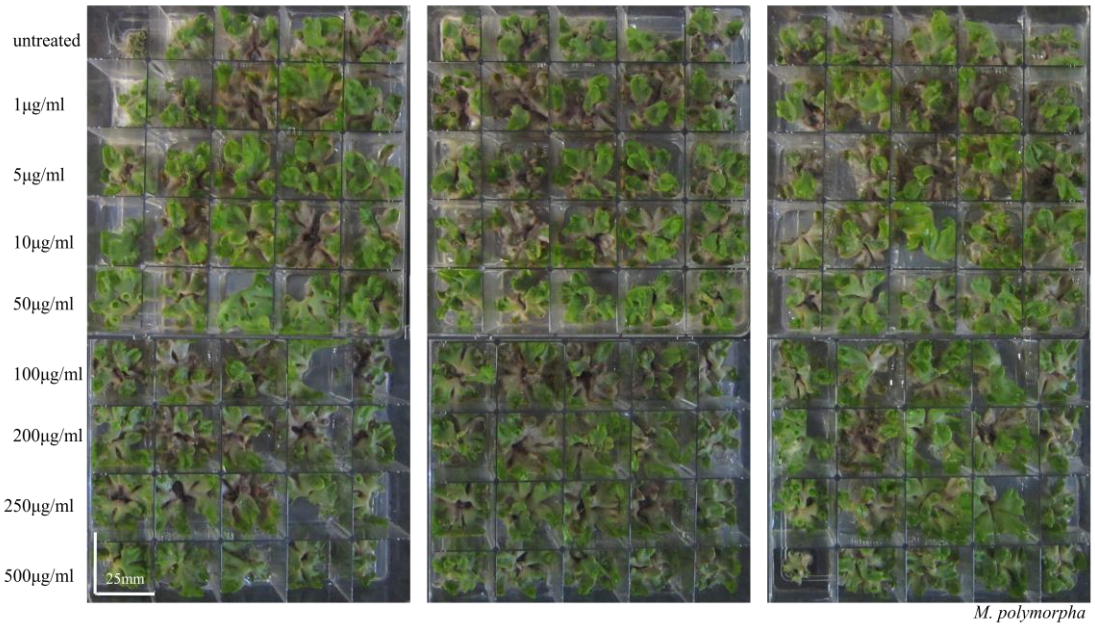

M. polymorpha

Chloramphenicol treatment

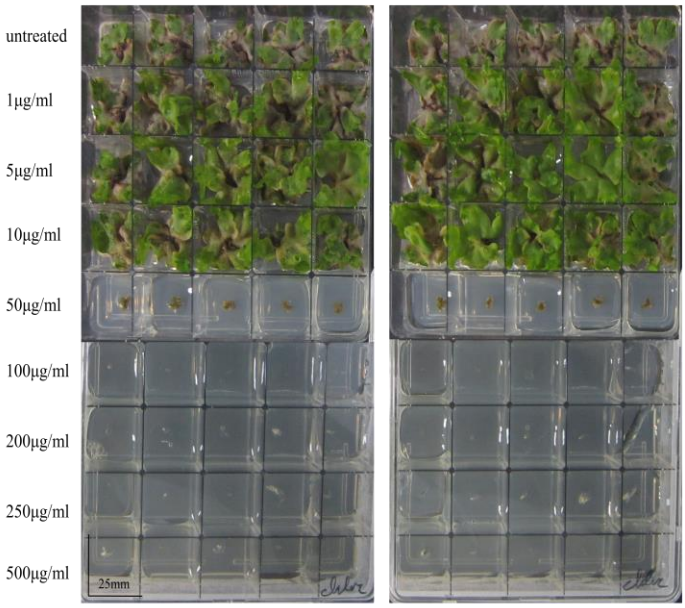

M. polymorpha

Kanamycin treatment

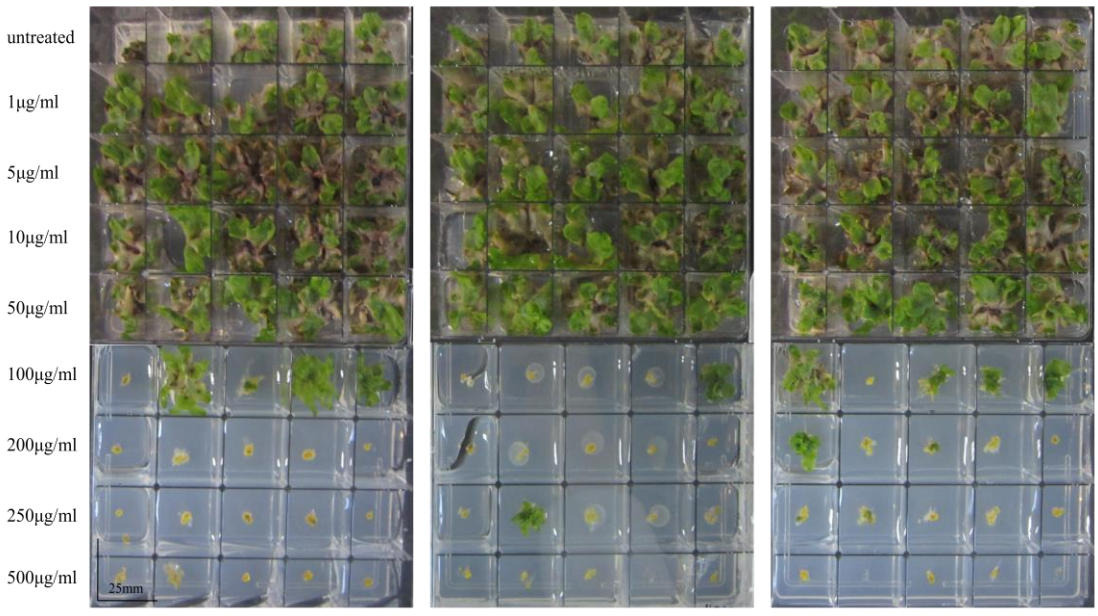

M. polymorpha

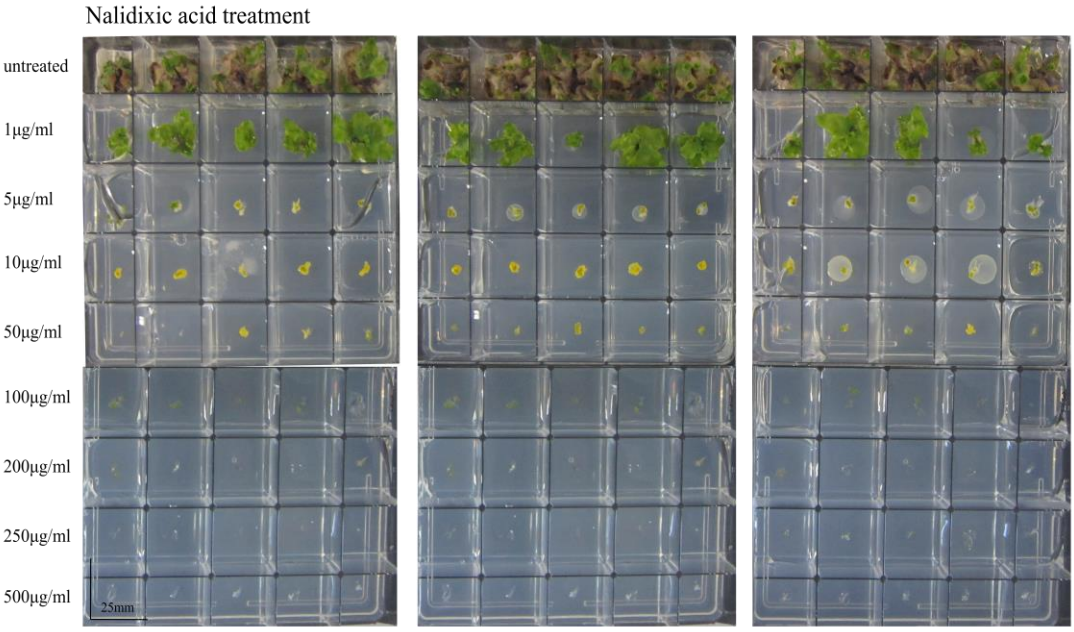

M. polymorpha